

IMIDAZOLE-BASED MOLECULES AS PREVENTATIVE THERAPEUTICS  
FOR ISCHEMIC NEURONAL DEGRADATION

by

Kale O'Neill

Submitted in partial fulfilment of the requirements  
for the degree of Master of Science

at

Dalhousie University  
Halifax, Nova Scotia  
September 2013

© Copyright by Kale O'Neill, 2013

*For my family.*

## TABLE OF CONTENTS

|   |      |
|---|------|
| <b>LIST OF TABLES</b> .....   | vii  |
| <b>LIST OF FIGURES</b> .....  | xiii |
| <b>ABSTRACT</b> .....   | xv   |
| <b>LIST OF ABBREVIATIONS USED</b> .....                                   | xvi  |
| <b>ACKNOWLEDGEMENTS</b> .....   | xvii |
| <b>CHAPTER 1 - INTRODUCTION</b> .....                                     | 1    |
| 1.1    COMPUTER-AIDED DESIGN.....   | 1    |
| 1.2    MOLECULAR MODELLING.....   | 3    |
| 1.2.1    Force Fields.....  | 3    |
| 1.2.2    The CHARMM22 Force Field and MOE.....                            | 5    |
| 1.2.3    Energy Minimization Algorithms.....                              | 8    |
| 1.2.3.1    The Newton-Raphson Method.....                                 | 9    |
| 1.2.3.2    The Steepest Descent Model.....                                | 10   |
| 1.2.3.3    Issue With Energy Minimization Techniques.....                 | 11   |
| 1.3    STROKE AND THE ROLE OF Ca <sup>2+</sup> AND Zn <sup>2+</sup> ..... | 12   |
| 1.3.1    The Ischemic Cascade.....  | 13   |
| 1.3.2    The Role of Ca <sup>2+</sup> .....                               | 15   |
| 1.3.3    The Role of Zn <sup>2+</sup> .....                               | 15   |
| 1.3.4    The Ischemic Penumbra.....                                       | 16   |
| 1.3.5    A Unique Approach.....   | 17   |
| 1.4    DEFINING A DRUG MOLECULE.....                                      | 18   |
| 1.4.1    Properties of Drug Molecules.....                                | 18   |
| 1.4.2    Lipinski's Rule of Five.....                                     | 20   |
| 1.5    RESEARCH GOALS.....  | 22   |
| <b>CHAPTER 2 - CARNOSINE</b> .....  | 24   |
| 2.1    IMIDAZOLES.....  | 24   |
| 2.1.1    Physical and Chemical Properties of Imidazoles.....              | 24   |
| 2.1.2    Imidazoles as Drug Molecules.....                                | 25   |
| 2.1.3    Hard-Soft Acid-Base Theory.....                                  | 25   |
| 2.2    THE METHOD.....  | 27   |

|                                    |   |           |
|------------------------------------|---|-----------|
| 2.2.1                              | Gas-Phase Simulations.....  | 28        |
| 2.2.2                              | Solution-Phase Simulations.....   | 29        |
| 2.2.3                              | A Reference Point.....  | 30        |
| 2.3                                | CASE STUDY: CARNOSINE.....  | 33        |
| 2.3.1                              | Carnosine as a Neuroprotective Molecule.....                              | 34        |
| 2.3.1.1                            | Cytosolic Buffer.....   | 34        |
| 2.3.1.2                            | Antioxidant Activity.....   | 34        |
| 2.3.1.3                            | Anti-Glutamatergic Excitotoxicity.....                                    | 35        |
| 2.3.1.4                            | Metal Ion Chelation.....  | 35        |
| 2.3.2                              | Gas-Phase Simulations with Carnosine.....                                 | 36        |
| 2.3.2.1                            | Carnosine and $Zn^{2+}$ <i>in vacuo</i> .....                             | 36        |
| 2.3.2.2                            | Carnosine and $Ca^{2+}$ <i>in vacuo</i> .....                             | 38        |
| 2.3.3                              | Solution-Phase Simulations with Carnosine.....                            | 40        |
| 2.3.3.1                            | Carnosine and $Zn^{2+}$ with Solvent.....                                 | 40        |
| 2.3.3.2                            | Carnosine and $Ca^{2+}$ with Solvent.....                                 | 42        |
| 2.3.4                              | Lead Molecules.....   | 44        |
| <b>CHAPTER 3 - IMIDAZOLES.....</b> |   | <b>45</b> |
| 3.1                                | IMIDAZOLE DATABASE.....   | 45        |
| 3.2                                | GAS-PHASE SIMULATIONS OF IMIDAZOLES<br>WITH $Zn^{2+}$ AND $Ca^{2+}$ ..... | 45        |
| 3.2.1                              | Imidazoles with Only Alkyl Substituents.....                              | 46        |
| 3.2.2                              | Imidazoles with Halide Substituents.....                                  | 50        |
| 3.2.3                              | Imidazoles with Nitro Substituents.....                                   | 51        |
| 3.2.4                              | Imidazoles with Amido and Amino Substituents.....                         | 55        |
| 3.2.5                              | Imidazoles with Cyano Substituents.....                                   | 58        |
| 3.2.6                              | Imidazoles with Hydroxyl Substituents.....                                | 60        |
| 3.2.7                              | Imidazoles with Aldehyde and Ketone Substituents.....                     | 62        |
| 3.2.8                              | Imidazoles with Carboxylic Acid and Ester Substituents.....               | 64        |
| 3.2.9                              | Imidazoles with Sulfur-Containing Substituents.....                       | 66        |
| 3.2.10                             | Imidazoles with Phenyl Substituents.....                                  | 71        |
| 3.2.11                             | Imidazolidinones.....   | 77        |

|        |   |     |
|--------|---|-----|
| 3.2.12 | Imidazolidinethione.....  | 79  |
| 3.2.13 | Benzimidazoles with Only Alkyl Substituents.....                      | 80  |
| 3.2.14 | Benzimidazoles with Halide Substituents.....                          | 82  |
| 3.2.15 | Benzimidazoles with Nitrogen-Containing Substituents.....             | 84  |
| 3.2.16 | Benzimidazoles with Oxygen-Containing Substituents.....               | 88  |
| 3.2.17 | Benzimidazoles with Sulfur-Containing Substituents.....               | 91  |
| 3.2.18 | Benzimidazoles with Phenyl Substituents.....                          | 93  |
| 3.2.19 | Exceptions and Atypical Imidazoles.....                               | 95  |
| 3.3    | <b>SOLUTION-PHASE SIMULATIONS OF IMIDAZOLES</b>                       |     |
|        | WITH Zn <sup>2+</sup> AND Ca <sup>2+</sup> .....                      | 97  |
| 3.3.1  | Imidazoles with Only Alkyl Substituents in Water.....                 | 98  |
| 3.3.2  | Imidazoles with Nitrogen-Containing Substituents in Water.....        | 101 |
| 3.3.3  | Imidazoles with Oxygen-Containing Substituents in Water.....          | 103 |
| 3.3.4  | Imidazoles with Sulfur-Containing Substituents in Water.....          | 106 |
| 3.3.5  | Imidazoles with Phenyl Substituents in Water.....                     | 110 |
| 3.3.6  | Imidazolidinones in Water.....  | 113 |
| 3.3.7  | Benzimidazoles with Only Alkyl Substituents in Water.....             | 114 |
| 3.3.8  | Benzimidazoles with Halide Substituents in Water.....                 | 116 |
| 3.3.9  | Benzimidazoles with Nitrogen-Containing<br>Substituents in Water..... | 117 |
| 3.3.10 | Benzimidazoles with Oxygen-Containing<br>Substituents in Water.....   | 118 |
| 3.3.11 | Benzimidazoles with Sulfur-Containing<br>Substituents in Water.....   | 120 |
| 3.3.12 | Benzimidazoles with Phenyl Substituents in Water.....                 | 121 |
| 3.3.13 | Exceptions and Atypical Imidazoles in Water.....                      | 122 |
| 3.4    | <b>COMMENTS AND CONCLUSIONS.....</b>                                  | 123 |
|        | <b>CHAPTER 4 - BIOLOGICALLY RELEVANT CATIONS.....</b>                 | 125 |
| 4.1    | GENERAL TRENDS.....   | 125 |
| 4.2    | GAS-PHASE SIMULATIONS WITH BIOLOGICALLY<br>RELEVANT CATIONS.....      | 127 |

|   |   |            |
|---|---|------------|
| 4.2.1   | Gas-Phase Simulations with $\text{Li}^+$ .....    | 128        |
| 4.2.2   | Gas-Phase Simulations with $\text{Be}^{2+}$ ..... | 129        |
| 4.2.3   | Gas-Phase Simulations with $\text{Na}^+$ .....    | 130        |
| 4.2.4   | Gas-Phase Simulations with $\text{Mg}^{2+}$ ..... | 131        |
| 4.2.5   | Gas-Phase Simulations with $\text{Al}^{3+}$ ..... | 132        |
| 4.2.6   | Gas-Phase Simulations with $\text{K}^+$ .....     | 133        |
| 4.2.7   | Gas-Phase Simulations with Chromium Ions.....     | 134        |
| 4.2.8   | Gas-Phase Simulations with Manganese Ions.....    | 135        |
| 4.2.9   | Gas-Phase Simulations with Cobalt Ions.....       | 137        |
| 4.2.10  | Gas-Phase Simulations with $\text{Ni}^{2+}$ ..... | 138        |
| 4.2.11  | Gas-Phase Simulations with Copper Ions.....       | 139        |
| 4.2.12  | Gas-Phase Simulations with $\text{Sr}^{2+}$ ..... | 140        |
| 4.2.13  | Gas-Phase Simulations with $\text{Pd}^{2+}$ ..... | 141        |
| 4.2.14  | Gas-Phase Simulations with $\text{Ag}^+$ .....    | 142        |
| 4.2.15  | Gas-Phase Simulations with $\text{Cd}^{2+}$ ..... | 143        |
| 4.2.16  | Gas-Phase Simulations with Tin Ions.....          | 144        |
| 4.2.17  | Gas-Phase Simulations with $\text{Ba}^{2+}$ ..... | 145        |
| 4.2.18  | Gas-Phase Simulations with $\text{Hg}^{2+}$ ..... | 146        |
| 4.2.19  | Gas-Phase Simulations with $\text{Pb}^{2+}$ ..... | 147        |
| 4.3   | CONCLUSION.....                                   | 148        |
| <b>CHAPTER 5 - FUTURE WORK AND CONCLUSIONS.....</b> |   | <b>149</b> |
| 5.1   | FUTURE EXPERIMENTAL WORK.....                     | 149        |
| 5.2   | CONCLUDING COMMENTS.....                          | 151        |
| <b>REFERENCES.....</b>                              |   | <b>153</b> |

## LIST OF TABLES

|            |  |    |
|------------|--|----|
| Table 2.1: | A table of hard and soft Lewis acids and bases.....  | 27 |
| Table 2.2: | Gas-phase data for aspartate, glutamate, cysteine and histidine binding to $Zn^{2+}$ ..... | 32 |
| Table 2.3: | Gas-phase data for aspartate, glutamate, cysteine and histidine binding to $Ca^{2+}$ ..... | 32 |
| Table 2.4: | Solvation data for aspartate, glutamate, cysteine and histidine binding to $Zn^{2+}$ ..... | 33 |
| Table 2.5: | Solvation data for aspartate, glutamate, cysteine and histidine binding to $Ca^{2+}$ ..... | 33 |
| Table 2.6: | Gas-phase data for carnosine binding to $Zn^{2+}$ .....                                    | 37 |
| Table 2.7: | Gas-phase data for carnosine binding to $Ca^{2+}$ .....                                    | 39 |
| Table 2.8: | Solvation data for carnosine binding to $Zn^{2+}$ .....                                    | 41 |
| Table 2.9: | Solvation data for carnosine binding to $Ca^{2+}$ .....                                    | 42 |
| Table 3.1: | Gas-phase data for imidazoles with only alkyl substituents binding with $Zn^{2+}$ .....    | 47 |
| Table 3.2: | Gas-phase data for imidazoles with only alkyl substituents binding with $Ca^{2+}$ .....    | 47 |
| Table 3.3: | Gas-phase data for imidazoles with halide substituents binding with $Zn^{2+}$ .....        | 50 |
| Table 3.4: | Gas-phase data for imidazoles with halide substituents binding with $Ca^{2+}$ .....        | 50 |
| Table 3.5: | Gas-phase data for imidazoles with nitro substituents binding with $Zn^{2+}$ .....         | 52 |
| Table 3.6: | Gas-phase data for imidazoles with nitro substituents binding with $Ca^{2+}$ .....         | 52 |
| Table 3.7: | Gas-phase data for imidazoles with amino substituents binding with $Zn^{2+}$ .....         | 56 |
| Table 3.8: | Gas-phase data for imidazoles with amino substituents binding with $Ca^{2+}$ .....         | 56 |

|             |  |    |
|-------------|--|----|
| Table 3.9:  | Gas-phase data for imidazoles with amido substituents binding with $Zn^{2+}$ .....                     | 56 |
| Table 3.10: | Gas-phase data for imidazoles with amido substituents binding with $Ca^{2+}$ .....                     | 56 |
| Table 3.11: | Gas-phase data for imidazoles with cyano substituents binding with $Zn^{2+}$ .....                     | 58 |
| Table 3.12: | Gas-phase data for imidazoles with cyano substituents binding with $Ca^{2+}$ .....                     | 59 |
| Table 3.13: | Gas-phase data for imidazoles with hydroxyl substituents binding with $Zn^{2+}$ .....                  | 60 |
| Table 3.14: | Gas-phase data for imidazoles with hydroxyl substituents binding with $Ca^{2+}$ .....                  | 61 |
| Table 3.15: | Gas-phase data for imidazoles with aldehyde and ketone substituents binding with $Zn^{2+}$ .....       | 63 |
| Table 3.16: | Gas-phase data for imidazoles with aldehyde and ketone substituents binding with $Ca^{2+}$ .....       | 63 |
| Table 3.17: | Gas-phase data for imidazoles with carboxylic acid and ester substituents binding with $Zn^{2+}$ ..... | 65 |
| Table 3.18: | Gas-phase data for imidazoles with carboxylic acid and ester substituents binding with $Ca^{2+}$ ..... | 65 |
| Table 3.19: | Gas-phase data for imidazolines with thioether substituents binding with $Zn^{2+}$ .....               | 67 |
| Table 3.20: | Gas-phase data for imidazolines with thioether substituents binding with $Ca^{2+}$ .....               | 68 |
| Table 3.21: | Gas-phase data for imidazoles with mercapto substituents binding with $Zn^{2+}$ .....                  | 68 |
| Table 3.22: | Gas-phase data for imidazoles with mercapto substituents binding with $Ca^{2+}$ .....                  | 69 |
| Table 3.23: | Gas-phase data for imidazoles with dithiocarboxylic acid substituents binding with $Zn^{2+}$ .....     | 70 |

|             |   |    |
|-------------|---|----|
| Table 3.24: | Gas-phase data for imidazoles with dithiocarboxylic acid substituents binding with $\text{Ca}^{2+}$ .....   | 70 |
| Table 3.25: | Gas-phase data for imidazoles with phenyl substituents binding with $\text{Zn}^{2+}$ .....                  | 74 |
| Table 3.26: | Gas-phase data for imidazoles with phenyl substituents binding with $\text{Ca}^{2+}$ .....                  | 75 |
| Table 3.27: | Gas-phase data for imidazolidinones with binding with $\text{Zn}^{2+}$ .....                                | 77 |
| Table 3.28: | Gas-phase data for imidazolidinones with binding with $\text{Ca}^{2+}$ .....                                | 78 |
| Table 3.29: | Gas-phase data for benzimidazoles with only alkyl substituents binding with $\text{Zn}^{2+}$ .....          | 81 |
| Table 3.30: | Gas-phase data for benzimidazoles with only alkyl substituents binding with $\text{Ca}^{2+}$ .....          | 81 |
| Table 3.31: | Gas-phase data for benzimidazoles with halide substituents binding with $\text{Zn}^{2+}$ .....              | 83 |
| Table 3.32: | Gas-phase data for benzimidazoles with halide substituents binding with $\text{Ca}^{2+}$ .....              | 83 |
| Table 3.33: | Gas-phase data for benzimidazoles with nitrogen-containing substituents binding with $\text{Zn}^{2+}$ ..... | 86 |
| Table 3.34: | Gas-phase data for benzimidazoles with nitrogen-containing substituents binding with $\text{Ca}^{2+}$ ..... | 86 |
| Table 3.35: | Gas-phase data for benzimidazoles with oxygen-containing substituents binding with $\text{Zn}^{2+}$ .....   | 89 |
| Table 3.36: | Gas-phase data for benzimidazoles with oxygen-containing substituents binding with $\text{Ca}^{2+}$ .....   | 89 |
| Table 3.37: | Gas-phase data for benzimidazoles with sulfur-containing substituents binding with $\text{Zn}^{2+}$ .....   | 92 |
| Table 3.38: | Gas-phase data for benzimidazoles with sulfur-containing substituents binding with $\text{Ca}^{2+}$ .....   | 92 |
| Table 3.39: | Gas-phase data for benzimidazoles with phenyl substituents binding with $\text{Zn}^{2+}$ .....              | 94 |

|             |   |     |
|-------------|---|-----|
| Table 3.40: | Gas-phase data for benzimidazoles with phenyl substituents binding with $\text{Ca}^{2+}$ .....          | 94  |
| Table 3.41: | Gas-phase data for atypical imidazoles binding with $\text{Zn}^{2+}$ .....                              | 96  |
| Table 3.42: | Gas-phase data for atypical imidazoles binding with $\text{Ca}^{2+}$ .....                              | 96  |
| Table 3.43: | Solvation data for imidazoles with only alkyl substituents binding with $\text{Zn}^{2+}$ .....          | 98  |
| Table 3.44: | Solvation data for imidazoles with only alkyl substituents binding with $\text{Ca}^{2+}$ .....          | 98  |
| Table 3.45: | Solvation data for imidazoles with nitrogen-containing substituents binding with $\text{Zn}^{2+}$ ..... | 101 |
| Table 3.46: | Solvation data for imidazoles with nitrogen-containing substituents binding with $\text{Ca}^{2+}$ ..... | 101 |
| Table 3.47: | Solvation data for imidazoles with oxygen-containing substituents binding with $\text{Zn}^{2+}$ .....   | 103 |
| Table 3.48: | Solvation data for imidazoles with oxygen-containing substituents binding with $\text{Ca}^{2+}$ .....   | 103 |
| Table 3.49: | Solvation data for imidazoles with sulfur-containing substituents binding with $\text{Zn}^{2+}$ .....   | 106 |
| Table 3.50: | Solvation data for imidazoles with sulfur-containing substituents binding with $\text{Ca}^{2+}$ .....   | 107 |
| Table 3.51: | Solvation data for imidazoles with phenyl substituents binding with $\text{Zn}^{2+}$ .....              | 110 |
| Table 3.52: | Solvation data for imidazoles with phenyl substituents binding with $\text{Ca}^{2+}$ .....              | 111 |
| Table 3.53: | Solvation data for imidazolidinones binding with $\text{Zn}^{2+}$ .....                                 | 113 |
| Table 3.54: | Solvation data for imidazolidinones binding with $\text{Ca}^{2+}$ .....                                 | 114 |
| Table 3.55: | Solvation data for benzimidazoles with only alkyl substituents binding with $\text{Zn}^{2+}$ .....      | 114 |
| Table 3.56: | Solvation data for benzimidazoles with only alkyl substituents binding with $\text{Ca}^{2+}$ .....      | 115 |

|             |  |     |
|-------------|--|-----|
| Table 3.57: | Solvation data for benzimidazoles with halide substituents binding with $Zn^{2+}$ .....              | 116 |
| Table 3.58: | Solvation data for benzimidazoles with halide substituents binding with $Ca^{2+}$ .....              | 116 |
| Table 3.59: | Solvation data for benzimidazoles with nitrogen-containing substituents binding with $Zn^{2+}$ ..... | 117 |
| Table 3.60: | Solvation data for benzimidazoles with nitrogen-containing substituents binding with $Ca^{2+}$ ..... | 117 |
| Table 3.61: | Solvation data for benzimidazoles with oxygen-containing substituents binding with $Zn^{2+}$ .....   | 118 |
| Table 3.62: | Solvation data for benzimidazoles with oxygen-containing substituents binding with $Ca^{2+}$ .....   | 119 |
| Table 3.63: | Solvation data for benzimidazoles with sulfur-containing substituents binding with $Zn^{2+}$ .....   | 120 |
| Table 3.64: | Solvation data for benzimidazoles with sulfur-containing substituents binding with $Ca^{2+}$ .....   | 120 |
| Table 3.65: | Solvation data for benzimidazoles with phenyl substituents binding with $Zn^{2+}$ .....              | 121 |
| Table 3.66: | Solvation data for benzimidazoles with phenyl substituents binding with $Ca^{2+}$ .....              | 121 |
| Table 3.67: | Solvation data for atypical imidazoles binding with $Zn^{2+}$ .....                                  | 122 |
| Table 3.68: | Solvation data for atypical imidazoles binding with $Ca^{2+}$ .....                                  | 122 |
| Table 4.1:  | Overview of the cations evaluated in this chapter.....   | 126 |
| Table 4.2:  | Gas-phase data for imidazoles binding with $Li^+$ .....  | 128 |
| Table 4.3:  | Gas-phase data for imidazoles binding with $Be^{2+}$ .....   | 129 |
| Table 4.4:  | Gas-phase data for imidazoles binding with $Na^+$ .....  | 130 |
| Table 4.5:  | Gas-phase data for imidazoles binding with $Mg^{2+}$ .....   | 131 |
| Table 4.6:  | Gas-phase data for imidazoles binding with $Al^{3+}$ .....   | 132 |
| Table 4.7:  | Gas-phase data for imidazoles binding with $K^+$ .....   | 133 |
| Table 4.8:  | Gas-phase data for imidazoles binding with $Cr^{2+}$ .....   | 134 |
| Table 4.9:  | Gas-phase data for imidazoles binding with $Cr^{3+}$ .....   | 135 |

|             |   |     |
|-------------|---|-----|
| Table 4.10: | Gas-phase data for imidazoles binding with $\text{Mn}^{2+}$ ..... | 136 |
| Table 4.11: | Gas-phase data for imidazoles binding with $\text{Mn}^{3+}$ ..... | 136 |
| Table 4.12: | Gas-phase data for imidazoles binding with $\text{Co}^{2+}$ ..... | 137 |
| Table 4.13: | Gas-phase data for imidazoles binding with $\text{Co}^{3+}$ ..... | 137 |
| Table 4.14: | Gas-phase data for imidazoles binding with $\text{Ni}^{2+}$ ..... | 138 |
| Table 4.15: | Gas-phase data for imidazoles binding with $\text{Cu}^{+}$ .....  | 139 |
| Table 4.16: | Gas-phase data for imidazoles binding with $\text{Cu}^{2+}$ ..... | 139 |
| Table 4.17: | Gas-phase data for imidazoles binding with $\text{Sr}^{2+}$ ..... | 140 |
| Table 4.18: | Gas-phase data for imidazoles binding with $\text{Pd}^{2+}$ ..... | 141 |
| Table 4.19: | Gas-phase data for imidazoles binding with $\text{Ag}^{+}$ .....  | 142 |
| Table 4.20: | Gas-phase data for imidazoles binding with $\text{Cd}^{2+}$ ..... | 143 |
| Table 4.21: | Gas-phase data for imidazoles binding with $\text{Sn}^{2+}$ ..... | 144 |
| Table 4.22: | Gas-phase data for imidazoles binding with $\text{Sn}^{4+}$ ..... | 144 |
| Table 4.23: | Gas-phase data for imidazoles binding with $\text{Ba}^{2+}$ ..... | 145 |
| Table 4.24: | Gas-phase data for imidazoles binding with $\text{Hg}^{2+}$ ..... | 146 |
| Table 4.25: | Gas-phase data for imidazoles binding with $\text{Pb}^{2+}$ ..... | 147 |

## LIST OF FIGURES

|             |  |    |
|-------------|--|----|
| Figure 1.1: | Illustrations depicting the changes that are accounted for in the first four terms of the potential energy equation for the CHARMM22 force field.....                      | 7  |
| Figure 1.2: | The first step in the Newton-Raphson Method.....   | 9  |
| Figure 1.3: | The Steepest Descent Method.....   | 10 |
| Figure 1.4: | Example of a potential energy surface with multiple minima.....  | 11 |
| Figure 1.5: | The NMDA receptor.....   | 14 |
| Figure 1.6: | Diagram of the ischemic focus and the surrounding ischemic penumbra.....   | 17 |
| Figure 1.7: | The imidazole functional group.....  | 22 |
| Figure 2.1: | (a) The protonated nitrogen in imidazole behaves like nitrogen in pyrrole.<br>(b) The unprotonated nitrogen in imidazole behaves like the nitrogen in pyridine.....        | 24 |
| Figure 2.2: | The zinc finger protein structural motif. The green sphere represents $Zn^{2+}$ . Note the presence of two cysteine residues and two histidine residues.....               | 31 |
| Figure 2.3: | EF hand structural motif. The purple sphere represents $Ca^{2+}$ . Note the presence of two aspartate residues and one glutamate residue.....                              | 32 |
| Figure 2.4: | The structure of carnosine, a dipeptide containing an imidazole ring, in its neutral form.....   | 34 |
| Figure 2.5: | Carnosine chelates iron ions to prevent the Fenton Reaction, which produces harmful reactive oxygen species.....   | 36 |
| Figure 2.6: | The complex formed as a result of a gas-phase molecular mechanics simulation of the interaction between carnosine and $Zn^{2+}$ .....                                      | 38 |
| Figure 2.7: | The complex formed as a result of a gas-phase molecular mechanics simulation of the interaction between carnosine and $Ca^{2+}$ .....                                      | 40 |
| Figure 2.8: | The complexes formed as a result of solvation molecular mechanics simulations of the interaction between carnosine and $Zn^{2+}$ (A) at N3 and (B) at the carboxylate..... | 42 |

|              |   |     |
|--------------|---|-----|
| Figure 2.9:  | The complexes formed as a result of solvation molecular mechanics simulations of the interaction between carnosine and $\text{Ca}^{2+}$ (A) at N3 and (B) at the carboxylate..... | 43  |
| Figure 3.1:  | Structures for imidazoles with only alkyl substituents.....   | 46  |
| Figure 3.2:  | Structures for imidazoles with halide substituents.....   | 50  |
| Figure 3.3:  | Structures for imidazoles with nitro substituents.....  | 52  |
| Figure 3.4:  | Charge distribution in a nitro group.....   | 53  |
| Figure 3.5:  | Nitro groups withdraw electron density by resonance.....  | 55  |
| Figure 3.6:  | Structures for imidazoles with amido and amino substituents.....  | 55  |
| Figure 3.7:  | Resonance structures of amido groups.....   | 57  |
| Figure 3.8:  | Structures for imidazoles with cyano substituents.....  | 58  |
| Figure 3.9:  | Structures for imidazoles with hydroxyl substituents.....   | 60  |
| Figure 3.10: | Structures for imidazoles with aldehyde and ketone substituents.....  | 62  |
| Figure 3.11: | Structures for imidazoles with carboxylic acid and ester substituents.....  | 65  |
| Figure 3.12: | Structures for imidazoles with sulfur-containing substituents.....  | 67  |
| Figure 3.13: | Imidazoline.....  | 68  |
| Figure 3.14: | Structures for imidazoles with phenyl substituents.....   | 73  |
| Figure 3.15: | Structures for imidazolidinones.....  | 77  |
| Figure 3.16: | Structure of imidazolidinethione.....   | 79  |
| Figure 3.17: | Benzimidazole.....  | 80  |
| Figure 3.18: | Structures for benzimidazoles with only alkyl substituents.....   | 81  |
| Figure 3.19: | Structures for benzimidazoles with halide substituents.....   | 83  |
| Figure 3.20: | Resonance of chloride in an aromatic ring.....  | 84  |
| Figure 3.21: | Structures for benzimidazoles with nitrogen-containing substituents.....  | 85  |
| Figure 3.22: | Structures for benzimidazoles with oxygen-containing substituents.....  | 88  |
| Figure 3.23: | Structures for benzimidazoles with sulfur-containing substituents.....  | 91  |
| Figure 3.24: | Structures for benzimidazoles with phenyl substituents.....   | 93  |
| Figure 3.25: | Structures for atypical imidazoles.....   | 95  |
| Figure 3.26: | The resulting system after a solution-phase simulation with molecule 041, $\text{Zn}^{2+}$ and $\text{Ca}^{2+}$ .....   | 109 |
| Figure 5.1:  | Apparatus for an <i>in vitro</i> study.....   | 150 |

## ABSTRACT

Computer-aided drug design is an exceptionally useful tool for screening a large number of potential drug molecules to evaluate their therapeutic potential. This technique is both effective and economical. Approximately 120 imidazole-containing molecules were computationally designed and evaluated using gas-phase and solution-phase simulations to assess their propensity for acting as a chelating agent with twenty-six biologically relevant cations. Of particular interest was their ability to chelate  $Zn^{2+}$  and  $Ca^{2+}$ , which play a key role in the degradation of neurons following an ischemic stroke. The ultimate goal was to design a small molecule that could be administered before a medical procedure that featured stroke as a possible side effect. In the event that a stroke occurred, the destruction of neurons caused by release of excess  $Ca^{2+}$  and  $Zn^{2+}$  would be diminished and the patient would maintain motor and cognitive function. Promising *in silico* results were obtained.

## LIST OF ABBREVIATIONS USED

|        |  |
|--------|--|
| AMPA   | 2-amino-3-(3-hydroxy-5-methyl-isoxazol-4-yl)propanoic acid |
| ATP    | Adenosine Triphosphate                                     |
| BBB    | Blood-Brain Barrier  |
| B-OA   | Born-Oppenheimer Approximation                             |
| CADD   | Computer-Aided Drug Design                                 |
| CHARMM | Chemistry at HARvard Macromolecular Mechanics              |
| HOMO   | Highest Occupied Molecular Orbital                         |
| HSAB   | Hard-Soft Acid-Base Theory                                 |
| LUMO   | Lowest Unoccupied Molecular Orbital                        |
| MOE    | Molecular Operating Environment                            |
| NMDA   | N-methyl-D-aspartic acid                                   |
| SAR    | Structure-Activity Relationship                            |
| USDA   | United States Department of Agriculture                    |

## **ACKNOWLEDGEMENTS**

I would like to thank my supervisor, Dr. Donald Weaver for his input and guidance in completing this thesis. His knowledge and support have been valuable assets throughout my time here.

I would also like to thank Dr. Autumn Meek for answering each and every one of my endless list of questions. Also, for teaching me to use the MOE computer program and giving advice when needed.

I would like to thank Cassandra Hawco for her patience and help.

I would like to thank all current and past members of the Weaver research group.

I would like to thank my family and friends for their love and support throughout my graduate degree.

# CHAPTER 1 – INTRODUCTION

Computational chemistry is consistently growing in its utility as a tool in the fields of medicinal chemistry and drug molecule design. The use of molecular dynamics, molecular mechanics and quantitative structure-activity relationships is becoming a more common practice as these techniques are refined and improved.

## *1.1 - Computer-Aided Design*

Designing novel drug molecules is one of the biggest challenges faced by the medicinal chemistry community today. The process of creating new therapeutics is academically challenging, financially expensive and time-consuming (Mandal, Mandal and Moudgil 2009). Consequently, research focused on developing new, less expensive, and faster methods of drug design is prevalent in the literature. One field, in particular, that is constantly being refined and improved is that of computer-aided drug design (CADD).

Traditional methods of drug discovery and development involve serendipity and trial and error. In some cases, scientists isolate and examine the activity of various natural products as potential therapeutics. For example, the mitotic inhibitor paclitaxel (marketed as Taxol) is used in cancer chemotherapy. It was discovered as a result of a plant screening operation organized by the National Cancer Institute in the United States. The institute commissioned USDA botanists to obtain samples from thousands of plants species in North America. One such plant was the Pacific Yew tree, which turned out to serve as the home for an endophytic fungus that synthesizes paclitaxel (Truelove 1999).

This is acceptable until the cost of the discovery is considered. Each screening test, whether useful or not, was expensive. High-throughput methods of screening are likewise expensive and time-consuming. From discovery to market, the process can cost hundreds of millions of dollars and take well over a decade. Considering the benefits to mankind and the excessive cost of drug discovery, a technique that makes any stage of the process more efficient would be a welcome addition to the drug design industry (Ooms 2000).

One effective and elegant solution to this problem is the use of virtual screening. This powerful approach allows a chemist to exploit state-of-the-art technologies to speed up the drug development process. It employs the use of a computer program (like Molecular Operating Environment or MOE) to make accurate predictions about interactions between a drug of interest and its target at the molecular level. The primary goal of this approach is to predict whether a given drug molecule is capable of binding to its target and, if so, to what extent. Programs like MOE use molecular mechanics or molecular dynamics to identify the lowest energy conformation of the small molecule to be tested for biological activity. The same techniques can then be used to model changes that occur in the target biomolecule after the drug binds to it. These methods will be discussed in detail later.

The aim of this thesis is to demonstrate the utility of CADD and its synergistic relationship with experimental medicinal chemistry. Setting aside the dramatic reduction in cost and time associated with the use of CADD, it also provides valuable insight into the physical and chemical properties and interactions in a complex system at the molecular level.

## ***1.2 - Molecular Modelling***

In molecular modelling, empirical molecular mechanics force fields are used to evaluate the activity and energy of molecules of interest. There are a variety of force fields at the disposal of the computational chemist. Some are used to assess a broad range of molecular systems, while others are tailored to a specific class of biomolecule (proteins, for example).

### **1.2.1 – Force Fields**

In molecular modelling, a force field is defined by the functional form and parameters used to calculate the potential energy of a molecular system. These functions and parameters are derived from both experimental work and advanced theoretical quantum mechanical calculations. Due to their empirical nature, there is not an exactly correct form for a force field. As such, force fields can be chosen based on how compatible they are with the molecular system a chemist is working with. For example, CHARMM22 is often used to model the interactions of proteins while CHARMM27 is used to model interactions of DNA, RNA and lipids. (Leach 2001)

Many force fields exist, but there are some characteristics that unify them. No matter which force field is being used, the terms of the force equations can be divided into two categories:

1. Terms that mathematically express bonding interactions. These terms describe deviations from equilibrium bond lengths and bond angles as well as torsions.
2. Terms that mathematically express non-bonding interactions. These include terms that describe the electrostatic and van der Waals energies of the system.

Simply put, the total potential energy of the molecular system ( $V_{\text{tot}}$ ) is equal to the sum of all bonding interactions ( $V_{\text{B}}$ ) and non-bonding interactions ( $V_{\text{NB}}$ ), as seen in (1) (Leach 2001).

$$V_{\text{Tot}} = V_{\text{B}} + V_{\text{NB}} \quad (1.1)$$

The bonding and non-bonding terms can further be broken down. The bonding term can be expressed as the sum of the energies caused by bond stretching ( $V_{\text{r}}$ ), bond angle bending ( $V_{\theta}$ ) and torsions ( $V_{\phi}$ ), as shown in (2). The non-bonding term can be expressed as the sum of the electrostatic energy and the van der Waals energy, as shown in (3) (Leach 2001).

$$V_{\text{B}} = V_{\text{r}} + V_{\theta} + V_{\phi} \quad (1.2)$$

$$V_{\text{NB}} = V_{\text{E}} + V_{\text{VDW}} \quad (1.3)$$

Depending on the force field, the composition and number of these terms may vary. The parameters that define each atom provide the various constants necessary to carry out the calculation of the total energy. Later in this thesis, the constants associated with the CHARMM22 force field will be discussed in detail. For now, suffice it to say that the terms of the force equation vary depending on atom types. Simple force fields assign all atoms of the same element the same atom type. In other words, when a simple force field is being used to evaluate a molecular interaction, all nitrogen atoms will be assessed using the same set of constants. This can lead to deviations from reality because a nitrogen atom in an amine group may not interact in the same way that a nitrogen atom in an amide group would. In more complex force fields (like CHARMM22), atom types are assigned to an element based on its local environment. For example, an amine

nitrogen atom would be assigned different constants than an amide nitrogen atom. (Leach 2001).

### 1.2.2 – The CHARMM22 Force Field and MOE

The software package used for this thesis is Molecular Operating Environment (MOE) by the Chemical Computing Group. MOE is a leading drug discovery software platform. It allows the user to visualize, model and simulate interactions at a molecular level. It is widely used by biologists, medicinal chemists and computational chemists in biotechnology, the pharmaceutical industry and in academic research (Mandal, Mandal and Moudgil 2009).

MOE is a program that is compatible with the CHARMM22 (Chemistry at HARvard Macromolecular Mechanics) force field. The CHARMM22 force field calculates the energy of a system using a potential energy function of the form (1.1). The bonding and non-bonding terms are as follows (Mackerell 1998):

$$V_{\text{Tot}} = V_r + V_\theta + V_\phi + V_\omega + V_U + V_{\text{VDW}} + V_E \quad (1.4)$$

The energy terms associated with bonding interactions are  $V_r$ ,  $V_\theta$ ,  $V_\phi$ , and  $V_\omega$ .  $V_r$  represents the energy associated with changes in bond length and is calculated using the following (Mackerell 1998):

$$V_r = \sum k_r (r-r_0)^2 \quad (1.5)$$

This term accounts for bond stretches.  $k_r$  is the bond force constant and  $r-r_0$  is the deviation from the equilibrium bond distance between the two atoms as seen in the top left diagram in Figure 1.1. Both the bond force constant and the equilibrium bond distance are selected based on the two atoms participating in the bond.

$$V_\theta = \sum k_\theta (\theta-\theta_0)^2 \quad (1.6)$$

The second term in the energy function considers bending and bond angles.  $k_\theta$  is the angle force constant and  $\theta-\theta_0$  is the deviation from equilibrium bond angles as seen in the bottom left diagram in Figure 1.1. Much like in the first term, the angle force constant and equilibrium bond angle are selected based on the three atoms that participate in the two bonds that created the angle. Both of the first two terms are variations of Hooke's Law and are treated as harmonic oscillators.

$$V_\phi = \sum k_\phi [1+\cos(n\phi-\delta)] \quad (1.7)$$

The third term concerns the torsion angles. As seen in the top right diagram in Figure 1.1, the torsional angle is the angle between atoms 1 and 4 of a four-atom chain whereby rotation occurs along the axis of the bond between atoms 2 and 3.  $k_\phi$  is the dihedral force constant,  $n$  is the multiplicity of the function (assigned automatically by CHARMM),  $\phi$  is the dihedral angle and  $\delta$  is the phase shift. Depending on the resource,  $\delta$  is sometimes written as  $\phi_0$ .

$$V_\omega = \sum k_\omega (\omega-\omega_0)^2 \quad (1.8)$$

The fourth term is exclusive to molecules with planar areas. It accounts for out-of-plane bending, as seen in the bottom right diagram in Figure 1.1. As in the first three terms,  $k_\omega$  is the associated force constant and  $\omega-\omega_0$  is the deviation from the equilibrium out-of-plane angle. Like the first two terms, this is a harmonic oscillator. The force constant and equilibrium value are selected based on the atoms present in the planar part of the molecule.

$$V_U = \sum k_U (U-U_0)^2 \quad (1.9)$$

The fifth term is the Urey-Bradley term, a cross-term that considers angle bending using 1,3 non-bonded interactions.  $k_U$  is the Urey-Bradley force constant and  $U-U_0$  is the

deviation from the equilibrium distance between the 1,3 atoms (i.e. atoms separated by one other atom). This term is also a harmonic oscillator. The force constant and equilibrium value are selected based on the atoms in question.

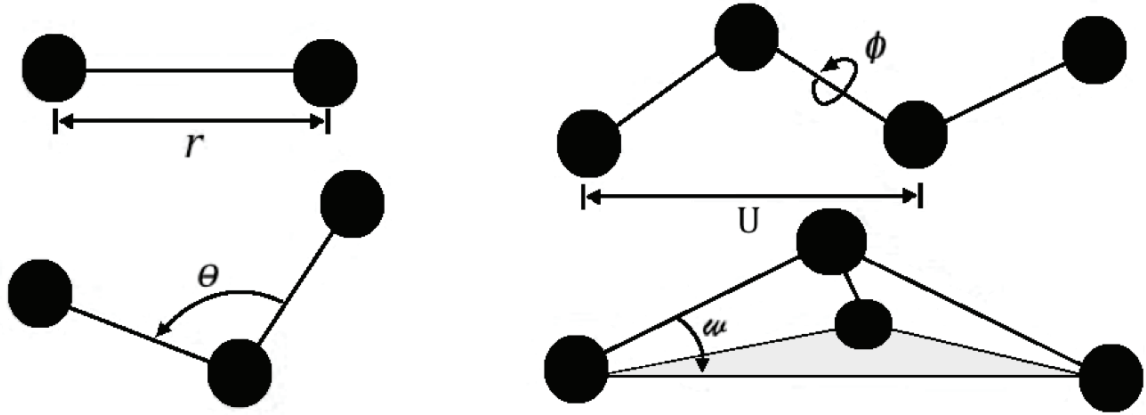


**Figure 1.1: Illustrations depicting the changes that are accounted for in the first four terms of the potential energy equation for the CHARMM22 force field.**

The final two terms consider non-bonding interactions between pairs of atoms,  $i$  and  $j$ , separated by at least three bonds. They are as follows:

$$V_{VDW} = \sum \epsilon_{i,j} [(R_{\min I,j} / d_{ij})^{12} - (R_{\min I,j} / d_{ij})^6] \quad (1.10)$$

The sixth term accounts for van der Waals interactions and is calculated using the 12-6 Lennard-Jones potential.  $\epsilon$  is the Lennard-Jones well depth (an atom-specific value),  $R_{\min}$  is the distance from the Lennard-Jones minimum and  $d$  is the distance between atoms  $i$  and  $j$ .

$$V_E = \sum q_i q_j / \epsilon_1 d_{ij} \quad (1.11)$$

The final term describes electrostatic interactions with a Coulombic potential. In this term,  $d$  represents the distance between atoms  $i$  and  $j$ ,  $q_i$  is the partial atomic charge of atom  $i$  (similar for  $q_j$ ) and  $\epsilon_1$  is the effective dielectric constant (MacKerell *et al* 1998).

Taken as a whole, equation 1.4 can seem daunting and overwhelming. However, when broken down into its component terms, it becomes a simple problem of classical mechanics. In general, molecular mechanics simulations all share three unifying characteristics. First, individual atoms are treated as single, distinct particles. Second, each atom is assigned a radius, polarizability and constant net charge. And third, bonds are treated as springs (Mackerell 1998).

### **1.2.3 – Energy Minimization Algorithms**

The computation of the potential energy of a molecule is an extremely complex exercise (Leach 2001). The energy will change if the positions of the atoms change in space. It is then possible to describe the energy of a molecular system using a potential energy surface, which depends on the nuclear coordinates of the atoms in the molecule. The easiest way to visualize this is to imagine a landscape of rolling hills, where moving along the surface of the hill in a North to South and East to West direction are independent variables and the height of the hill is the potential energy associated with a particular set of coordinates. The ultimate objective of an energy minimization algorithm is to find the lowest point of the deepest valley, which corresponds to the lowest-energy conformation of the system. There are many algorithms for minimization available to a computational chemist. It is important to choose a technique that is compatible with the system being studied. Some minimization techniques (Newton Raphson for example) are designed for use with small systems that contain 200 atoms or fewer, while others (Steepest Descent for example) are designed for use with large systems (Leach 2001).

### 1.2.3.1 – The Newton-Raphson Method

The Newton-Raphson Method of energy minimization can be traced back almost 400 years to Isaac Newton and Joseph Raphson. Its elegance is only exceeded by its simplicity. For clarity, the one-dimensional case of the algorithm will be described. Let the potential energy function be  $V_{\text{Tot}}(x)$ , where  $x$  represents a variable that determines the value of the potential energy function. Let  $V_{\text{Tot}}'(x)$  be the first derivative of the potential energy function and let  $(x_0, V_{\text{Tot}}(x_0))$  be an arbitrary point on the potential energy curve (Figure 1.2).

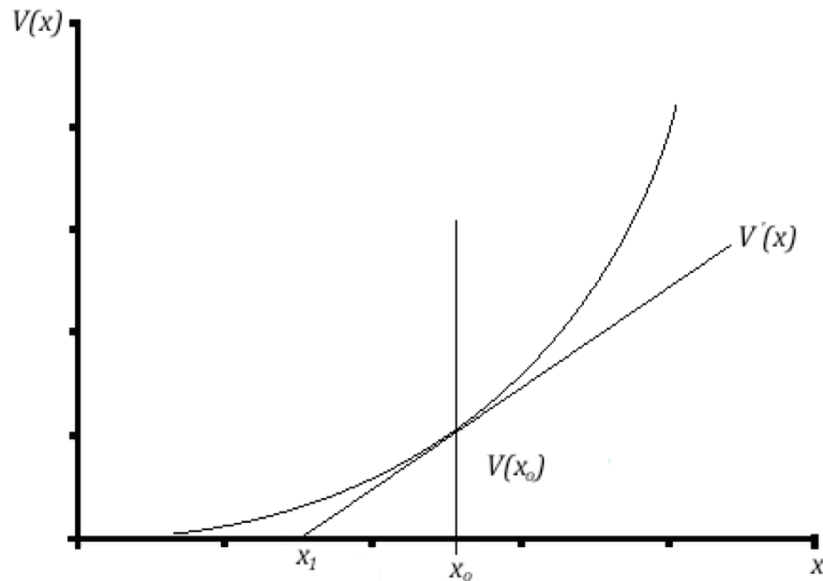


**Figure 1.2: The first step in the Newton-Raphson Method.**

Notice that the intersection of the slope and the  $x$ -axis at  $x_1$  is closer to the minimum value of the function than  $x_0$ . Repeating this process  $n$  times, the point  $x_n$  is reached, which is arbitrarily close to the minimum value of the function. The larger the value of  $n$ , the closer the value will be to the true minimum (Rogers 2003).

### 1.2.3.2 – The Steepest Descent Method

This steepest descent method is effective when the starting conformation of the molecule is in a high-energy state. The steepest descent algorithm is a first order minimization technique that involves making small, step-wise changes to the nuclear coordinates and evaluating the energy function at every step. This method is more gradual than the Newton-Raphson method, which leaps down the potential energy surface quickly. This is of particular importance when dealing with large systems (Leach 2001).

Once again, an arbitrary point on the potential energy surface is chosen as a starting point. The program then identifies the gradient of the potential energy surface at that point. The gradient is the direction of steepest descent. Next, the necessary conformational changes are made to move along the gradient, deeper into the potential energy well (Figure 1.3). Each successive step is orthogonal to the last (Leach 2001).

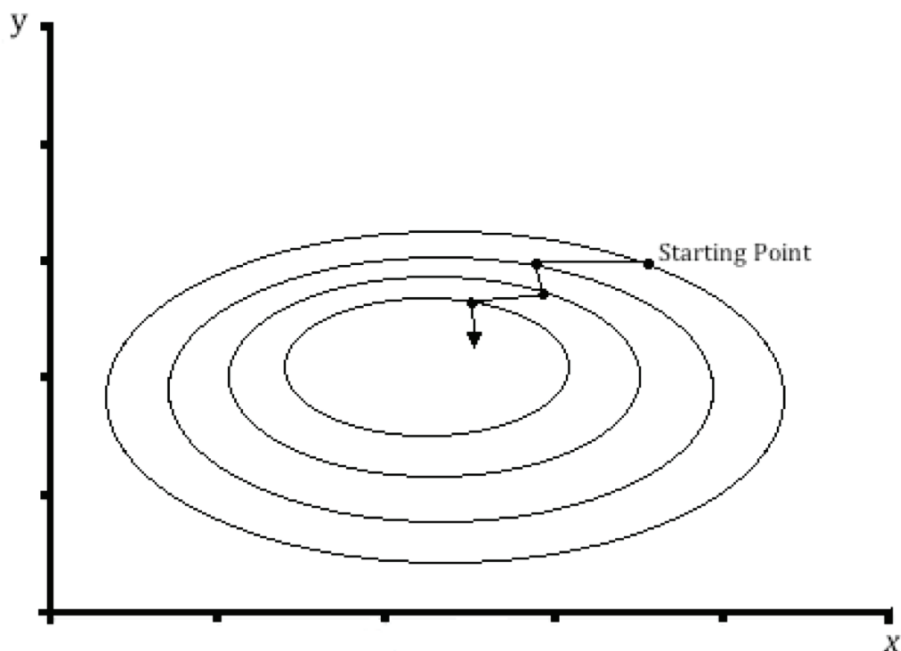


**Figure 1.3: The Steepest Descent Method.**

The question then becomes: how large should the movements along the gradient be? The most common method is to take a line search approach. Essentially, the line search approach brackets a minimum point on the gradient line, where the minimum point is lower in energy than the two bracket points. Next, the distance between the bracketing points is reduced at each iteration until the minimum is reached (Leach 2001).

### *1.2.3.3 – Issues With Energy Minimization Techniques*

Two major problems can arise when using energy minimization techniques. First, if more than one minimum exists on the potential energy surface (Figure 1.4), the algorithm may get ‘stuck’ in one of the valleys (a local minimum). When this occurs, the true, global minimum may not be found. One technique used to combat this problem is to impose a large change to the system instead of the usual small perturbations. This large change corresponds to a large leap across the potential energy surface. Ideally, the leap would land in the energy well that contains the global minimum (Leach 2001).

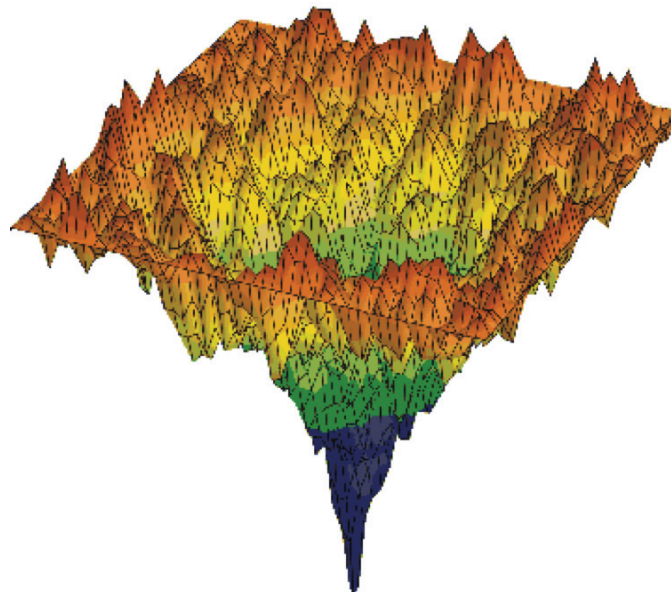


**Figure 1.4: Example of a potential energy surface with multiple minima.**

Second, sometimes the conformation that a drug molecule takes in reality does not correspond to the lowest energy conformation. In other words, the conformation that results in the minimum of the potential energy surface may not correspond to the active form of the molecular system in an organism (Leach 2001).

### ***1.3 – Stroke and the Role of $Ca^{2+}$ and $Zn^{2+}$***

In this section, an overview of the disease state of interest for this study (ischemic stroke) will be given. Cerebral stroke is the most common cause of disability resulting in loss of physical independence in the world. It is the third leading cause of death in the North America, after heart disease and cancer. Consequently, it is a very well researched disease state and many approaches to alleviating its symptoms are being pursued by medicinal chemists worldwide (Aggarwal, Aggarwal, Khatak and Khatak 2010).

Stroke is the sudden interruption of blood supply to a part of the brain that leads to a decrease in neurologic function. There are two types of stroke: haemorrhagic and ischemic. A haemorrhagic stroke occurs when a blood vessel in the brain tears or breaks. Diminished cerebral blood flow to the areas of the brain beyond the break causes cells in this region to not receive the necessary oxygen and glucose to survive (Aggarwal, Aggarwal, Khatak and Khatak 2010). The focus of this thesis will be the second type: ischemic stroke. Approximately 87% of strokes are a result of ischemia (Li and Zhang 2012). An ischemic stroke occurs when a blood vessel is obstructed or blocked. Similar to the haemorrhagic stroke, neurons beyond the point of the blockage do not receive the necessary oxygen and glucose to sustain ATP production and begin to die (Aggarwal, Aggarwal, Khatak and Khatak 2010). Ischemic stroke will be discussed in detail shortly.

This section will include a summary of the series of chemical reactions that take place in the brain following a stroke event, known as the ischemic cascade. Next, the unique approach taken to tackle this problem will be presented. Finally, a comprehensive look at the target species: zinc and calcium ions in the brain, will be provided.

### **1.3.1 – The Ischemic Cascade**

Ischemic stroke occurs when an artery is occluded and blood flow to the neurons beyond the blockage is decreased or cut off completely. There are two broad categories of ischemic stroke: thrombotic and embolic. A thrombotic stroke is caused by the formation of a blood clot inside an artery. This occurs most commonly in the middle cerebral artery, but may also occur in the internal carotid artery, proximal and intracranial vertebral arteries or the basilar artery. Embolic strokes happen when a clot formed elsewhere in the body breaks away from the arterial wall, travels to another blood vessel and causes a blockage (Aggarwal, Aggarwal, Khatak and Khatak 2010).

The ischemic cascade is the series of biochemical reactions that takes place following the interruption of blood flow to a tissue. Ischemia refers to a shortage of oxygen and glucose required for the production of adenosine triphosphate (ATP). When a cerebral blood vessel is obstructed by a thrombus or an embolus, cerebral blood flow to neurons surrounding the clot is reduced or interrupted entirely. As a result, the supply of oxygen to these neurons is depleted and the cells are forced to switch to anaerobic metabolism. Lactic acid, one of the major by-products of anaerobic metabolism, accumulates and lowers the pH (Aggarwal, Aggarwal, Khatak and Khatak 2010). Sources have reported that the pH can drop to as low as 6.3-6.7 in the regions of ischemia (Orlowski, Chappell, Sub Park, Grau and Payne 2011). This causes mitochondrial

activity to decrease, resulting in a marked decrease in production of ATP. Many ion pumps in the neuronal membrane require ATP to move ions against their concentration gradient from the intracellular space into the bloodstream.  $\text{Ca}^{2+}$ - $\text{H}^+$  ATPase and the  $\text{Ca}^{2+}$ - $\text{Na}^+$  antiporter are two such ion pumps. Normally, both of these transporters move  $\text{Ca}^{2+}$  out of the cell. However, in the absence of ATP, the action of the ion pumps is interrupted and the neuron is not able to remove  $\text{Ca}^{2+}$  from the cytosol. There is a concurrent influx of  $\text{Na}^+$  and  $\text{Cl}^-$  and efflux of  $\text{K}^+$ . The result of this ion movement is a net depolarization of the neuron. In a state of depolarization, neurotransmitters (glutamate in particular) are released. Glutamate then acts on two of its receptors, NMDA (Figure 1.5) and AMPA. When activated, both the NMDA and AMPA receptors open an ion channel that allows for  $\text{Ca}^{2+}$  to enter the cell. This event further depolarizes the cell and glutamate release is further increased. This part of the cascade is known as excitotoxicity (Aggarwal and Khatak 2010).

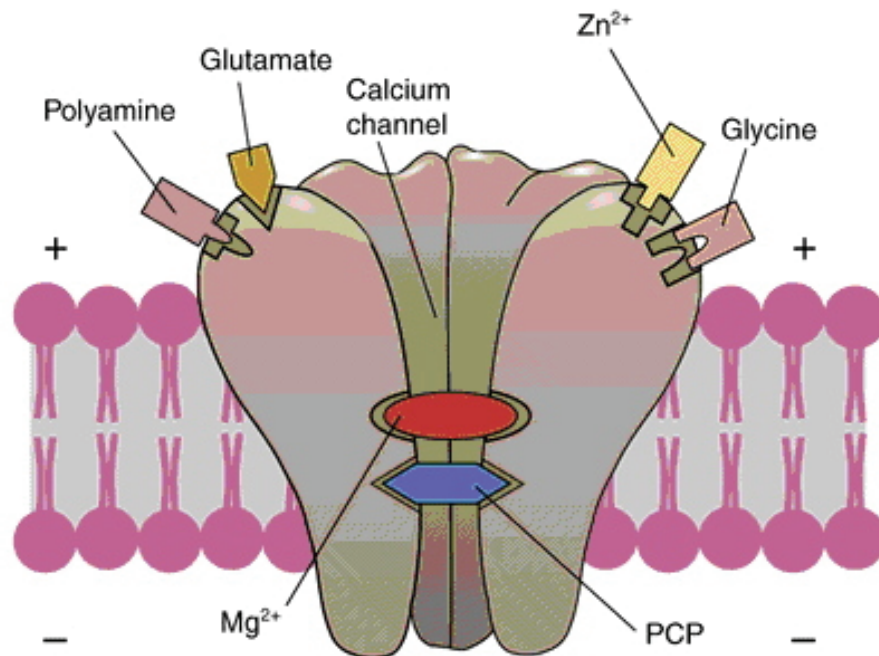


**Figure 1.5: The NMDA receptor (Rang, Dale and Ritter 2001).**

### **1.3.2 – The Role of Ca<sup>2+</sup>**

At this point, Ca<sup>2+</sup> is present in the neuron in great excess and exerts a number of detrimental effects on the cell. The mitochondrion has a very delicate relationship with calcium ions. In the correct amount, Ca<sup>2+</sup> plays an important role in the production of ATP. However, when excess Ca<sup>2+</sup> moves into the mitochondrion, it stimulates a sequence of reactions that ultimately lead to apoptosis (programmed cell death) and necrosis (Aggarwal and Khatak 2010).

Ca<sup>2+</sup> influx within a mitochondrion leads to the formation of reactive oxygen species, producing a state of oxidative stress in the neuron. Neuronal nitric oxide synthase (nNOS) is a Ca<sup>2+</sup> dependent enzyme that causes the formation of toxic peroxynitrite, a potent reactive oxygen species. Ca<sup>2+</sup> influx causes inflammatory mediators to be activated, leading to edema (swelling). Swelling increases pressure in the brain and can cause further injury (Aggarwal and Khatak 2010).

It is known that Ca<sup>2+</sup> plays a central role in the events of the ischemic cascade for decades (Li and Zhang 2012). It is intuitive to a medicinal chemist to view the Ca<sup>2+</sup> ion as a potential target for a drug molecule.

### **1.3.3 – The Role of Zn<sup>2+</sup>**

Recent research indicates that Ca<sup>2+</sup> is not the only cation that has a profound effect on ischemic neuronal degradation. In fact, it may not even be the primary player in the cascade. It has been proposed that toxic elevations in levels of Ca<sup>2+</sup> may, in part or entirely, be induced by Zn<sup>2+</sup> present in the neuronal cytosol (Dyck and Kasso 2007).

Like Ca<sup>2+</sup>, Zn<sup>2+</sup> also plays an important role in the normal functioning of the brain when present in the right concentration. Also like Ca<sup>2+</sup>, an excess of zinc ions in the

cytosol can wreak havoc on ion homeostasis. In the brain,  $Zn^{2+}$  is stored in synaptic vesicles with glutamate (Dyck and Kasso 2007). As mentioned, the influx of  $Ca^{2+}$  and the associated depolarization of the neuron induce the release of glutamate from synaptic vesicles.  $Zn^{2+}$  that was stored in those same vesicles is also released. Once in the cytosol,  $Zn^{2+}$  elicits a number of responses. As seen in Figure 1.5,  $Zn^{2+}$  can bind to a modulatory site on the NMDA receptor. This interaction alters the conformation of the receptor, making it more permeable to  $Ca^{2+}$ . Similarly,  $Zn^{2+}$  can also bind to an allosteric site on the AMPA receptor. This interaction makes the ion channel more permeable to both  $Ca^{2+}$  and  $Zn^{2+}$ . Once in the cell,  $Zn^{2+}$  has a toxic effect on mitochondria and is also involved in the production of reactive oxygen species, ultimately contributing to neuronal cell death (Dyck and Galasso 2007).

#### **1.3.4 – The Ischemic Penumbra**

Neuronal degradation due to ischemia starts as an isolated event. The starting point is known as the ischemic focus. As ischemia persists, the damage branches out from the ischemic focus until phagocytic cells engulf and destroy the damaged neurons to arrest the ischemic cascade and prevent further damage. The area surrounding the ischemic focus that is at risk is known as the ischemic penumbra (Figure 1.6) (Bogousslavsky and Fisher 2000). From a clinical perspective, researchers look at the ischemic penumbra as an area of potentially reversible neuronal damage. The ischemic penumbra is characterized by reduced cerebral blood flow and a decrease in aerobic metabolism. As the cells in the ischemic focus die, their membranes are broken down by phospholipases. As the membrane disappears, the contents of the cell are released into the extracellular fluid. The toxins that destroyed the first cell can then migrate to other,

nearby cells and destroy them. This causes a rippling effect whereby the ischemic penumbra expands outward from the ischemic focus.

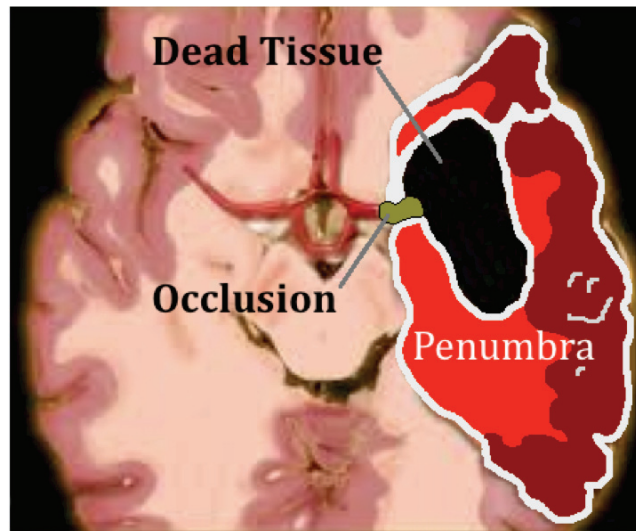


**Figure 1.6: Diagram of the ischemic focus and the surrounding ischemic penumbra (von Kummer 1997).**

The ischemic penumbra evolves at different rates in each patient. It depends on a number of factors including the extent of the vascular blockage and the patient's age. The period of time after the onset of ischemia in which the damage in the ischemic penumbra is reversible is known as the therapeutic time window. The variation in the rate at which the penumbra evolves from patient to patient makes it difficult to create a therapeutic that can be administered after the ischemic event and still be effective (von Kummer 1997)).

### **1.3.5 – A Unique Approach**

Under normal circumstances, it is difficult to predict the onset of a stroke. There are several risk factors for stroke including high blood pressure, diabetes, smoking, obesity and old age, but none of these are definitive indicators that a stroke is imminent (Aggarwal, Aggarwal, Khatak and Khatak 2010). Having said that, there are a number of medical procedures and surgeries (coronary artery bypass surgery for example) in which

stroke is a fairly common side effect (Selnes, Gottesman, Grega, Baumgartner, Zeger and McKhann 2012). A drug molecule that could be administered prior to these procedures as a protective measure against stroke would be an extremely valuable discovery. The ultimate goal is to abate the neuronal degradation associated with ischemia. If the ischemic cascade can be interrupted, then the evolution of the ischemic penumbra would be terminated and neurons would be saved (von Kummer 1997).

The target for such a drug could be any of the species involved in the ischemic cascade. As indicated earlier,  $\text{Ca}^{2+}$  is one of the primary players in the ischemic cascade. The approach of chelating  $\text{Ca}^{2+}$  has been attempted with only modest success.  $\text{Zn}^{2+}$  is the major inducer of  $\text{Ca}^{2+}$  influx in the neuron. Conveniently, both of these are divalent metal cations. In this study, a strategy was devised to design a drug molecule that is able to chelate both  $\text{Ca}^{2+}$  and  $\text{Zn}^{2+}$  in an effort to disrupt the ischemic cascade (discussed in chapter 2).

## ***1.4 – Defining a Drug Molecule***

In order to fully appreciate the complexity of the drug design process, particularly for drugs that must enter the brain to act on their target receptor, it is important investigate what physical and chemical properties make a drug molecule bioavailable.

### **1.4.1 – Properties of Drug Molecules**

Drugs can be administered in a number of different ways, each with its own benefits and associated challenges. For example, drugs that are given orally must survive the acidic environment of the stomach before they can be absorbed into the bloodstream in the small intestine. This is why drugs that contain an ester in the pharmacophore (the

part of the drug molecule that interacts with the target receptor) are not given orally. The acidic environment of the stomach would hydrolyze the ester to produce a carboxylic acid, rendering the drug obsolete. Instead, these types of drugs can be administered intravenously to avoid hydrolysis and skip the absorption step in the small intestine. The functional groups and geometric arrangement of a drug molecule affect the way it moves around the body and the way it interacts with its target receptor. The chemical and physical properties of a drug molecule are defined by its atomic makeup (i.e. the functional groups present) (Nogrady and Weaver 2005).

Arguably the most important feature of a drug molecule is specificity. A perfect drug molecule is capable of moving freely about the body and exists in a conformation such that it will only react with the desired target receptor. When a drug molecule is flexible, it may interact with other receptors in the body, leading to potential toxic effects (Nogrady and Weaver 2005).

As previously mentioned, the pharmacophore is the region of the drug molecule that interacts with the target receptor. It follows that relatively reactive functional groups are typically found in the pharmacophore. Conversely, structural framework of the drug is usually made up of chemically inert groups (i.e. a hydrocarbon chain). It is also advantageous to have a rigid framework to minimize conformational changes and increase specificity for the desired target (Nogrady and Weaver 2005).

It is also important that a drug molecule be capable of travelling through the body to its target receptor. A drug molecule must be capable of travelling through the hydrophilic and lipophilic regions of the body on its way to its final destination. This presents a particularly difficult challenge when designing novel drugs whose targets are

in the brain. In order for a drug molecule to access its receptor in the brain, it must traverse the blood-brain barrier (BBB). The BBB is composed of several lipid bilayers, therefore drugs must be lipophilic enough to pass through them. On the other hand, drugs must also be hydrophobic to dissolve in the aqueous environment of the blood. Consequently, a fine balance must be achieved between hydrophilicity and lipophilicity to gain access to the brain (Nogrady and Weaver 2005).

### **1.4.2 - Lipinski's Rule of Five**

The previous section states that there are a number of fairly stringent qualities that a drug molecule must have to be effective. In 1997, Christopher A. Lipinski noticed a trend in the pharmaceutical industry. He noticed that the majority of drug molecules were small and slightly lipophilic. Later, he developed a set of guidelines known as the Rule of Five: a sort of instructional manual for medicinal chemists. The rules are as follows:

1. A drug molecule should have a molecular weight of less than 500 g/mol, as it needs to be small enough to travel throughout the body (Lipinski, Lombardo, Dominy and Feeny 2001).
2. A drug molecule should have a logP value of less than 5, where logP is the logarithm of the octanol-water partition coefficient (1.13) (Lipinski, Lombardo, Dominy and Feeny 2001).

$$\log P = \log( [\text{Solute}]_{\text{oct}} / [\text{Solute}]_{\text{water}} ) \quad (1.13)$$

3. A drug molecule should have no more than five hydrogen bonding donors (i.e. amines, alcohols, etc.) (Lipinski, Lombardo, Dominy and Feeny 2001).

4. A drug molecule should have no more than ten hydrogen bond acceptors (i.e. functional groups containing C, N, O, F) (Lipinski, Lombardo, Dominy and Feeny 2001).
5. There are exceptions to the above rules in the event that the drug molecule is analogous to a natural molecule that is actively transported across lipid membranes in the body. Most drugs travel by passive diffusion, but rules 1-4 can be relaxed for molecules of this type (Lipinski, Lombardo, Dominy and Feeny 2001).

Rule one is fairly intuitive: the smaller the molecule, the more likely it will be able to diffuse across the lipid membranes of the body. Rule two is a guide to achieving the required balance between hydrophilicity and lipophilicity. Rules three and four are a preventative measure for rapid drug excretion. Highly polar molecules are eliminated from the body very quickly by the kidneys. As such, drugs that violate rules four and five are likely to have a short half-life and may never reach their target receptor.

When Lipinski was creating this set of guidelines, he was making observations about all types of drugs. It should be noted that drugs that must cross the BBB have a more stringent set of guidelines. For optimal BBB penetration, drug molecules should have a molecular weight that does not exceed 450 g/mol. A lower molecular weight allows for a better chance of the drug passively diffusing across the BBB. Secondly, neurological drugs should have a logP value between 1.5 and 3.0. This range corresponds to a class of drugs that are just hydrophilic enough to travel in the blood to the brain and just lipophilic enough to pass through the BBB. Thirdly, the molecule should contain even fewer hydrogen donors and acceptors (no more than three). Finally,

neurological drugs should not have a net charge because it becomes even more difficult to traverse the BBB.

The challenge that a neurological medicinal chemist faces is a considerable one. The strict guidelines and set of chemical properties that a molecule must have to permeate the BBB make neurological drug design a complex puzzle. For those willing to meet the challenge, the rewards are worth it.

### ***1.5 – Research Goals***

The ultimate goal of my this thesis was to design a novel drug molecule that has the ability to cross the BBB, form a complex with both  $\text{Ca}^{2+}$  and  $\text{Zn}^{2+}$ , and subsequently remove these two potentially neurotoxic cations from the central nervous system to be metabolized and/or excreted. As mentioned, attempts have been made to attack  $\text{Ca}^{2+}$  as a potential drug target. The approach of removing  $\text{Zn}^{2+}$ , one of the primary regulators of intracellular levels of  $\text{Ca}^{2+}$ , and  $\text{Ca}^{2+}$  itself simultaneously has never been tried before.

This thesis will focus on one particular class of molecules as a potential chelating agent for both  $\text{Zn}^{2+}$  and  $\text{Ca}^{2+}$ : imidazoles. Imidazoles are molecules that contain a five-membered heterocycle as seen in Figure 1.7 (Note the numbering scheme, as it will be referenced numerous times in the remainder of this thesis).

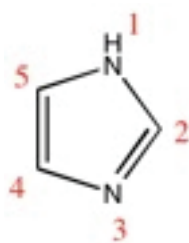


**Figure 1.7: The imidazole functional group.**

In Chapter 2 provides an overview of the physical and chemical properties that make imidazoles an excellent candidate for this research. Next, the computational methods used to calculate the potential energy of the molecular systems being studied will be summarized. This chapter will conclude with a case study of L-carnosine (Figure 2.4), an imidazole-containing dipeptide that has been investigated as a potential therapeutic for stroke.

Chapter 3 will analyze and discuss the results that have been gathered during this research. The interactions of approximately 120 imidazole-containing molecules with both  $Zn^{2+}$  and  $Ca^{2+}$  were simulated *in silico*. Each molecule will be presented in turn and their potential for use as a therapeutic for ischemic neuronal degradation will be discussed.

Chapter 4 will shift the focus away from  $Zn^{2+}$  and  $Ca^{2+}$ . For thoroughness, simulations of the interactions of the same 120 imidazole-containing molecules were performed with twenty-four other biologically relevant (i.e. present in the human body) cations. These include:  $Li^+$ ,  $Be^{2+}$ ,  $Na^+$ ,  $Mg^{2+}$ ,  $Al^{3+}$ ,  $K^+$ ,  $Cr^{2+}$ ,  $Cr^{3+}$ ,  $Mn^{2+}$ ,  $Mn^{3+}$ ,  $Co^{2+}$ ,  $Co^{3+}$ ,  $Ni^{2+}$ ,  $Cu^+$ ,  $Cu^{2+}$ ,  $Sr^{2+}$ ,  $Pd^{2+}$ ,  $Ag^+$ ,  $Cd^{2+}$ ,  $Sn^{2+}$ ,  $Sn^{4+}$ ,  $Ba^{2+}$ ,  $Hg^{2+}$  and  $Pb^{2+}$ . Each ion will be discussed in turn and the results of the simulations will be analyzed.

Chapter 5 will offer concluding remarks, a brief look at ongoing experimental studies that are being performed in collaboration with other members of the Weaver group, and a proposal of future experimental work that could be done to complement the computational data that has been gathered.

## CHAPTER 2 - CARNOSINE

### 2.1 – Imidazoles

For this thesis, imidazoles were evaluated for their ability to chelate both  $Zn^{2+}$  and  $Ca^{2+}$ . This proved to be challenging because the ions in question are quite different from one another in terms of their chemistry.

#### 2.1.1 – Physical and Chemical Properties of Imidazoles

Imidazoles are a class of molecules that contain a five-membered aromatic heterocycle called the imidazole ring. They are highly polar and, consequently, readily soluble in water. As per the definition of aromaticity, all atoms in the heterocycle are  $sp^2$  hybridized, the molecule is planar, and contains a Hückel's number of  $\pi$ -electrons (6). Four of the  $\pi$ -electrons reside in the double bonds and the other two reside in the p atomic orbital on the protonated, pyrrole-type nitrogen (N1) (2.1a). Imidazoles are amphoteric and can behave as both an acid and a base. For the purpose of this thesis, the basic properties of imidazole were used to chelate  $Zn^{2+}$  and  $Ca^{2+}$ , which are both Lewis acids. When acting as a base, the  $pK_a$  of imidazole is approximately 7. The lone pair on N3 does not participate in the aromaticity of the molecule and is able to behave as a base, much like the lone pair in pyridine (Figure 2.1b) (Bhatnagar, Sharma and Kumar 2011).

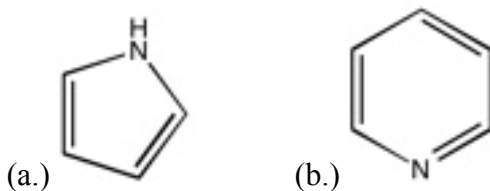


**Figure 2.1: (a) The protonated nitrogen in imidazole behaves like nitrogen in pyrrole. (b) The unprotonated nitrogen in imidazole behaves like the nitrogen in pyridine.**

### **2.1.2 – Imidazoles as Drug Molecules**

Imidazole has a molecular weight of 68 g/mol. This small size affords a computational chemist a lot of opportunity to explore a variety of possible hydrocarbon frameworks because neurological drugs can be up to 450 g/mol.

Imidazole rings are present in a number of endogenous molecules in the human body. The most obvious example of this is the amino acid side chain of histidine. Histidine readily crosses the BBB and is very common in the metal binding sites of metalloproteins. Histamine, a hormone involved in local immune responses, also contains an imidazole ring (Sakurai, Sakurai, Watanabe and Yanai 2009).

The presence of imidazole rings in endogenous molecules is very encouraging, because it means that the body is less likely to eliminate other molecules containing the same functionality. Also, the fact that histidine is able to penetrate the BBB with relative ease suggests that other imidazoles may be able to act as a mimic of histidine and traverse the BBB as well (Sakurai, Sakurai, Watanabe and Yanai 2009).

In fact, there are many examples of drugs that are currently on the market that contain imidazole rings in their pharmacophore. Imidazoles are commonly used as anti-inflammatory agents, anti-fungal agents (miconazole, ketoconazole, clotrimazole), anti-cancer agents, and much more. This bodes well as a drug design platform.

### **2.1.3 – Hard-Soft Acid-Base Theory**

Hard-Soft Acid-Base (HSAB) theory is widely used in chemistry (especially transition metal chemistry) to explain compound stability and reaction pathways. Chemical species are assigned hardness and softness based on a number of physical and

chemical properties. They are also distinguished as acids and bases based on their ability to donate or accept electron pairs.

Hard acids and bases typically have small radii, high oxidation states and very low polarizability. Hard bases tend to have a high electronegativity and a low-energy highest-occupied molecular orbital (HOMO). Contrarily, hard acids have a lowest-unoccupied molecular orbital (LUMO) of relatively high energy. In hard acids and bases, the HOMO and LUMO have a large gap between them (compared to soft acids and bases). This explains the low polarizability of hard species. Interactions between hard acids and bases are primarily ionic in nature and are dependent on the positive and negative charges on the acid and base (Pearson 1968).

Soft acids and bases typically have large radii, low or zero oxidation state and are highly polarizable. They have low electronegativity. Soft bases have a high-energy HOMO and soft acids have a low-energy LUMO. The gap between the frontier orbitals is smaller in soft species. This explains the high polarizability of soft acids and bases. Interactions between soft acids and bases tend to be covalent in nature and depend on the energies of the participating frontier molecular orbitals (Pearson 1968).

Mathematically, chemical hardness is proportional to the difference between the ionization energy and the electron affinity of the species being studied (Equation 2.1).

$$\eta_M = \frac{1}{2} (IE - EA) \quad (2.1)$$

The larger the gap between the ionization energy and electron affinity, the harder the species is. In general, hard acids tend to form adducts with hard bases and, similarly, soft acids tend to form adducts with soft bases (Pearson 1968).

## 2.2 – The Method

The challenge of this research was the fact that the  $\text{Ca}^{2+}$  and  $\text{Zn}^{2+}$  cations are physically and chemically dissimilar. The ultimate goal of finding a molecule to chelate both cations proved to be a challenge. As indicated in Table 2.1,  $\text{Ca}^{2+}$  is a hard acid and  $\text{Zn}^{2+}$  is an intermediate acid (Dyck and Kasso 2007).

**Table 2.1: A table of hard and soft Lewis acids and bases.**

|              | Acids   | Bases  |
|--------------|---|--|
| Hard         | $\text{H}^+$ , $\text{Li}^+$ , $\text{Na}^+$ , $\text{K}^+$ , $\text{Mg}^{2+}$ , $\text{Ca}^{2+}$ , $\text{Mn}^{2+}$<br>$\text{Al}^{3+}$ , $\text{Ln}^{3+}$ ,<br>$\text{Cr}^{3+}$ , $\text{Co}^{3+}$ , $\text{Fe}^{3+}$ , $\text{VO}^{2+}$ , $\text{MoO}^{3+}$ ,<br>$\text{SO}_3$ , $\text{CO}_2$ | $\text{H}_2\text{O}$ , $\text{ROH}$ , $\text{NH}_3$ , $\text{RNH}_2$<br>$\text{RCO}_2^-$ , $\text{Cl}^-$ , $\text{F}^-$<br>$\text{PO}_4^{3-}$ , $\text{HPO}_4^{2-}$ , $\text{H}_2\text{PO}_4^-$ , $\text{SO}_4^{2-}$ |
| Intermediate | $\text{Fe}^{2+}$ , $\text{Co}^{2+}$ , $\text{Ni}^{2+}$ , $\text{Cu}^{2+}$ , $\text{Zn}^{2+}$<br>$\text{Pb}^{2+}$ , $\text{Sn}^{2+}$ , $\text{SO}_2$ , $\text{NO}^+$ , $\text{Ru}^{2+}$  | Imidazole, pyridine  |
| Soft         | $\text{Cu}^+$ , $\text{Ag}^+$ , $\text{Au}^+$ , $\text{Tl}^+$ , $\text{Hg}^+$<br>$\text{Cd}^{2+}$ , $\text{Pd}^{2+}$ , $\text{Pt}^{2+}$ , $\text{Hg}^{2+}$  | $\text{RSH}$ , $\text{R}_2\text{S}$<br>$\text{CN}^-$ , $\text{I}^-$<br>$\text{S}_2\text{O}_3^{2-}$   |

As indicated,  $\text{Ca}^{2+}$  is a hard acid and  $\text{Zn}^{2+}$  is an intermediate/borderline acid. In order to chelate both cations, the drug molecule should ideally be an intermediate-hard base. The literature was searched to investigate the binding sites of proteins that bind  $\text{Ca}^{2+}$  or  $\text{Zn}^{2+}$ . It was found that several  $\text{Zn}^{2+}$  binding sites and a few  $\text{Ca}^{2+}$  binding sites contain histidine residues (Lewit-Bentley and Rety 2000). In both cases, the metals were chelated via the pyridine-like nitrogen in the imidazole ring of histidine. Not surprisingly, imidazole falls on the border between intermediate and hard on the spectrum of bases, as indicated in Table 2.1. With this starting point, several synthetically feasible molecules containing the imidazole functionality were designed and tested systematically. Later in this chapter, the characterization of carnosine, a dipeptide containing an imidazole ring, will

be discussed in detail. First, the computational method used to analyze the activity of imidazoles will be presented.

### **2.2.1 – Gas-Phase Simulations**

In this study, two types of molecular mechanics simulations were performed: gas-phase and solvated simulations. First, gas-phase (or *in vacuo*) simulations were carried out as a virtual screening technique. The absence of solvent interactions in the gas phase allows for a very large number of rapid calculations. This technique is computationally inexpensive, making it an ideal method for screening a large number of compounds in a short period of time. However, the relaxed conditions can lead to problems when searching for the lowest energy conformation of the molecule. The lack of solvent interaction can result in artifacts in molecular geometry, especially in charged molecules. Charged pieces of the molecule that would typically interact with solvent molecules end up interacting with one another, leading to inaccurate conformations. At physiological pH, some of the molecules in the testing set exist as zwitterions or charged species. To account for the aforementioned problem, all conformation searches were performed with the molecules in their neutral form. This prevented any intramolecular, electrostatic interactions, thus improving the reliability and accuracy of the lowest energy conformation given by MOE. Once minimized, the correct charges were manually applied on the appropriate functional groups. At this point, the system's total energy, van der Waals energy and electrostatic energy were recorded. Next, one of the target metal cations ( $\text{Zn}^{2+}$  or  $\text{Ca}^{2+}$ ) was added to the system. The system was then manipulated so that the target was in close proximity (distances are given in column 1 of the upcoming tables) to the predicted active site of the molecule of interest (i.e. near the imidazole

ring). Energy minimization calculations were again performed to examine whether or not the molecule would interact with the target. At this point, the systems total energy, van der Waals energy and electrostatic energy were recorded. The differences in energy between the final system and the naked molecule were then used to rank the molecules from most stable metal complex formed to least stable metal complex formed. All molecules that were calculated to have a negative energy difference and showed coordination of the imidazoles with the cation moved on to the solvation simulation stage.

### **2.2.2 – Solution-Phase Simulations**

In the solvation simulations, the lowest energy conformations that were calculated in the gas-phase simulations were loaded in the program. Again, charges were manually assigned to the appropriate functional groups. Next, a solvent box was created with the molecule of interest at the centre. The solvent box was given a cubic shape and water was chosen as the solvent to imitate the aqueous environment of human blood. Once the solvent was built, the system was minimized to determine whether or not the presence of solvent molecules would have any effect on the lowest energy conformation. After the minimization was complete, the solvent was deleted and the total energy, van der Waals energy and electrostatic energy of the naked molecule were recorded. The system was then solvated again in the same way as before (with water in a solvent cube). Next, one of the target metal cations ( $Zn^{2+}$  or  $Ca^{2+}$ ) was added to the system. The system was, again, manipulated so that the target was in close proximity to the predicted active site of the molecule of interest (i.e. near the imidazole ring). Energy minimization calculations were performed to examine whether or not the molecule would interact with the target in

solvent. As before, the solvent molecules were deleted, leaving the metal-ligand complex by itself. At this point, the systems total energy, van der Waals energy and electrostatic energy were recorded. Any differences in interactions between the gas-phase and solvation simulations were noted. The differences in energy between the final system and the naked molecule were then used to rank the molecules from most stable metal complex formed to least stable metal complex formed. Separate, ranked lists were created for both  $Zn^{2+}$  complexes and  $Ca^{2+}$  complexes. Among the highest ranked molecules, a few were purchased to evaluate experimentally.

### **2.2.3 – A Reference Point**

Before beginning to test imidazole-containing compounds as chelators for both  $Ca^{2+}$  and  $Zn^{2+}$ , it was necessary to find a point of reference. A search of the literature was conducted to find naturally occurring proteins that possess binding sites for both metal cations. Several protein structural motifs were found for each cation. Zinc fingers (McDowall 2007) are present in a variety of different proteins in the human body. They possess a binding site for  $Zn^{2+}$ , which typically consists of two histidine residues and two cysteine residues (Figure 2.2). As a reference for  $Zn^{2+}$  binding, histidine and cysteine were constructed in MOE and minimized with and without zinc and calcium ions in the usual way.

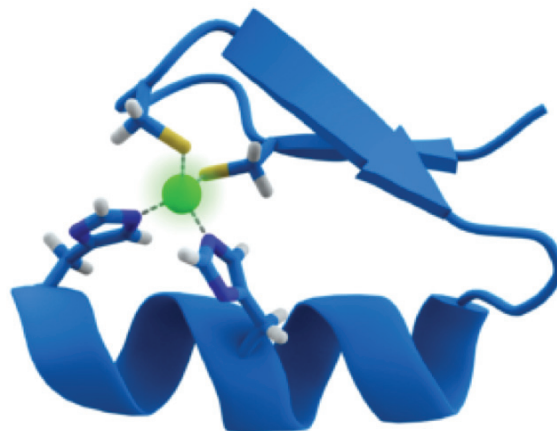


**Figure 2.2: The zinc finger protein structural motif. The green sphere represents  $Zn^{2+}$ . Note the presence of two cysteine residues and two histidine residues (Splettstoesser 2007).**

The EF hand motif (Lewit-Bentley and Rety 2000) is also present in several proteins in the human body. This motif acts as a binding site for  $Ca^{2+}$ , which consists of several aspartate and glutamate residues (Figure 2.3). As a reference for  $Ca^{2+}$  binding, glutamate and aspartate were constructed in MOE and minimized with and without zinc and calcium ions in the usual way. Tables 2.2-2.5 contain gas-phase and solvation simulation data for each of these four amino acids bound to both calcium and zinc ions. The energies given in these tables represent the difference in energy between the metal-ligand complex and the bare drug molecule (equation 2.1). This will be the case for all data tables in this thesis.

$$\Delta E_{\text{binding}} = E_{\text{metal-drug complex}} - E_{\text{drug}} \quad (2.1)$$

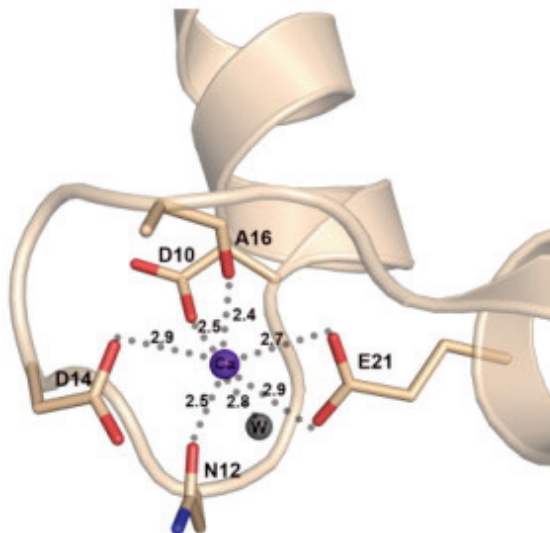


**Figure 2.3: EF hand protein structural motif. The purple sphere represents  $\text{Ca}^{2+}$ . Note the presence of two aspartate residues and one glutamate residue.**

**Table 2.2: Gas Phase data for aspartate, glutamate, cysteine and histidine binding to  $\text{Zn}^{2+}$ .**

| File Name | Distance (angstroms) | $\Delta$ Energy kcal/mol | $\Delta$ vdW kcal/mol | $\Delta$ Electrostatic kcal/mol |
|-----------|----------------------|--------------------------|-----------------------|---------------------------------|
| AspZn     | 3.5                  | -123.5                   | 5.8                   | -95.1                           |
| GluZn     | 3.5                  | -127.6                   | 5.8                   | -99.3                           |
| CysZn     | 3.0                  | -59.5                    | 1.1                   | -38.7                           |
| HisZn     | 3.5                  | -110.4                   | 7.2                   | -98.8                           |

**Table 2.3: Gas Phase data for aspartate, glutamate, cysteine and histidine binding to  $\text{Ca}^{2+}$ .**

| File Name | Distance (angstroms) | $\Delta$ Energy kcal/mol | $\Delta$ vdW kcal/mol | $\Delta$ Electrostatic kcal/mol |
|-----------|----------------------|--------------------------|-----------------------|---------------------------------|
| AspCa     | 3.5                  | -106.8                   | 5.7                   | -78.3                           |
| GluCa     | 3.5                  | -120.9                   | 4.6                   | -91.1                           |
| CysCa     | 3.0                  | -53.6                    | 1.5                   | -32.2                           |
| HisCa     | 3.5                  | -121.5                   | 6.4                   | -107.8                          |

**Table 2.4: Solvation data for aspartate, glutamate, cysteine and histidine binding to  $Zn^{2+}$ .**

| File Name  | Distance (angstroms) | $\Delta$ Energy kcal/mol | $\Delta$ vdW kcal/mol | $\Delta$ Electrostatic kcal/mol |
|------------|----------------------|--------------------------|-----------------------|---------------------------------|
| AspZn Solv | 3.0                  | -41.7                    | 3.3                   | -44.3                           |
| GluZn Solv | 3.0                  | -61.8                    | -3.2                  | -55.8                           |
| CysZn Solv | 3.0                  | 0.3                      | 1.8                   | 6.3                             |
| HisZn Solv | 3.0                  | -50.4                    | 0.5                   | -54.4                           |

**Table 2.5: Solvation data for aspartate, glutamate, cysteine and histidine binding to  $Ca^{2+}$ .**

| File Name  | Distance (angstroms) | $\Delta$ Energy kcal/mol | $\Delta$ vdW kcal/mol | $\Delta$ Electrostatic kcal/mol |
|------------|----------------------|--------------------------|-----------------------|---------------------------------|
| AspCa Solv | 3.0                  | -45.5                    | 3.1                   | -48.5                           |
| GluCa Solv | 3.0                  | -58.8                    | 3.3                   | -63.0                           |
| CysCa Solv | 3.0                  | -3.5                     | 1.8                   | 3.1                             |
| HisCa Solv | 3.0                  | -47.9                    | 1.9                   | -50.8                           |

### **2.3 – Case Study: Carnosine**

Once the reference point had been established, construction and analysis imidazole-containing molecules could begin. In this chapter, data for one of the most promising molecules, carnosine, will be presented. Figure 2.4 shows the structure of L-carnosine, a dipeptide consisting of beta-alanine and histidine, in its neutral form. In reality, carnosine exists as a zwitterion in which the carboxylic acid is deprotonated and the terminal amine is protonated. In other words, the molecule has a net charge of 0, but features charged ends.

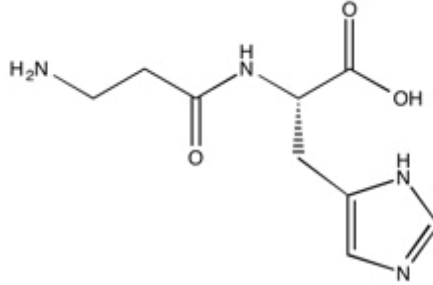


**Figure 2.4: The structure of carnosine, a dipeptide containing an imidazole ring, in its neutral form.**

### **2.3.1 – Carnosine as a Neuroprotective Molecule**

Carnosine is an endogenous dipeptide that is found in several types of tissue in the human body, including the central nervous system (CNS). In the CNS, carnosine is most commonly found in glial and ependymal cells in concentrations ranging from 0.7 mM-2.0 mM (Boldyrev, Song, Lawrence and Carpenter 1999). It is able to readily traverse the BBB and is known to have neuroprotective properties (Rajanikant, Zemke, Senut, Frenkel, Chen, Gupta and Majid 2007).

#### *2.3.1.1 – Cytosolic Buffer*

First, it can act as a cytosolic buffer (Rajanikant, Zemke, Senut, Frenkel, Chen, Gupta and Majid 2007). Remember that one of the features of the ischemic focus and penumbra is a sub-physiological pH due to the presence of lactic acid, a product of anaerobic metabolism. The ability of imidazoles to act as a base allows for the neutralization of some of the lactic acid, slowing down the evolution of the ischemic cascade.

#### *2.3.1.2 – Antioxidant Activity*

Second, carnosine is known to act as an antioxidant (Kohen, Yamamoto, Cundy and Ames 1988). Antioxidants are broadly defined as molecules that prevent oxidative

damage to lipids, proteins, DNA and other essential macromolecules. Recall that part of the ischemic cascade involves the production of reactive oxygen species, which can wreak havoc on the aforementioned macromolecules, leading to destruction of neurons. In fact, free radicals mediate most of the ischemia-induced damage in the brain (Kohen, Yamamoto, Cundy and Ames 1988). The primary antioxidant activity of carnosine (and other imidazoles) is to reduce the peroxy radical ( $\text{HO}_2\bullet$ ) (Kohen, Yamamoto, Cundy and Ames 1988).

### *2.3.1.3 – Anti-Glutamatergic Excitotoxicity*

Third, carnosine acts to counter the activity of glutamate in the ischemic cascade and prevents excitotoxicity. Recall that, during the early stages of the ischemic cascade, large amounts of glutamate are released from vesicles in the affected neuron. Conveniently, carnosine is co-localized in these glutamate vesicles, perhaps indicating that it is an endogenous agent that acts to protect against glutamate-induced excitotoxicity. One of the negative effects that glutamate evokes is the production of reactive oxygen species. As before, carnosine acts as a scavenger and reduces these species before they can destroy the neuron (Boldyrev, Song, Lawrence and Carpenter 1999).

### *2.3.1.4 – Metal Ion Chelation*

Carnosine is known to be an effective chelator of  $\text{Zn}^{2+}$  (Rajanikant, Zemke, Senut, Frenkel, Chen, Gupta and Majid 2007).  $\text{Zn}^{2+}$ -carnosine chelate compound Z-103 is used to treat gastric ulcers. In fact, carnosine has been reported to chelate copper, cadmium and mercury cations, among others (Brown and Antholine 1979). This thesis will focus primarily on the efficacy with which imidazoles chelate  $\text{Zn}^{2+}$  and  $\text{Ca}^{2+}$ , but that is not to

say that these are the only two metal cations involved in stroke. Actually, several metal ions have been linked to the pathophysiology of stroke. These include endogenous ions of potassium, magnesium, copper, manganese, selenium and exogenous ions of cadmium, nickel, arsenic, mercury and aluminum. For example, carnosine is known to chelate copper and iron ions, preventing them from participating in Fenton Reactions and producing harmful reactive oxygen species (Kohen, Yamamoto, Cundy and Ames 1988).

### **Fenton Reaction**

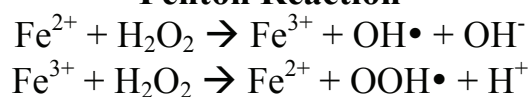


**Figure 2.5: Carnosine chelates iron ions to prevent the Fenton Reaction, which produces harmful reactive oxygen species.**

### **2.3.2 – Gas-Phase Simulations with Carnosine**

There is no pre-existing structure for carnosine in MOE, so it had to be built in the program. First, the carbon backbone was constructed using the ‘Build’ feature and then functional groups were added in the appropriate regions. Next, a systematic conformational search was performed to determine the lowest energy conformation, which was then loaded into MOE. At physiological pH, the amino group is protonated and the carboxyl group is deprotonated. These charges were manually assigned and carnosine was tested as described in section 2.2 using molecular mechanics in gas-phase simulations. The results are very promising.

#### *2.3.2.1 – Carnosine and Zn<sup>2+</sup> in vacuo*

Table 2.6 shows the results from the gas-phase binding study using carnosine to chelate Zn<sup>2+</sup>. When complexed with Zn<sup>2+</sup>, carnosine showed a difference in energy of -134.8 kcal/mol. For convenience, the calculated energies for the amino acids that were

used as a reference point are included in Table 2.6. Compared to the four reference compounds, carnosine showed the most significant change in energy. This suggests that the carnosine- $Zn^{2+}$  adduct is more stable than the complexes formed between  $Zn^{2+}$  and the four amino acids. Also, note that the interactions between  $Zn^{2+}$  and carnosine are primarily electrostatic, as indicated by the large negative value for the difference in electrostatic energy.

**Table 2.6: Gas-phase data for carnosine binding with  $Zn^{2+}$ .**

| File Name | Distance<br>(angstroms) | $\Delta$ Energy<br>kcal/mol | $\Delta$ vdW<br>kcal/mol | $\Delta$ Electrostatic<br>kcal/mol |
|-----------|-------------------------|-----------------------------|--------------------------|------------------------------------|
| AspZn     | 3.5                     | -123.5                      | 5.8                      | -95.1                              |
| GluZn     | 3.5                     | -127.6                      | 5.8                      | -99.3                              |
| CysZn     | 3.0                     | -59.5                       | 1.1                      | -38.7                              |
| HisZn     | 3.5                     | -110.4                      | 7.2                      | -98.8                              |
| CarnZn    | 3.0                     | -134.8                      | 7.1                      | -133.7                             |

Figure 2.6 shows the resulting complex after a gas-phase molecular mechanics simulation using carnosine and  $Zn^{2+}$ .  $Zn^{2+}$  was placed in the plane of the imidazole ring 3 angstroms away from the pyridine-like nitrogen. Upon minimization, a clear electrostatic interaction occurred between  $Zn^{2+}$  and the carboxylate group of carnosine. Furthermore,  $Zn^{2+}$  moved closer to the imidazole ring without the presence of an electrostatic interaction. Because the imidazole ring is a planar, aromatic functional group, this is likely a  $\pi$ -type interaction. In summary, the imidazole nitrogen and carboxylate oxygen act as a bidentate pincer-type ligand when chelating  $Zn^{2+}$ .

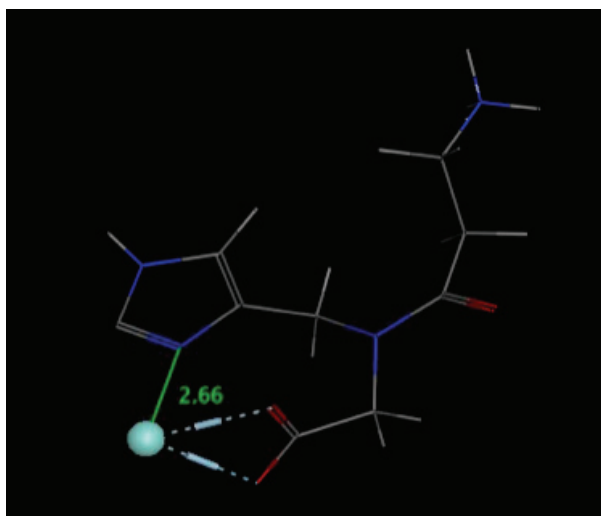


**Figure 2.6: The complex formed as a result of a gas-phase molecular mechanics simulation of the interaction between carnosine and  $Zn^{2+}$ .**

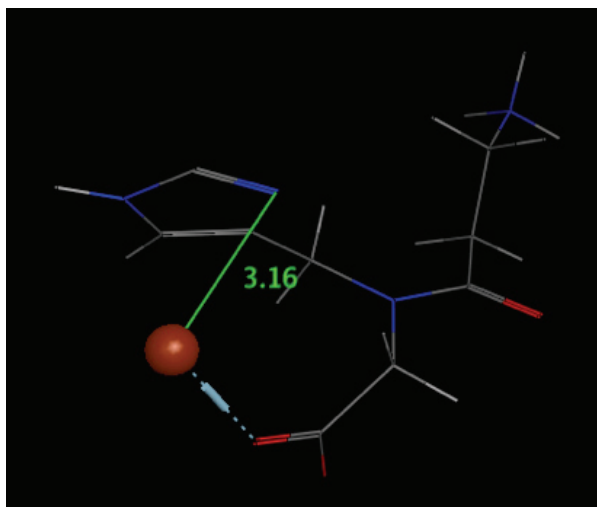
#### 2.3.2.2 – Carnosine and $Ca^{2+}$ in vacuo

Table 2.7 shows the results from the gas-phase binding study using carnosine to chelate  $Ca^{2+}$ . When complexed with  $Ca^{2+}$ , carnosine showed a difference in energy of -116.9 kcal/mol. Carnosine was able to bind  $Ca^{2+}$  more strongly than aspartate and cysteine, as indicated by the changes in energy on going from bare carnosine to the carnosine- $Ca^{2+}$  complex. Also, carnosine is comparable to both histidine and glutamate in terms of its ability to chelate  $Ca^{2+}$ . Note that the interactions between  $Ca^{2+}$  and carnosine are primarily electrostatic, as indicated by the large negative value for the difference in electrostatic energy.

**Table 2.7: Gas-phase data for carnosine binding with Ca<sup>2+</sup>.**

| File Name | Distance (angstroms) | $\Delta$ Energy kcal/mol | $\Delta$ vdW kcal/mol | $\Delta$ Electrostatic kcal/mol |
|-----------|----------------------|--------------------------|-----------------------|---------------------------------|
| AspCa     | 3.5                  | -106.8                   | 5.7                   | -78.3                           |
| GluCa     | 3.5                  | -120.9                   | 4.6                   | -91.1                           |
| CysCa     | 3.0                  | -53.6                    | 1.5                   | -32.2                           |
| HisCa     | 3.5                  | -121.5                   | 6.4                   | -107.8                          |
| CarnCa    | 3.0                  | -116.9                   | 7.8                   | -113.2                          |

Figure 2.7 shows the resulting complex after a gas-phase molecular mechanics simulation using carnosine and Ca<sup>2+</sup>. Ca<sup>2+</sup> was placed in the plane of the imidazole ring 3 angstroms away from the pyridine-like nitrogen. Upon minimization, a clear electrostatic interaction occurred between Ca<sup>2+</sup> and the carboxylate group of carnosine. However, unlike Zn<sup>2+</sup>, Ca<sup>2+</sup> moved further away from the imidazole. This raises doubts as to whether or not a  $\pi$ -type interaction is taking place, as it did with Zn<sup>2+</sup>. Upon further inspection, the Ca<sup>2+</sup> ion is seemingly suspended in space below the imidazole ring. This arrangement in space is indicative of a  $\pi$ -type interaction because the  $\pi$ -orbitals of the imidazole ring sit above and below the plane of the heterocycle. In summary, the imidazole nitrogen and carboxylate oxygen act as a bidentate pincer-type ligand when chelating Ca<sup>2+</sup>.



**Figure 2.7: The complex formed as a result of a gas-phase molecular mechanics simulation of the interaction between carnosine and  $\text{Ca}^{2+}$ .**

### **2.3.3 – Solution-Phase Simulations with Carnosine**

The strong binding of carnosine with both of the cations being studied makes carnosine an excellent candidate for a solvation study. Explicit solvation was used to carry out these calculations. Explicit solvation is the best way to mimic a biological system (Leach 2001). Implicit solvation involves the dielectric constant. The dielectric constant is adjusted to imitate the shielding effect that water has on a charged species, but it is more informative to use explicit solvation for systems of this type. By explicitly building a solvent system of water molecules, the interactions indicated in the simulations become truer to reality. Both the drug molecule and the cation in the system may interact with water molecules in such a way that it alters the way that they interact with each other. For example, water molecules may further stabilize the interaction by coordinating with the cation as it binds to the drug molecule.

The solvent was constructed using the ‘Solvate’ command in MOE. The solvent cube was filled with a periodic array of water molecules with carnosine at the centre. A

margin of six angstroms was selected, meaning that the edge of the solvent box were six angstroms away from the extremities of the carnosine molecule.

The gas-phase simulations with carnosine indicated two possible binding sites for the cations: the pyridine-like nitrogen in the imidazole ring and the oxygens of the carboxylate group. For completeness, two separate solvation simulations were performed. In the first one, the cation was placed in the plane of the imidazole ring, approximately three angstroms away from N3 ('CarnZn Sol N' in Table 2.8 and 'CarnCa Sol N' in Table 2.9). In the second, the cation was placed approximately three angstroms away from the carboxylate oxygens ('CarnZn Sol O' in Table 2.8 and 'CarnCa Sol O' in Table 2.9).

### 2.3.3.1 – Carnosine and $Zn^{2+}$ with Solvent

**Table 2.8: Solvation data for carnosine binding with  $Zn^{2+}$ .**

| File Name    | Distance (angstroms) | $\Delta$ Energy kcal/mol | $\Delta$ vdW kcal/mol | $\Delta$ Electrostatic kcal/mol |
|--------------|----------------------|--------------------------|-----------------------|---------------------------------|
| AspZn Solv   | 3.0                  | -41.7                    | 3.3                   | -44.3                           |
| GluZn Solv   | 3.0                  | -61.8                    | -3.2                  | -55.8                           |
| CysZn Solv   | 3.0                  | 0.3                      | 1.8                   | 6.3                             |
| HisZn Solv   | 3.0                  | -50.4                    | 0.5                   | -54.4                           |
| CarnZn Sol N | 3.0                  | -58.4                    | 3.1                   | -64.6                           |
| CarnZn Sol O | 3.0                  | -78.2                    | 2.6                   | -84.8                           |

Table 2.8 shows the results from the solvation binding study using carnosine to chelate  $Zn^{2+}$ . When the cation was placed in proximity to the imidazole ring, carnosine showed a change in energy of -58.4 kcal/mol. Unlike in the gas-phase simulations, this time, there was no indication of an ionic-type interaction. Also, although the cation moved closer in space to carnosine, it does not sit directly above the plane of the imidazole ring, which may indicate that this is not a  $\pi$ -type interaction (Figure 2.8A).

When the cation was placed in proximity to the carboxylate group, carnosine showed a change in energy of -78.2 kcal/mol. Furthermore, there is a very clear electrostatic interaction between the cation and the negatively charged oxygen of the carboxylate group (Figure 2.8B). Also note that the change in energy is the most negative for this simulation, indicating carnosine's high affinity for binding zinc ions.

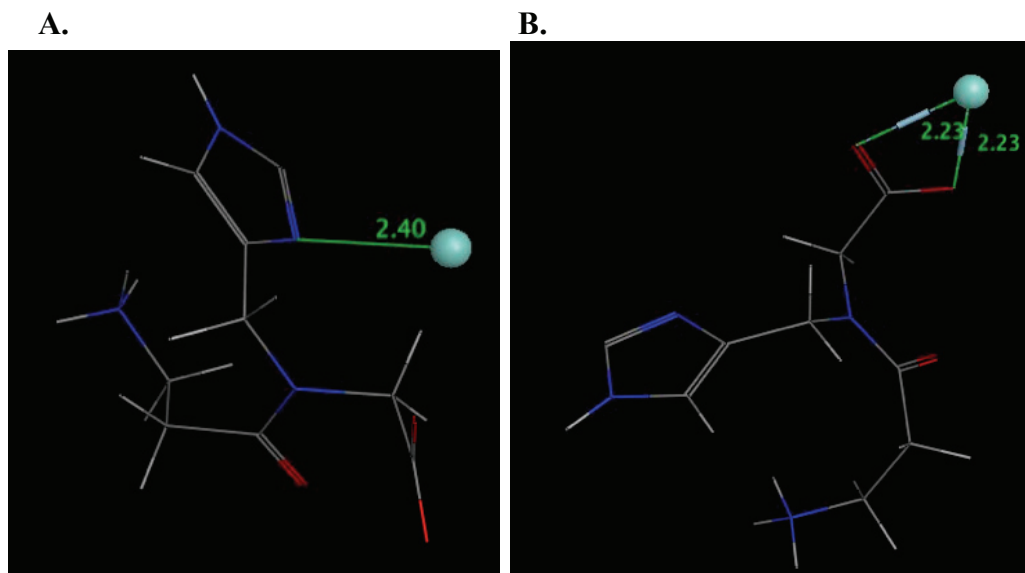


**Figure 2.8:** The complexes formed as a result of a solvation molecular mechanics simulations of the interaction between carnosine and  $Zn^{2+}$  (A) at N3 and (B) at the carboxylate.

### 2.3.3.2 – Carnosine and $Ca^{2+}$ with Solvent

**Table 2.9:** Solvation data for carnosine binding with  $Ca^{2+}$ .

| File Name    | Distance (angstroms) | $\Delta$ Energy kcal/mol | $\Delta$ vdW kcal/mol | $\Delta$ Electrostatic kcal/mol |
|--------------|----------------------|--------------------------|-----------------------|---------------------------------|
| AspCa Solv   | 3.0                  | -45.5                    | 3.1                   | -48.5                           |
| GluCa Solv   | 3.0                  | -58.8                    | 3.3                   | -63.0                           |
| CysCa Solv   | 3.0                  | -3.5                     | 1.8                   | 3.1                             |
| HisCa Solv   | 3.0                  | -47.9                    | 1.9                   | -50.8                           |
| CarnCa Sol N | 3.0                  | -43.7                    | 4.7                   | -55.4                           |
| CarnCa Sol O | 3.0                  | -73.2                    | 8.5                   | -81.2                           |

Table 2.9 shows the results from the solvation binding study using carnosine to chelate  $\text{Ca}^{2+}$ . When the cation was placed in proximity to the imidazole ring, carnosine showed a change in energy of -43.7 kcal/mol. Unlike in the  $\text{Zn}^{2+}$  solvation simulation, there was an electrostatic interaction (Figure 2.9A). In this case, carnosine did not show the most favourable binding interaction. Having said that, the energy difference for carnosine is comparable to that of aspartate, which is present in naturally occurring  $\text{Ca}^{2+}$ -binding sites in proteins.

When the cation was placed in proximity to the carboxylate group, carnosine showed a change in energy of -73.2 kcal/mol. Furthermore, there is a very clear electrostatic interaction between the cation and the negatively charged oxygen of the carboxylate group (Figure 2.9B). Also note that the change in energy is the most negative for this simulation, indicating carnosine's high affinity for binding  $\text{Ca}^{2+}$ .

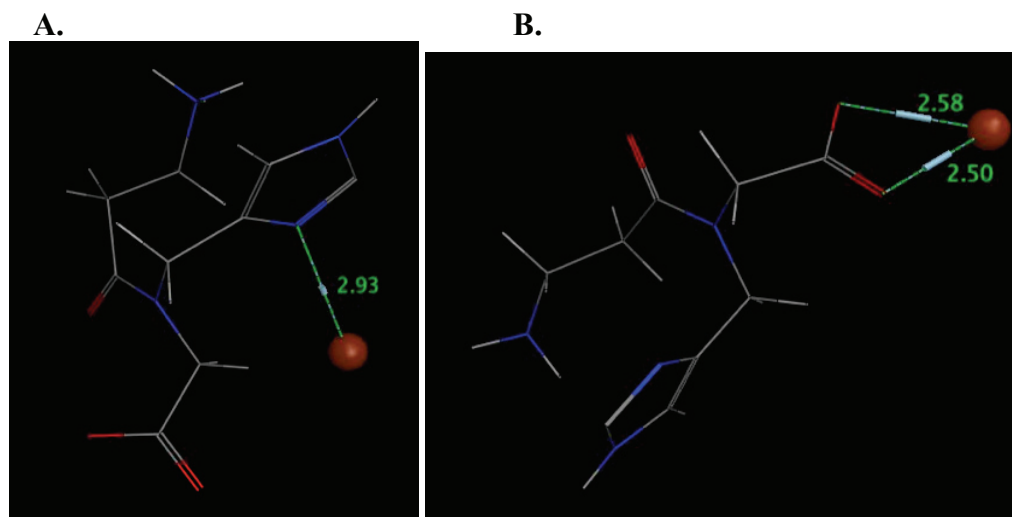


**Figure 2.9: The complexes formed as a result of solvation molecular mechanics simulations of the interaction between carnosine and  $\text{Ca}^{2+}$  (A) at N3 and (B) at the carboxylate.**

### 2.3.4 – Lead Molecules

The above results for carnosine are very promising from a computational perspective. The gas-phase simulations indicated that carnosine has a strong affinity for binding both zinc and calcium ions. This was confirmed in the solvation studies, in which the electrostatic interactions were maintained and binding still occurred in the presence of the explicit solvent, water. Taken together, the results for carnosine indicate that it is an excellent lead compound for further investigation.

Lead compounds are drug molecules that have shown promising results *in silico* or *in vitro*. The next step in the drug design process is lead optimization, in which lead molecules are refined and evaluated to increase their efficacy as potential therapeutics. Subsequently, Cassandra Hawco from the Weaver Group began to experimentally evaluate these compounds.

In the next chapter, the results of similar simulations performed on approximately 120 imidazole-containing molecules will be presented. Carnosine is only one of several hit compounds that have shown promising results for both  $\text{Ca}^{2+}$  and  $\text{Zn}^{2+}$  chelation.

## CHAPTER 3 – IMIDAZOLES

### *3.1 – Imidazole Database*

The first task in this research was to develop a library of imidazoles that could be tested systematically and then compare the results. The characteristics that each molecule needed to have were as follow:

1. They had to contain an imidazole ring.
2. They had to possess the drug-like properties discussed in chapter 1.
3. They had to be synthetically feasible.

A search of the literature was conducted and a database of imidazole-based molecules produced by Wako Pure Chemical Industries, Ltd was identified. The database contains approximately 175 imidazoles that Wako provides to laboratories. All of the compounds in the database satisfy rules 1 and 3 above: they all contain an imidazole ring and are synthetically feasible. Each molecule in the database was evaluated and those molecules that did not satisfy Lipinski's Rule of Five were eliminated. In the end, a working set of about 120 molecules was subjected to the same simulations as carnosine in Chapter 2.

### *3.2 – Gas-Phase Simulations of Imidazoles with $Zn^{2+}$ and $Ca^{2+}$*

After narrowing the database down to a working set, the 120 molecules were systematically tested with both of the cations of interest. First, each molecule was subjected to gas-phase molecular mechanics simulations in MOE. In this section, a summary the interactions of each imidazole with  $Zn^{2+}$  and  $Ca^{2+}$  will be given. In each table, column one lists the molecule number, column two lists the absolute energy of the

drug molecule *in vacuo*, column three lists the energy of the drug-metal complex *in vacuo*, column four lists the binding energy and column five indicates whether an interaction occurred. In column five, N indicates that no interaction occurred, P indicates a  $\pi$ -type interaction and integers (1 or 2) indicate the number of electrostatic interactions that formed during the simulations in the system. The results have been organized into groups based on the functional groups present in each molecule in hopes of establishing a structure-activity relationship (SAR).

### 3.2.1 – Imidazoles with Only Alkyl Substituents

To begin, imidazole itself was evaluated, as well as imidazoles with only alkyl substituents. Tables 3.1 and 3.2 summarize the results.

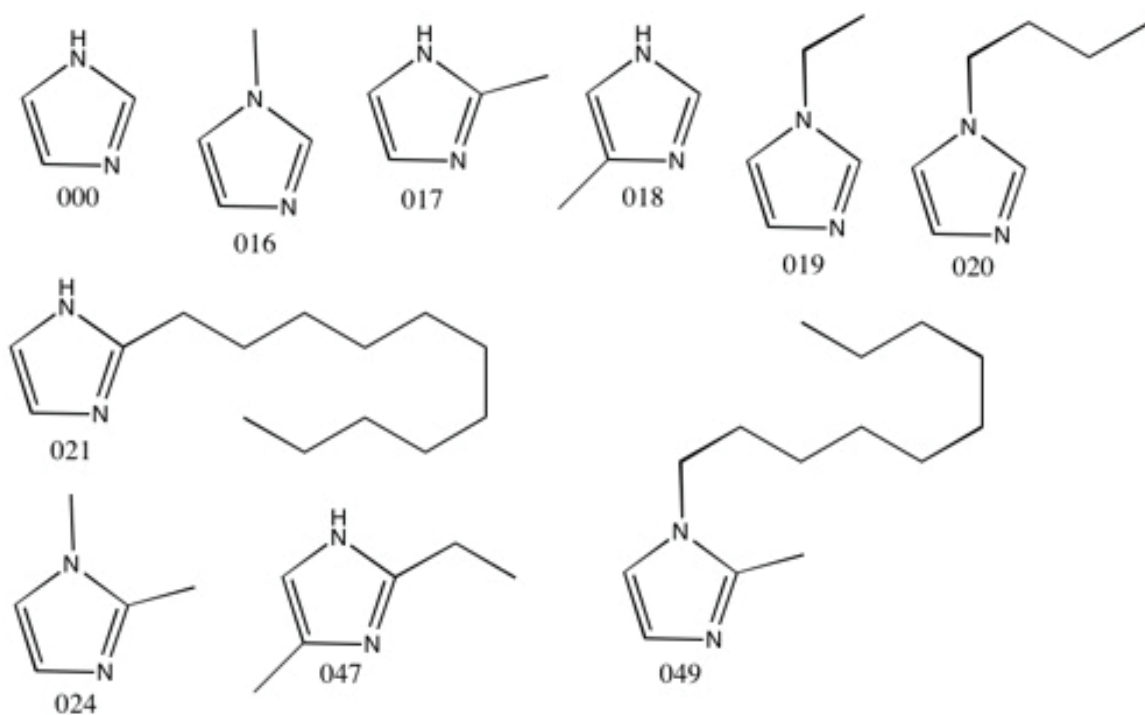


**Figure 3.1: Structures for imidazoles with only alkyl substituents.**

**Table 3.1: Gas-phase data for imidazoles with only alkyl substituents binding with  $Zn^{2+}$ .**

| Molecule | Energy of Drug<br>kcal/mol | Energy of Complex<br>kcal/mol | $\Delta$ Energy<br>kcal/mol | Interactions |
|----------|----------------------------|-------------------------------|-----------------------------|--------------|
| 000      | -1.058                     | -17.650                       | -16.592                     | 1            |
| 016      | 25.829                     | 21.994                        | -3.835                      | 1            |
| 017      | 2.307                      | -26.787                       | -29.094                     | 1            |
| 018      | 1.248                      | -24.663                       | -25.911                     | 1            |
| 019      | 35.418                     | 19.916                        | -15.502                     | 1            |
| 020      | 38.650                     | 20.953                        | -17.697                     | 1            |
| 021      | 17.018                     | -14.968                       | -31.986                     | 1            |
| 024      | 34.864                     | 19.571                        | -15.293                     | 1            |
| 047      | 2.821                      | -26.175                       | -28.996                     | 1            |
| 049      | 48.896                     | 24.060                        | -24.836                     | 1            |

**Table 3.2: Gas-phase data for imidazoles with only alkyl substituents binding with  $Ca^{2+}$ .**

| Molecule | Energy of Drug<br>kcal/mol | Energy of Complex<br>kcal/mol | $\Delta$ Energy<br>kcal/mol | Interactions |
|----------|----------------------------|-------------------------------|-----------------------------|--------------|
| 000      | -1.058                     | -13.065                       | -12.007                     | 1            |
| 016      | 25.829                     | 22.602                        | -3.227                      | 1            |
| 017      | 2.307                      | -22.169                       | -24.476                     | 1            |
| 018      | 1.248                      | -19.812                       | -21.060                     | 1            |
| 019      | 35.418                     | 20.531                        | -14.887                     | 1            |
| 020      | 38.650                     | 21.442                        | -17.208                     | 1            |
| 021      | 17.018                     | -10.434                       | -27.452                     | 1            |
| 024      | 34.864                     | 20.282                        | -14.582                     | 1            |
| 047      | 2.821                      | -21.299                       | -24.120                     | 1            |
| 049      | 48.896                     | 24.028                        | -24.868                     | 1            |

In general, these molecules were moderately efficient at binding both  $Zn^{2+}$  and  $Ca^{2+}$ . This is likely due to the electron-donating property of alkyl substituents. Alkyl groups are known to donate electron density to conjugated  $\pi$  systems by induction. The

extra electron density in the imidazole ring increases the capacity of the pyridine-like nitrogen to act as a base. Consequently, these molecules are able to form an acid-base adduct with  $\text{Zn}^{2+}$  and  $\text{Ca}^{2+}$ .

Molecule 000 is imidazole. It will serve as a reference point for all other molecules in this chapter. Compared to the other molecules in this group, imidazole was moderately successful in chelating both cations.

Molecules 016, 017 and 018 each contain a methyl substituent at different positions on the imidazole ring. In 016 (1-methylimidazole), the methyl group is on N1. In 017 (2-methylimidazole), the methyl group is on the carbon between the two nitrogens. In 018 (4-methylimidazole), the methyl group is on the carbon adjacent to N3, but not N1. In the cases of both cations, the trend of binding energy is as follows:  $017 > 018 \gg 016$ . Because the electron-donating effect of alkyl groups is inductive in nature, it follows that the closer the alkyl substituent is to the basic site of the molecule, the more it will enhance its ability to act as a base. Therefore, it is reasonable that 017 and 018, in which the methyl group is adjacent to N3, are better at binding with the cations than 016, in which the methyl group is three bonds away.

In comparing 017 and 018, it is hard to say why 017 is slightly better at binding both cations. Hypothetically, the methyl group in 017 should help to 'shield' N3 from the electron-withdrawing effect of N1. This results in slightly better binding in 017 as compared to 018.

Molecules 016, 019 and 020 are useful for making observations about the effect of alkyl chain length. As mentioned, 016 has a methyl group on N1. Similarly, 019 (1-ethylimidazole) and 020 (1-butylimidazole) have an ethyl and butyl group, respectively,

on N1. The trend of binding energy is as follows: 020>019>>>016. Similarly, the binding energies of 017 and 021 (2-undecylimidazole) can be compared to evaluate the effect of changing the alkyl chain length at C2. In both cases, the longer the alkyl chain was, the stronger the binding energy became.

Molecules 024, 047 and 049 each have multiple alkyl chains on the imidazole ring. 024 (1,2-dimethylimidazole) has methyl groups at N1 and C2. It has a larger binding energy than 016 and a smaller binding energy than 017, which indicates that an alkyl group on N1 may actually be detrimental to cation binding. This is corroborated by the fact that bare imidazole (000) has a larger binding energy than 1-methylimidazole (016). In 047 (2-ethyl-4-methylimidazole), N3 is flanked on either side by an ethyl group and a methyl group. It has a larger binding energy than 018 (methyl group on C4) and a lower binding energy than 017 (methyl group at C2). This indicates that the most favourable binding energy is achieved when there is one alkyl group on C2. 049 (1-decyl-2-methylimidazole) is very similar to 024. 049 has a higher binding energy than 024, which further shows that binding improves as alkyl chains are lengthened.

In summary, there appear to be two factors that influence binding energy when dealing with imidazoles that only feature alkyl substituents. First, the position of the alkyl chain can have a significant effect on binding energy. It is most preferable if the alkyl chain is on C2 and most detrimental if it is on N1. Second, the length of the alkyl chain affects binding energy. The trend shows that binding energy increases in magnitude as alkyl chain length increases.

### 3.2.2 – Imidazoles with Halide Substituents

Next, simulations were performed using imidazoles with halide substituents.

Tables 3.3 and 3.4 summarize the results.

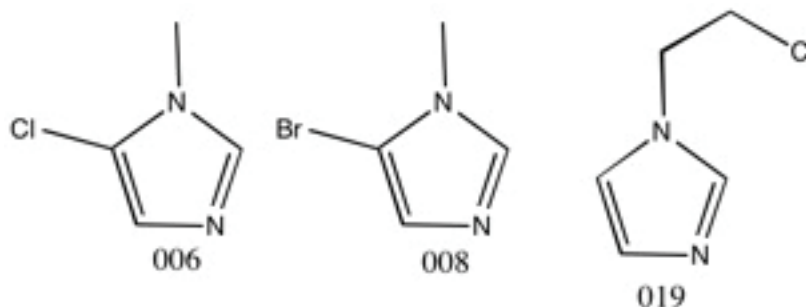


Figure 3.2: Structures for imidazoles with halide substituents.

Table 3.3: Gas-phase data for imidazoles with halide substituents binding with  $Zn^{2+}$ .

| Molecule | Energy of Drug<br>kcal/mol | Energy of Complex<br>kcal/mol | $\Delta$ Energy<br>kcal/mol | Interactions |
|----------|----------------------------|-------------------------------|-----------------------------|--------------|
| 006      | 27.218                     | 24.807                        | -2.411                      | 1            |
| 008      | 0.115                      | -14.781                       | -14.896                     | 1            |
| 028      | 35.631                     | 22.554                        | -13.077                     | 1            |

Table 3.4: Gas-phase data for imidazoles with halide substituents binding with  $Ca^{2+}$ .

| Molecule | Energy of Drug<br>kcal/mol | Energy of Complex<br>kcal/mol | $\Delta$ Energy<br>kcal/mol | Interactions |
|----------|----------------------------|-------------------------------|-----------------------------|--------------|
| 006      | 27.218                     | 25.242                        | -1.976                      | 1            |
| 008      | 0.115                      | -10.484                       | -10.599                     | 1            |
| 028      | 35.631                     | 23.209                        | -12.422                     | 1            |

In general, imidazoles featuring halide substituents are less proficient at chelating the zinc and calcium ions than imidazole itself. This is likely due to the electron-withdrawing property of halides. Halides are known to withdraw electron density from

conjugated  $\pi$  systems by induction. When electron density in the imidazole ring is diminished, so is the ability of N3 to act as a base. In this case, the acid-base adduct is still formed with the cations, but the binding energy is smaller in magnitude than that of imidazole. This indicates that the halide substituents have a detrimental effect on the ability of N3 to interact with the cations.

Molecules 006 (5-chloro-1-methylimidazole) and 008 (5-bromoimidazole) each feature a halide substituent at C5. Recall that molecule 016 (Table 3.1 and 3.2) had binding energies of -3.832 kcal/mol and -3.227 kcal/mol for  $\text{Zn}^{2+}$  and  $\text{Ca}^{2+}$ , respectively. Both binding energies for 006 are lower than those for 016. 006 and 016 only differ by the chloride present in 016, so it is confirmed that halides decrease the binding ability of imidazoles. This is substantiated by the fact that the binding energies for 008 are both smaller in magnitude than those for imidazole (000). A similar argument can be made in comparing 028 with 019.

In summary, halide substituents inhibit the binding of imidazoles with zinc and calcium ions. Though the effect is quite small, it would be best to avoid halide substituents going forward.

### **3.2.3 – Imidazoles with Nitro Substituents**

Imidazoles containing nitro substituents were tested next. Tables 3.5 and 3.6 summarize the results.

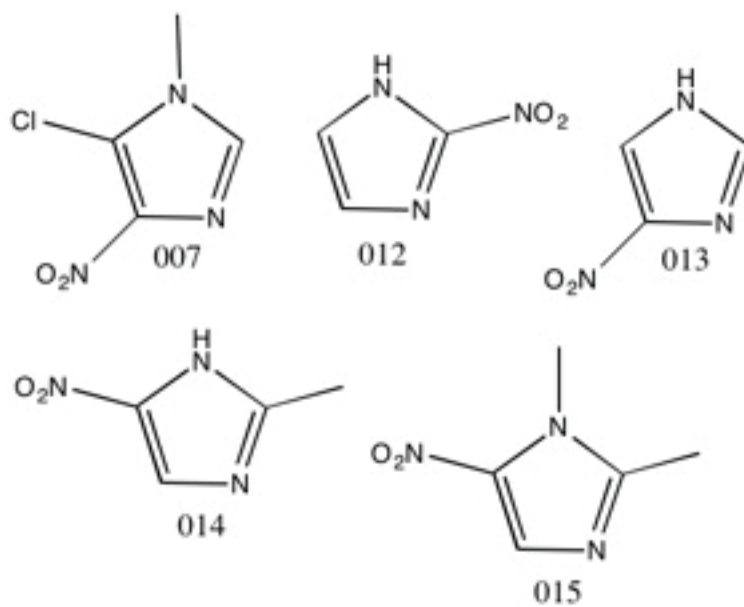


Figure 3.3: Structures for imidazoles with nitro substituents.

Table 3.5: Gas-phase data for imidazoles with nitro substituents binding with  $Zn^{2+}$ .

| Molecule | Energy of Drug<br>kcal/mol | Energy of Complex<br>kcal/mol | $\Delta$ Energy<br>kcal/mol | Interactions |
|----------|----------------------------|-------------------------------|-----------------------------|--------------|
| 007      | 9.046                      | -5.078                        | -14.124                     | 2            |
| 012      | 19.816                     | -11.505                       | -31.321                     | 2            |
| 013      | 16.240                     | -9.637                        | -25.877                     | 2            |
| 014      | 16.708                     | -21.588                       | -38.296                     | 1            |
| 015      | 47.041                     | 27.434                        | -19.607                     | 1            |

Table 3.6: Gas-phase data for imidazoles with nitro substituents binding with  $Ca^{2+}$ .

| Molecule | Energy of Drug<br>kcal/mol | Energy of Complex<br>kcal/mol | $\Delta$ Energy<br>kcal/mol | Interactions |
|----------|----------------------------|-------------------------------|-----------------------------|--------------|
| 007*     | 9.046                      | -1.315                        | -10.361                     | 2            |
| 012      | 19.816                     | -7.493                        | -27.309                     | 2            |
| 013      | 16.240                     | -5.522                        | -21.762                     | 2            |
| 014      | 16.708                     | -17.339                       | -34.047                     | 1            |
| 015      | 47.041                     | 27.948                        | -19.093                     | 1            |

In general, the results in the tables above are quite promising. With the exception of 007, all of the molecules in this set showed better binding than imidazole. In fact, some of these molecules acted as a bidentate ligand on both zinc and calcium ions. Nitro groups are strong electron-withdrawing groups, so nitro substituents are expected to have an unfavourable effect on the binding energies of imidazoles. However, nitro groups have a negative charge that is shared between the two oxygens (Figure 3.1). This negative charge acts as an enticing target for an electrostatic interaction with the positive cations being studied.

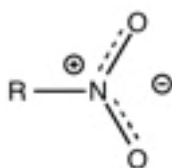


**Figure 3.4: Charge distribution in a nitro group.**

Molecules 012 (2-nitroimidazole) and 013 (4-nitroimidazole) feature a nitro substituent at C2 and C4 respectively. In both cases, the nitro group sits on the carbon adjacent to N3. As predicted, the negatively charged oxygens in the nitro group form an electrostatic interaction with the metal cations. Furthermore, because of the proximity of the nitro group to N3, another interaction occurs between the cations and N3. Notice that the binding energy of 012 is more favourable than that of 013, indicating that a nitro group at C2 is more beneficial than a nitro group at C4.

Molecule 007 (5-chloro-1-methyl-4-nitroimidazole) also features a nitro group on C4. Recall that in section 3.2.1 it was established that an alkyl group at N1 strongly decreases binding energy. Also recall that halide substituents have the same effect to a lesser extent. Despite the presence of both of these detrimental groups, 007 still has a

binding energy comparable to that of imidazole. This indicates that the electrostatic interactions formed between the cations, N3 and the nitro oxygens are very energetically favourable.

Molecules 014 (2-methyl-5-nitroimidazole) and 015 (1,2-dimethyl-5-nitroimidazole) have the nitro group at C5 instead of C4. Remember that, in all simulations, the cation was originally placed three angstroms away from N3 in the plane of the imidazole ring. At C5, the nitro group is a significant distance from the cation to start. At that distance, the force of attraction between the oxygen and cation is not strong enough to show up as an electrostatic interaction in MOE. Instead, MOE produces an electrostatic interaction between the cation and N3. This seems counterintuitive. Since nitro groups are strong electron-withdrawing groups, it follows that the binding energy for 014 and 015 should be smaller than that of imidazole. According to MOE, the opposite is true. Taking a closer look, the reason for this becomes clear.

Unlike halides, which withdraw electron density through induction, nitro groups withdraw electron density via resonance. Figure 3.2 shows several resonance structures of nitrobenzene. Notice that a partial positive charge exists on the carbons adjacent (*ortho*) to the nitro-carbon and the carbon *para* to the nitro group. A similar phenomenon occurs in 5-nitroimidazoles. Fortuitously, N3 is not adjacent to the nitro-carbon. As a result, it does not bear a positive charge and is free to interact with zinc and calcium ions.

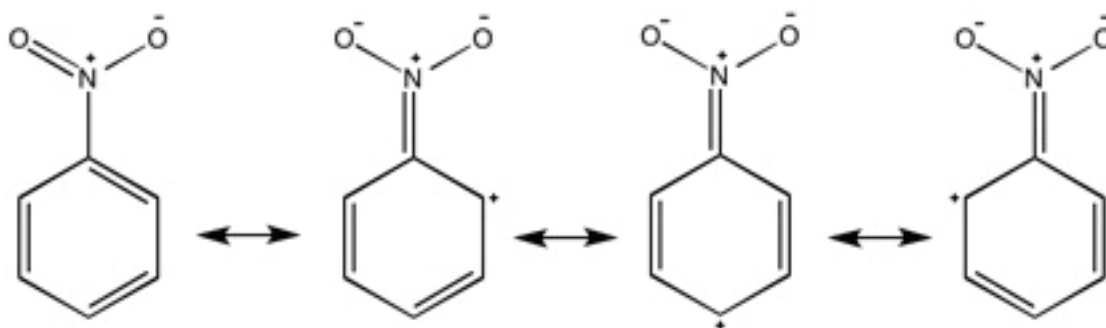


**Figure 3.5: Nitro groups withdraw electron density by resonance.**

In summary, nitro groups have a positive effect on the ability of imidazoles to chelate zinc and calcium ions. Also, molecules with a nitro group on the carbons adjacent to N3 act as bidentate ligands via the oxygens in the nitro group and N3.

### 3.2.4 – Imidazoles with Amido and Amino Substituents

The next several simulations included imidazoles with amino or amido substituents. Tables 3.7-3.10 summarize the results.

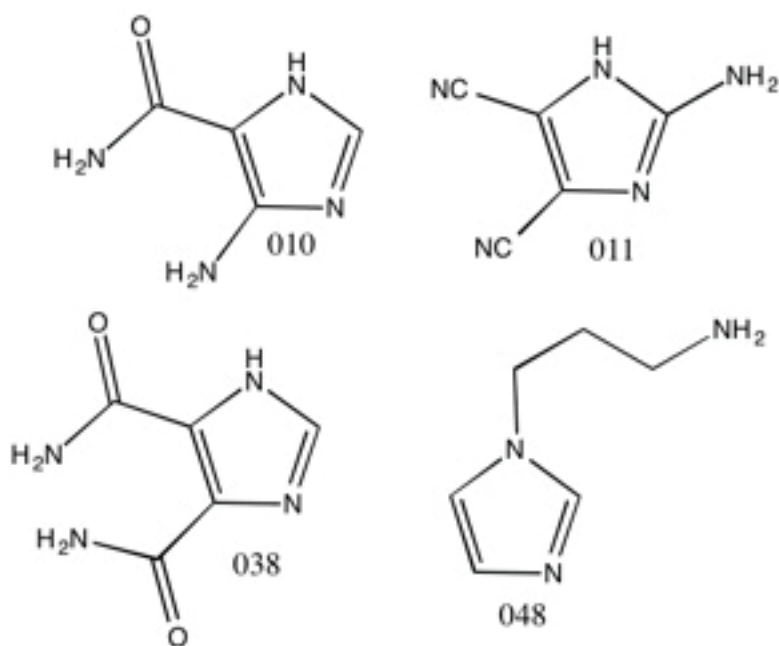


**Figure 3.6: Structures for imidazoles with amido and amino substituents.**

**Table 3.7: Gas-phase data for imidazoles with amino substituents binding with Zn<sup>2+</sup>.**

| Molecule | Energy of Drug<br>kcal/mol | Energy of Complex<br>kcal/mol | $\Delta$ Energy<br>kcal/mol | Interactions |
|----------|----------------------------|-------------------------------|-----------------------------|--------------|
| 010      | -11.137                    | -19.905                       | -8.768                      | N            |
| 011      | 25.922                     | -19.029                       | -44.951                     | N            |
| 048      | 42.202                     | 24.060                        | -18.142                     | N            |

**Table 3.8: Gas-phase data for imidazoles with amino substituents binding with Ca<sup>2+</sup>.**

| Molecule | Energy of Drug<br>kcal/mol | Energy of Complex<br>kcal/mol | $\Delta$ Energy<br>kcal/mol | Interactions |
|----------|----------------------------|-------------------------------|-----------------------------|--------------|
| 010      | -11.137                    | -19.907                       | -8.770                      | N            |
| 011      | 25.922                     | -7.337                        | -33.259                     | N            |
| 048      | 42.202                     | 24.044                        | -18.158                     | N            |

**Table 3.9: Gas-phase data for imidazoles with amido substituents binding with Zn<sup>2+</sup>.**

| Molecule | Energy of Drug<br>kcal/mol | Energy of Complex<br>kcal/mol | $\Delta$ Energy<br>kcal/mol | Interactions |
|----------|----------------------------|-------------------------------|-----------------------------|--------------|
| 010      | -11.137                    | -19.905                       | -8.768                      | N            |
| 038      | 15.367                     | -15.423                       | -30.790                     | 2            |

**Table 3.10: Gas-phase data for imidazoles with amido substituents binding with Ca<sup>2+</sup>.**

| Molecule | Energy of Drug<br>kcal/mol | Energy of Complex<br>kcal/mol | $\Delta$ Energy<br>kcal/mol | Interactions |
|----------|----------------------------|-------------------------------|-----------------------------|--------------|
| 010      | -11.137                    | -19.907                       | -8.770                      | N            |
| 038      | 15.367                     | -8.196                        | -23.563                     | 2            |

In general, amino substituents effectively eliminate the ability of imidazole to bind with zinc and calcium ions, while amido substituents enhance this same property.

As can be seen in 010 (4-amino-5-carboxamide), which contains both an amino and an amido substituent, the amino effect dominates and no interaction takes place.

At physiological pH, all of the amines in this set exist in their protonated form. When protonated, the amino nitrogen bears a positive charge, therefore, the molecule has a net positive charge. The positive charge of the molecule repels the positive charge of the metal ions and a metal-ligand complex is not formed.

Molecule 011 (2-amino-4,5-imidazoledicarbonitrile) bears a protonated amino group on the carbon adjacent to N3. The repulsive effect of the amino group is compounded by the electron withdrawing effect of the cyano groups. Taken together, it makes sense that no binding takes place with 011.

Molecule 048 (3-(2-methyl-1H-imidazolyl)propylamine) shows that the amine effect is still potent even if the positively charged nitrogen is removed from the ring by three carbons. The repulsion of the positive charge is stronger than the attractive effect of N3; therefore, no interaction takes place.

The only molecule in this set that showed any binding 038 (4,5-imidazoledicarboxamide). In fact, 038 acted as a bidentate ligand, binding via N3 and the amido oxygen. As was the case with nitro groups, amido groups also have resonance structures that bear a negative charge on the oxygen (Figure 3.3).

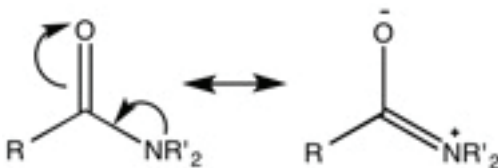


**Figure 3.7: Resonance structures of amido groups.**

The cations interacted with the oxygen of the amido group adjacent to N3. The proximity and arrangement of the amido group allowed for another electrostatic interaction to take place between the cation and N3. The interaction at N3 was facilitated by the electron-donating capability of the other amido group on C5.

In summary amino groups effectively eliminate any potential interaction between imidazoles and the cations being studied. This is largely due to electrostatic repulsion. Conversely, amido groups are beneficial to the binding capability of imidazoles due to the partial negative charge on the amido oxygen and their ability to donate electron density to the imidazole ring.

### 3.2.5 – Imidazoles with Cyano Substituents

Imidazoles with cyano substituents were also tested for their ability to chelate zinc and calcium ions. The results are summarized in Tables 3.11 and 3.12.

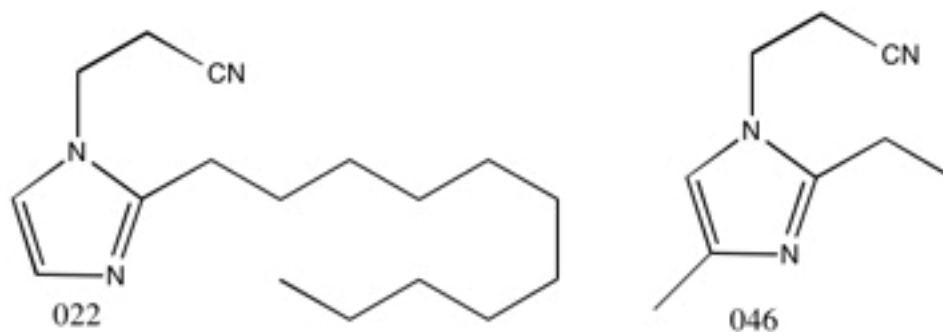


**Figure 3.8: Structures for imidazoles with cyano substituents.**

**Table 3.11: Gas-phase data for imidazoles with cyano substituents binding with  $Zn^{2+}$ .**

| Molecule | Energy of Drug<br>kcal/mol | Energy of Complex<br>kcal/mol | $\Delta$ Energy<br>kcal/mol | Interactions |
|----------|----------------------------|-------------------------------|-----------------------------|--------------|
| 022      | 60.979                     | 28.656                        | -32.323                     | 1            |
| 046      | 46.421                     | 21.485                        | -24.936                     | 1            |

**Table 3.12: Gas-phase data for imidazoles with cyano substituents binding with  $\text{Ca}^{2+}$ .**

| Molecule | Energy of Drug<br>kcal/mol | Energy of Complex<br>kcal/mol | $\Delta$ Energy<br>kcal/mol | Interactions |
|----------|----------------------------|-------------------------------|-----------------------------|--------------|
| 022      | 60.979                     | 29.538                        | -31.441                     | N            |
| 046      | 46.421                     | 22.081                        | -24.340                     | P            |

In general, imidazoles bearing cyano groups are very slightly less effective at binding zinc and calcium ions than their analogues without a cyano group. Cyano groups, like nitro groups, are known to withdraw electron density from conjugated  $\pi$  systems. Also similar to nitro groups, cyano groups have resonance structures in which a partial negative charge is placed on the nitrogen and a partial positive charge is placed on the carbon. However, in the case of cyano groups, this resonance form is not very favourable (compared to that of the nitro group). This is because the oxygen in a nitro group has a higher electronegativity and can bare a more negative charge. In the case of cyano groups in MOE, no electrostatic interaction takes place between the cyano nitrogen and the cations.

Instead, the cyano groups in 022 (1-cyanoethyl-2-undecylimidazole) and 046 (1-cyanoethyl-2-ethyl-4-methylimidazole) act solely as a weak electron withdrawing group. 021 (Tables 3.1 and 3.2) and 022 only differ by a cyanoethyl substituent on N1. Comparing the two, it becomes clear that the effect of the cyanoethyl group is not significant. In 022, the dominant substituent is the undecyl group, which donates electron density to the neighbouring N3. Furthermore, notice that 022 was able to bind  $\text{Zn}^{2+}$ , but not  $\text{Ca}^{2+}$ . This is likely a steric effect, whereby the undecyl group inhibits the electrostatic interaction with  $\text{Ca}^{2+}$ . This makes sense considering the fact that  $\text{Ca}^{2+}$  and

$Zn^{2+}$  have ionic radii of 114 pm and 88 pm respectively (Jolly 1984). Essentially, the zinc ion is small enough to sneak around the undecyl group and bind to the imidazole at N3, while the calcium ion is not.

In the case of 046, the cyanoethyl group appears to be the dominant substituent. Both cations are still able to interact with the imidazole, indicating that the effect is quite weak.  $Zn^{2+}$  forms an electrostatic interaction at N3, while  $Ca^{2+}$  moves to the space directly above the plane of the ring and forms a  $\pi$ -type interaction. Going from 046 to 047 (Tables 3.1 and 3.2), which only differ by the cyanoethyl group, there is a slight increase in the magnitude of the binding energy. This confirms that cyano groups have a very small detrimental effect on cation binding.

### 3.2.6 – Imidazoles with Hydroxyl Substituents

The results of imidazoles with hydroxyl substituents are in Tables 3.13 and 3.14.

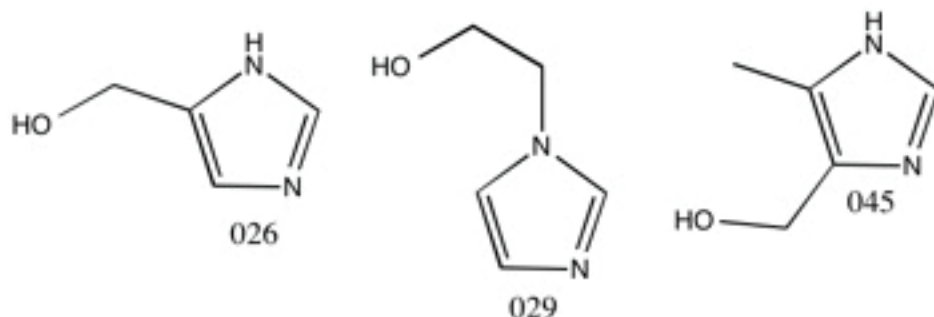


Figure 3.9: Structures for imidazoles with hydroxyl substituents.

Table 3.13: Gas-phase data for imidazoles with hydroxyl substituents binding with  $Zn^{2+}$ .

| Molecule | Energy of Drug<br>kcal/mol | Energy of Complex<br>kcal/mol | $\Delta$ Energy<br>kcal/mol | Interactions |
|----------|----------------------------|-------------------------------|-----------------------------|--------------|
| 026      | 3.285                      | -14.826                       | -18.111                     | 1            |
| 029      | 36.916                     | 21.033                        | -15.883                     | 1            |
| 045      | 1.368                      | -21.739                       | -23.107                     | 2            |

**Table 3.14: Gas-phase data for imidazoles with hydroxyl substituents binding with  $\text{Ca}^{2+}$ .**

| Molecule | Energy of Drug<br>kcal/mol | Energy of Complex<br>kcal/mol | $\Delta$ Energy<br>kcal/mol | Interactions |
|----------|----------------------------|-------------------------------|-----------------------------|--------------|
| 026      | 3.285                      | -10.303                       | -13.588                     | 1            |
| 029      | 36.916                     | 21.268                        | -15.648                     | N            |
| 045      | 1.368                      | -13.470                       | -14.838                     | 2            |

In general, the addition of a hydroxyl substituent on the imidazole ring has very little effect on the binding ability of N3. In all three molecules, the hydroxyl group is more than one bond away from the imidazole ring. This prevents the hydroxyl group from donating electron density into the ring by resonance. Instead, the hydroxyl group exhibits a weak electron-withdrawing effect by induction.

Molecule 026 (5-hydroxymethylimidazole) has a binding energy slightly lower in magnitude than that of imidazole itself. This is indicative of the weak electron withdrawing effect of the hydroxymethyl substituent. In 029 (1-hydroxyethylimidazole), the hydroxyl group is an extra bond away from the imidazole ring compared to 026. As expected, the binding energy for 029 is slightly larger in magnitude than that of 026. This shows that the further the hydroxyl group is away from the ring, the weaker its inductive electron withdrawal becomes.

In molecule 045 (5-methyl-4-hydroxymethylimidazole), the hydroxymethyl group is on the carbon adjacent to N3. Molecule 045 acts as a bidentate ligand for both cations via the hydroxyl oxygen and N3. The interaction at the oxygen in 045 is weaker than the analogous interaction on the nitro-containing imidazoles. This may indicate that the interaction at the hydroxyl group in 045 is more hydrogen bond-like than ionic in nature.

### 3.2.7 – Imidazoles with Aldehyde and Ketone Substituents

Imidazoles containing aldehyde and ketone functionalities were evaluated as well.

Results are summarized in Tables 3.15 and 3.16.

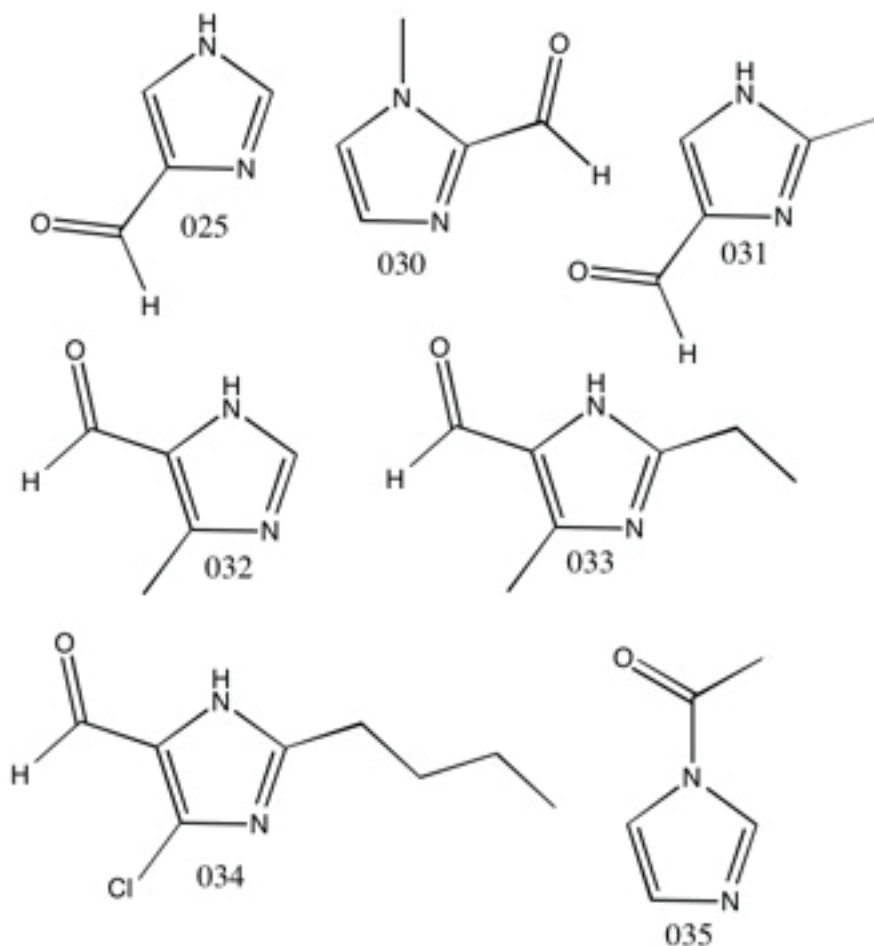


Figure 3.10: Structures for imidazoles with aldehyde and ketone substituents.

**Table 3.15: Gas-phase data for imidazoles with aldehyde and ketone substituents binding with Zn<sup>2+</sup>.**

| File Name | Energy of Drug<br>kcal/mol | Energy of Complex<br>kcal/mol | $\Delta$ Energy<br>kcal/mol | Interactions |
|-----------|----------------------------|-------------------------------|-----------------------------|--------------|
| 025       | 5.067                      | -3.153                        | -8.220                      | 1            |
| 030       | 37.411                     | 20.579                        | -16.832                     | 1            |
| 031       | 4.653                      | -13.083                       | -17.736                     | 1            |
| 032       | 5.356                      | -17.174                       | -22.530                     | 1            |
| 033       | 7.006                      | -19.355                       | -26.361                     | 1            |
| 034       | 13.990                     | -14.556                       | -28.546                     | 1            |
| 035       | 35.121                     | 8.553                         | -26.568                     | 1            |

**Table 3.16: Gas-phase data for imidazoles with aldehyde and ketone substituents binding with Ca<sup>2+</sup>.**

| Molecule | Energy of Drug<br>kcal/mol | Energy of Complex<br>kcal/mol | $\Delta$ Energy<br>kcal/mol | Interactions |
|----------|----------------------------|-------------------------------|-----------------------------|--------------|
| 025      | 5.067                      | 0.460                         | -4.607                      | 1            |
| 030      | 37.411                     | 24.231                        | -13.180                     | 1            |
| 031      | 4.653                      | -9.299                        | -13.952                     | 1            |
| 032      | 5.356                      | -12.706                       | -18.062                     | 1            |
| 033      | 7.006                      | -14.810                       | -21.816                     | 1            |
| 034      | 13.990                     | -10.838                       | -24.828                     | 1            |
| 035      | 35.121                     | 4.508                         | -30.613                     | N            |

Aldehydes and ketones are known to withdraw electron density from conjugated  $\pi$  systems. In theory, one would expect that an imidazole with one of these substituents would have less affinity for binding zinc and calcium ions. 025 (4-formylimidazole) confirms this because its binding energy is significantly smaller in magnitude than that of bare imidazole.

Molecules 030 (1-methyl-2-imidazolecarbaldehyde), 031 (2-methyl-4-formylimidazole) and 032 (4-methyl-5-imidazolecarbaldehyde) each have an aldehyde substituent and a methyl substituent. In both 030 and 031, the aldehyde is adjacent to the N3 cation-binding site of the imidazole ring. The electron-withdrawing effect of the aldehyde is felt more strongly in these two molecules than it is in 032, in which the aldehyde is an extra bond away. This is corroborated by the fact that 032 exhibited the largest binding energy.

Also, 033 (2-ethyl-4-methyl-formylimidazole) differs from 032 by an ethyl group at C2. The binding energy of 033 is more favourable than that of 032, confirming that alkyl groups are favourable substituents because of their electron-donating capability.

The binding energy of 034 (2-butyl-5-chloro-4-imidazolecarbaldehyde) seems counterintuitive. Before running the simulations with zinc and calcium ions, it was hypothesized that 034 would be less efficient at binding the cations than imidazole. It was hypothesized that the presence of two electron-withdrawing groups (the aldehyde and the chloride) would outweigh the effect of the butyl substituent adjacent to N3. According to MOE, the opposite is true, as evidenced by the binding energy being significantly larger in magnitude than that of imidazole.

Finally, 035 (1-acetylimidazole) features a ketone at N1. Like 032, the carbonyl is three bonds away from N3, so the electron-withdrawing effect is negligible.

### **3.2.8 – Imidazoles with Carboxylic Acid and Ester Substituents**

Carboxylic acid-containing imidazoles were some of the most promising molecules in the working set. Esters are also included in this section because they are a

carboxylic acid derivative. The results of these simulations are given in Tables 3.17 and 3.18.

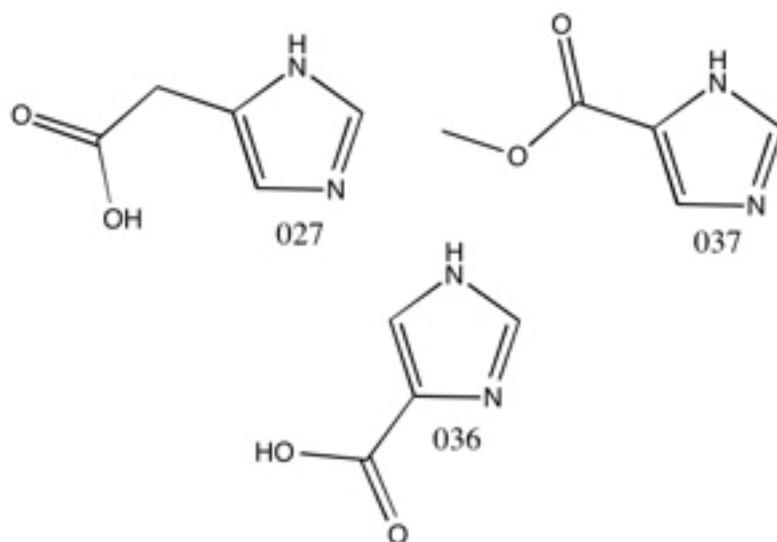


**Figure 3.11: Structures for imidazoles with carboxylic acid and ester substituents.**

**Table 3.17: Gas-phase data for imidazoles with carboxylic acid and ester substituents binding with  $Zn^{2+}$ .**

| Molecule | Energy of Drug<br>kcal/mol | Energy of Complex<br>kcal/mol | $\Delta$ Energy<br>kcal/mol | Interactions |
|----------|----------------------------|-------------------------------|-----------------------------|--------------|
| 027      | 7.921                      | -81.491                       | -89.412                     | 1            |
| 036      | 15.352                     | -49.294                       | -64.646                     | 2            |
| 037      | 21.242                     | -0.642                        | -21.884                     | 1            |

**Table 3.18: Gas-phase data for imidazoles with carboxylic acid and ester substituents binding with  $Ca^{2+}$ .**

| Molecule | Energy of Drug<br>kcal/mol | Energy of Complex<br>kcal/mol | $\Delta$ Energy<br>kcal/mol | Interactions |
|----------|----------------------------|-------------------------------|-----------------------------|--------------|
| 027      | 7.921                      | -69.116                       | -77.037                     | 1            |
| 036      | 15.352                     | -36.757                       | -52.109                     | 2            |
| 037      | 21.242                     | 2.517                         | -18.725                     | 1            |

Molecules 027 (imidazole-5-acetic acid) and 036 (4-imidazolecarboxylic acid) have carboxylic acid groups at C4 and C5, respectively. At physiological pH, the carboxylic acids will be deprotonated, so a negative charge was assigned to the oxygen before the simulation began. The charged carboxylate group in both molecules served as an ideal binding site for zinc and calcium ions. Because of the ionic-type interaction, it is no surprise that the complexes formed showed some of the best binding energies of the 120 molecules tested.

As mentioned, in 036, the carboxylate group is on C4, adjacent to N3. This molecule acted as a bidentate ligand for both  $Zn^{2+}$  and  $Ca^{2+}$ . In this case, the two interactions may be less favourable than the single interaction in 027. It is hypothesized that the carboxylate in 036 is too close to N3 and, when the metal binds to both the oxygen and nitrogen, there is an unfavourable repulsion between the carboxylate and N3. This is why the binding energy of 036 is smaller in magnitude than that of 027.

037 (methyl-5-imidazolecarboxylate) has an ester group on C5. Esters typically withdraw electron density from conjugate  $\pi$  systems. In this case, the effect is negligible because the ester is three bonds away from N3.

### **3.2.9 – Imidazoles with Sulfur-Containing Substituents**

Three different types of sulfur-containing substituents were evaluated for their effect on the binding energy of imidazole with zinc and calcium ions. The data are summarized in Tables 3.19-3.24.

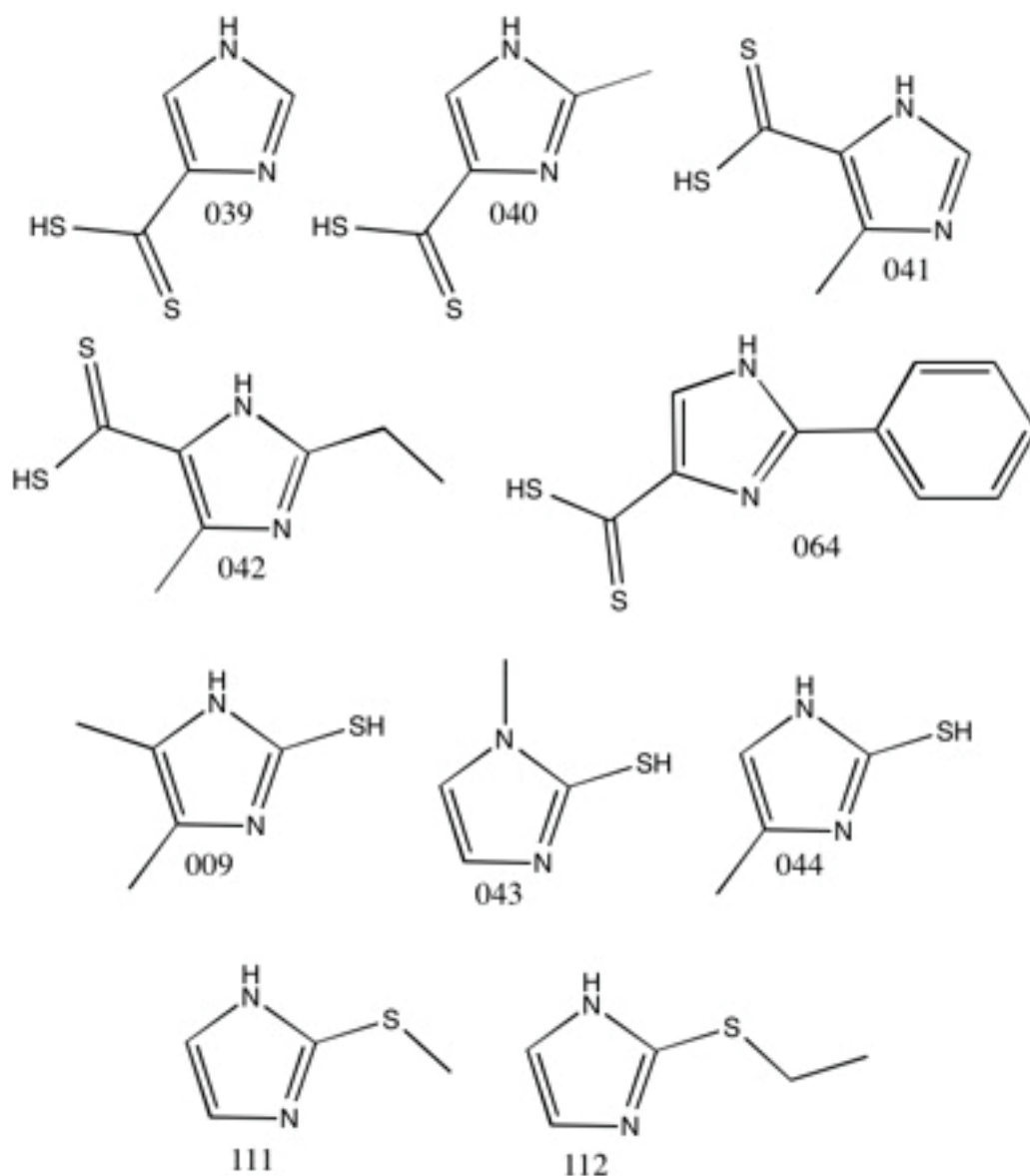


Figure 3.12: Structures for imidazoles with sulfur-containing substituents.

Table 3.19: Gas-phase data for imidazolines with thioether substituents binding with  $Zn^{2+}$ .

| Molecule | Energy of Drug<br>kcal/mol | Energy of Complex<br>kcal/mol | $\Delta$ Energy<br>kcal/mol | Interactions |
|----------|----------------------------|-------------------------------|-----------------------------|--------------|
| 111      | 37.118                     | 8.603                         | -28.515                     | N            |
| 112      | 40.034                     | 8.449                         | -31.585                     | 1            |

**Table 3.20: Gas-phase data for imidazolines with thioether substituents binding with  $\text{Ca}^{2+}$ .**

| Molecule | Energy of Drug<br>kcal/mol | Energy of Complex<br>kcal/mol | $\Delta$ Energy<br>kcal/mol | Interactions |
|----------|----------------------------|-------------------------------|-----------------------------|--------------|
| 111      | 37.118                     | 9.596                         | -27.522                     | N            |
| 112      | 40.034                     | 9.588                         | -30.446                     | 1            |

Molecules 111 (2-methylthio-2-imidazoline) and 112 (2-ethylthio-2-imidazoline) are both imidazoline (Figure 3.4) derivatives with thioether substituents. Thioethers, like their oxygen-containing counterparts, are weak electron donating groups. They transfer electron density into the imidazoline ring and increase the basicity at N3. As indicated, the cations only showed binding with 112. This may be due to the fact that the longer alkyl chain in 112 donates more electron density to N3, or it may be a computational anomaly.

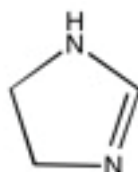


**Figure 3.13: Imidazoline.**

**Table 3.21: Gas-phase data for imidazoles with mercapto substituents binding with  $\text{Zn}^{2+}$ .**

| Molecule | Energy of Drug<br>kcal/mol | Energy of Complex<br>kcal/mol | $\Delta$ Energy<br>kcal/mol | Interactions |
|----------|----------------------------|-------------------------------|-----------------------------|--------------|
| 009      | -14.819                    | -31.618                       | -16.799                     | 1            |
| 043      | 40.394                     | 18.815                        | -21.579                     | N            |
| 044      | 7.718                      | -29.928                       | -37.646                     | 1            |

**Table 3.22: Gas-phase data for imidazoles with mercapto substituents binding with  $\text{Ca}^{2+}$ .**

| Molecule | Energy of Drug<br>kcal/mol | Energy of Complex<br>kcal/mol | $\Delta$ Energy<br>kcal/mol | Interactions |
|----------|----------------------------|-------------------------------|-----------------------------|--------------|
| 009      | -14.819                    | -26.768                       | -11.949                     | 1            |
| 043      | 40.394                     | 20.014                        | -20.380                     | N            |
| 044      | 7.718                      | -25.172                       | -32.890                     | 1            |

Similar to thioethers, mercapto groups also act as a weak electron-donating group. 009 (2-mercapto-4,5-dimethylimidazole), 043 (2-mercapto-1-methylimidazole) and 044 (2-mercapto-4-methylimidazole) each contain a mercapto group at C2 and methyl group(s) at various positions on the imidazole ring. 009 has three electron donating groups and, as expected, shows a better binding energy than imidazole itself.

In comparing 043 and 044, which each contain a single methyl group, it becomes clear that the position of the methyl group greatly affects the binding energy. Recall molecule 016, which had a methyl group on N1, and 018, which had a methyl group on C4, from Table 3.1 and 3.2. The binding energies of 043 and 044 are consistent with the binding energies of 016 and 018. In other words, the methyl group on N1 is detrimental to binding affinity in both cases, as evidenced by the lack of electrostatic interaction with molecule 043.

**Table 3.23: Gas-phase data for imidazoles with dithiocarboxylic acid substituents binding with Zn<sup>2+</sup>.**

| File Name | Energy of Drug<br>kcal/mol | Energy of Complex<br>kcal/mol | ΔEnergy<br>kcal/mol | Interactions |
|-----------|----------------------------|-------------------------------|---------------------|--------------|
| 039       | 23.300                     | -14.697                       | -37.997             | 2            |
| 040       | 22.495                     | -24.434                       | -46.929             | 2            |
| 041       | 27.454                     | -16.295                       | -43.749             | 1            |
| 042       | 43.675                     | -18.517                       | -62.192             | 1            |
| 064       | 40.062                     | 1.583                         | -38.479             | 1            |

**Table 3.24: Gas-phase data for imidazoles with dithiocarboxylic acid substituents binding with Ca<sup>2+</sup>.**

| Molecule | Energy of Drug<br>kcal/mol | Energy of Complex<br>kcal/mol | ΔEnergy<br>kcal/mol | Interactions |
|----------|----------------------------|-------------------------------|---------------------|--------------|
| 039      | 23.300                     | -9.865                        | -33.165             | 2            |
| 040      | 22.495                     | -19.657                       | -42.152             | 2            |
| 041      | 27.454                     | -11.577                       | -39.031             | 1            |
| 042      | 43.675                     | -13.770                       | -57.445             | 1            |
| 064      | 40.062                     | 5.974                         | -34.088             | 1            |

Molecules 039 (4-imidazoledithiocarboxylic acid) and 040 (2-methylimidazole-4-dithiocarboxylic acid) only differ by a methyl group present at C2 in 040. Both molecules have a dithiocarboxylic acid group at C4. Prior to running the simulations, a negative charge was manually assigned to one of the sulfurs because at physiological pH, the dithiocarboxylic acid would be deprotonated. The negatively charged dithiocarboxylate group sits adjacent to N3 and acts as a prime binding target for the cations of interest. In fact, the dithiocarboxylate is close enough to N3, that both molecules 039 and 040 act as a bidentate ligand for both calcium and zinc ions. As usual, the presence of the methyl group in 040 further improves the binding energy.

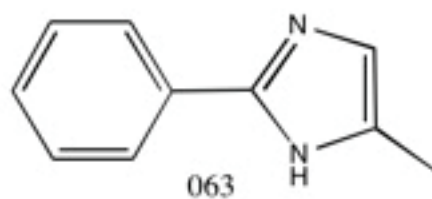
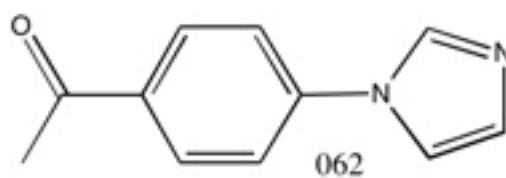
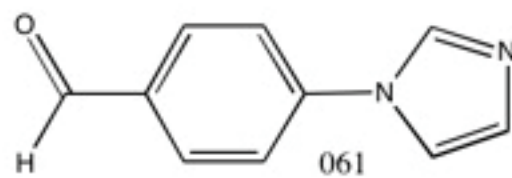
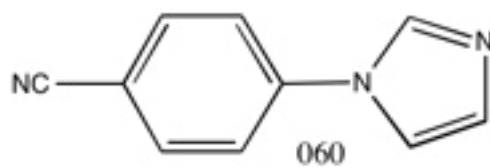
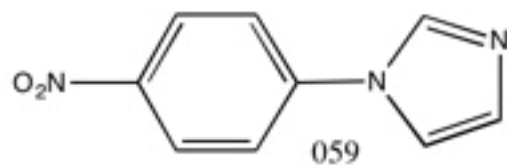
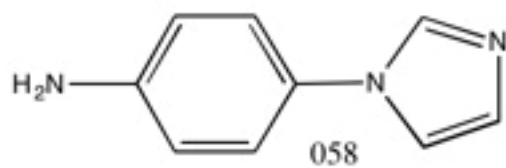
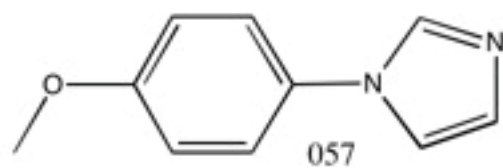
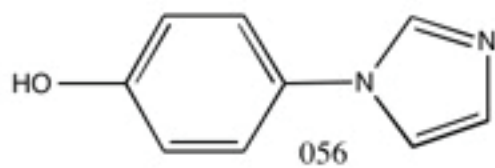
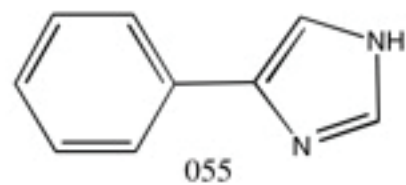
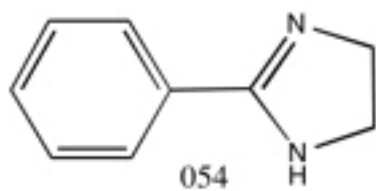
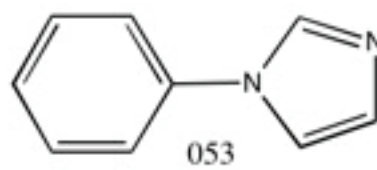
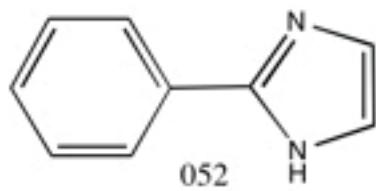
Molecules 041 (5-methylimidazole-4-dithiocarboxylic acid) and 042 (2-ethyl-4-methylimidazole-5-dithiocarboxylic acid) both feature the dithiocarboxylate group at C5 instead of C4. Similar to the carboxylic acids in section 3.2.8, the binding energy is stronger when the dithiocarboxylate group is not adjacent to N3. This is likely due to repulsion between the negatively charged sulfur and N3 in molecules 039 and 040. Once again, the binding energy improves on going from 041 to 042, which only differ by an ethyl group on C2.

In 064 (2-phenylimidazole-4-dithiocarboxylic acid), N3 is flanked by a dithiocarboxylate group and a phenyl ring substituent. Phenyl rings are capable of acting as very weak electron-donating groups. Also, the phenyl ring is quite large in comparison to the other alkyl substituents that have been studied, so it may sterically hinder the binding of the cations. This appears to be the case in 064. The only difference between 040 and 064 is the size of the substituent at C2. The larger phenyl substituent slightly inhibits the binding of both cations, as evidenced by the superior binding energy of 040.

In summary, dithiocarboxylate groups are by far the most beneficial to the binding affinity of imidazoles. Thioethers and mercapto groups inhibit binding in some cases (043 and 111) and should not be included in the solvation studies.

### **3.2.10 – Imidazoles with Phenyl Substituents**

The largest group of molecules that was tested was a set of phenyl-substituted imidazoles. The results are tabulated in Tables 3.25 and 3.26.



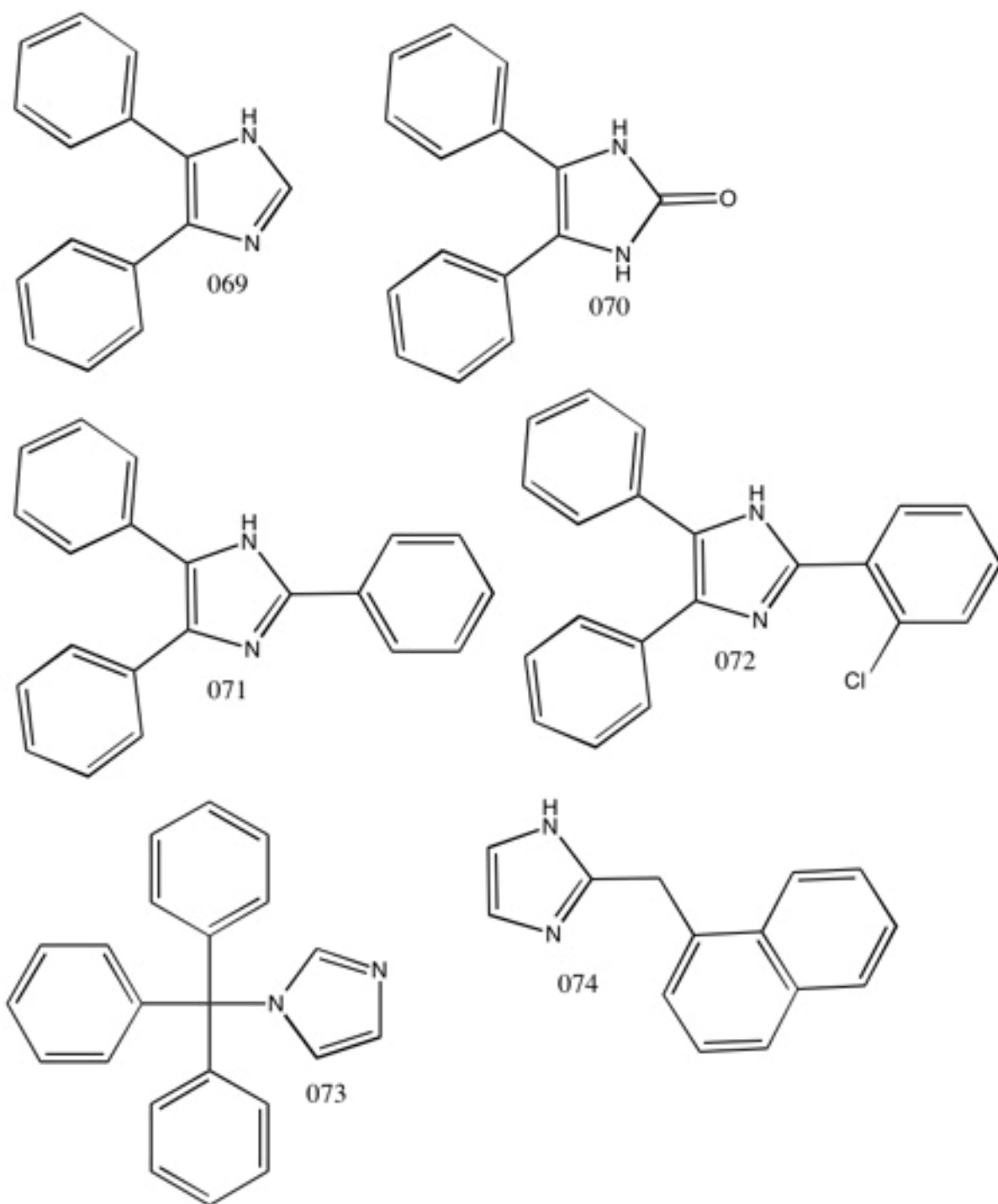


Figure 3.14: Structures for imidazoles with phenyl substituents.

**Table 3.25: Gas-phase data for imidazoles with phenyl substituents binding with  $Zn^{2+}$ .**

| Molecule | Energy of Drug<br>kcal/mol | Energy of Complex<br>kcal/mol | $\Delta$ Energy<br>kcal/mol | Interactions |
|----------|----------------------------|-------------------------------|-----------------------------|--------------|
| 052      | 20.175                     | -1.040                        | -21.215                     | 1            |
| 053      | 50.343                     | 28.537                        | -21.806                     | 1            |
| 054      | 44.926                     | 21.292                        | -23.634                     | N            |
| 055      | 18.695                     | -0.843                        | -19.538                     | 1            |
| 056      | 48.515                     | 27.427                        | -21.088                     | 1            |
| 057      | 56.091                     | 35.002                        | -21.089                     | N            |
| 058      | 78.450                     | 49.468                        | -28.982                     | N            |
| 059      | 65.212                     | 36.800                        | -28.412                     | 1            |
| 060      | 60.092                     | 31.018                        | -29.074                     | 1            |
| 061      | 53.173                     | 34.565                        | -18.608                     | 1            |
| 062      | 53.543                     | 34.304                        | -19.239                     | 1            |
| 063      | 18.319                     | -8.374                        | -26.693                     | 1            |
| 069      | 35.738                     | 14.990                        | -20.748                     | 1            |
| 070      | 58.313                     | 20.826                        | -37.487                     | 1            |
| 071      | 55.152                     | 31.533                        | -23.619                     | 1            |
| 072      | 59.239                     | 31.240                        | -27.999                     | 1            |
| 073      | 102.119                    | 66.436                        | -35.683                     | N            |
| 074      | 59.757                     | 28.652                        | -31.105                     | 1            |

**Table 3.26: Gas-phase data for imidazoles with phenyl substituents binding with  $\text{Ca}^{2+}$ .**

| Molecule | Energy of Drug<br>kcal/mol | Energy of Complex<br>kcal/mol | $\Delta$ Energy<br>kcal/mol | Interactions |
|----------|----------------------------|-------------------------------|-----------------------------|--------------|
| 052      | 20.175                     | 3.516                         | -16.659                     | 1            |
| 053      | 50.343                     | 29.204                        | -21.139                     | 1            |
| 054      | 44.926                     | 23.746                        | -21.180                     | N            |
| 055      | 18.695                     | 3.813                         | -14.882                     | 1            |
| 056      | 48.515                     | 27.641                        | -20.874                     | 1            |
| 057      | 56.091                     | 35.054                        | -21.037                     | N            |
| 058      | 78.450                     | 49.465                        | -28.985                     | N            |
| 059      | 65.212                     | 36.983                        | -28.229                     | 1            |
| 060      | 60.092                     | 31.508                        | -28.584                     | 1            |
| 061      | 53.173                     | 35.055                        | -18.118                     | 1            |
| 062      | 53.543                     | 34.789                        | -18.754                     | 1            |
| 063      | 18.319                     | -3.632                        | -21.951                     | 1            |
| 069      | 35.738                     | 19.098                        | -16.640                     | 1            |
| 070      | 58.313                     | 25.448                        | -32.865                     | 1            |
| 071      | 55.152                     | 35.400                        | -19.752                     | 1            |
| 072      | 59.239                     | 35.033                        | -24.206                     | 1            |
| 073      | 102.119                    | 66.491                        | -35.628                     | N            |
| 074      | 59.757                     | 29.296                        | -30.461                     | 1            |

In general, the phenyl-substituted imidazoles chelated both calcium and zinc ions quite effectively. As mentioned the previous section, phenyl rings are able to act as weak electron donors, increasing the basicity of N3.

Molecules 052 (2-phenylimidazole), 053 (1-phenylimidazole) and 055 (4-phenylimidazole) each feature a phenyl substituent at a different atom of the imidazole ring. The effect of moving the phenyl group around the ring is very small. The order of binding energy for phenyl substitution is as follows: N1>C2>C4. Next, a number of

analogues of 1-phenyl imidazole featuring substituents *para* to the imidazole ring were evaluated.

Molecules 056 (*p*-(1-imidazolyl)-phenol), 057 (1-(4-methoxyphenyl)-1H-imidazole), 058 (4-(1H-imidazol-1-yl)aniline), 059 (1-(4-nitrophenyl)-1H-imidazole), 060 (4-(1H-imidazol-1-yl)benzotrile), 061 (4-(1H-imidazol-1-yl)benzaldehyde) and 062 (4-(imidazol-1-yl)acetophenone) each have a substituent on the phenyl ring *para* to the imidazole. The order of binding energy is as follows: CN>NO<sub>2</sub>>OH>ketone>aldehyde (excluding the two molecules that showed no binding with Ca<sup>2+</sup> or Zn<sup>2+</sup>).

Molecules 063 (4-methyl-2-phenylimidazole) and 052 only differ by a methyl group at C4. As expected, the binding energy of 063 is larger in magnitude than that of 052 due to the electron donating ability of the alkyl substituent.

Molecules 069 (4,5-diphenylimidazole) and 070 (4,5-diphenyl-2-imidazolinone) have phenyl groups on both C4 and C5. Molecule 069 shows a slightly better binding energy than imidazole, perhaps due to the electron-donating effects of the phenyl rings. In 070, C2 is a carbonyl. Instead of binding via N3 in the usual way, both Ca<sup>2+</sup> and Zn<sup>2+</sup> interacted with the carbonyl oxygen instead. This proves to be a more favourable interaction than the one via N3 in 069. Imidazolidinones, which also feature a carbonyl at C2, will be investigated in the next section.

Molecules 071 (2,4,5-triphenylimidazole) and 072 (2-(*o*-chlorophenyl)-4,5-diphenylimidazole) each have three phenyl substituents at C2, C4 and C5. The only difference being that 072 has a chloro substituent on the phenyl ring at C2. Both of these molecules show binding with both Zn<sup>2+</sup> and Ca<sup>2+</sup>. In fact both have a more favourable

binding energy than imidazole itself. Also, the addition of the chloro substituent is favourable, as evidenced by 072 have a better binding energy than 071.

Molecule 073 (1-tritylimidazole) showed no electrostatic interaction with either cation. The trityl group (which consists of three phenyl groups attached to a central carbon) is large and likely sterically hinders the binding of the cations to N3.

Molecule 074 (2-(1-naphthylmethyl)-2-imidazoline) features a large naphthyl substituent at C2, adjacent to N3. Unlike in the case of the trityl substituent, the naphthyl substituent is separated from the imidazole ring by an  $sp^3$ -hybridized carbon. Since there is free rotation about the carbon bond, the naphthyl group can effectively swing out the way so as not to sterically hinder the binding of the cations at N3.

### 3.2.11– Imidazolidinones

Imidazolidinones are five-membered heterocycles containing two nitrogens and a carbonyl group. Tables 3.3 and 3.4 summarize the results.

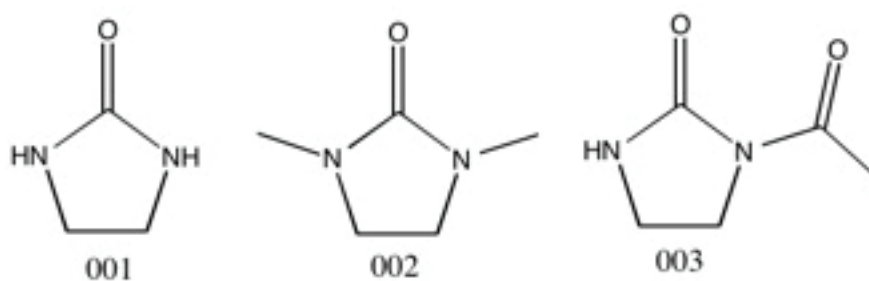


Figure 3.15: Structures for imidazolidinones.

Table 3.27: Gas-phase data for imidazolidinones binding with  $Zn^{2+}$ .

| Molecule | Energy of Drug<br>kcal/mol | Energy of Complex<br>kcal/mol | $\Delta$ Energy<br>kcal/mol | Interactions |
|----------|----------------------------|-------------------------------|-----------------------------|--------------|
| 001      | 8.638                      | -8.310                        | -16.948                     | 1            |
| 002      | 33.828                     | 19.784                        | -14.044                     | 1            |
| 003      | 17.896                     | 5.542                         | -12.354                     | 1            |

**Table 3.28: Gas-phase data for imidazolidinones binding with Ca<sup>2+</sup>.**

| Molecule | Energy of Drug<br>kcal/mol | Energy of Complex<br>kcal/mol | $\Delta$ Energy<br>kcal/mol | Interactions |
|----------|----------------------------|-------------------------------|-----------------------------|--------------|
| 001      | 8.638                      | -4.013                        | -12.651                     | 1            |
| 002      | 33.828                     | 23.551                        | -10.277                     | 1            |
| 003      | 17.896                     | 9.076                         | -8.820                      | 1            |

In general, these molecules were not very effective at binding either cation. This is most likely due to a loss of basicity at the nitrogens. A resonance structure can be drawn in which two electrons in the carbonyl double bond move to the oxygen. This means that there is a slight negative charge at the oxygen and a slight positive charge at the carbonyl carbon. The positive charge on C2 pulls electron density away from the nitrogens, decreasing their ability to act as a base and form an acid-base adduct with the metal cations. Also, instead of binding at nitrogen in the usual way, the partial negative charge on the oxygen interacts electrostatically with the cations to form weak attractions.

Molecules 001 (2-imidazolidinone) and 002 (1,3-dimethylimidazolidinone) interacted with the cations via the carbonyl oxygen inside the imidazole ring. Contrarily, 003 (1-acetyl-2-imidazolidinone) interacted with the cations via the peripheral carbonyl attached to N1. This is likely due to the inductive effect of the nitrogens. In 003, the carbonyl in the imidazole ring is flanked by two nitrogens, whereas the peripheral carbonyl only has one nitrogen neighbour. The ring carbonyl oxygen experiences more of an electron pull from two nitrogens than the peripheral carbonyl does from one nitrogen. Therefore, the peripheral carbonyl has more electron density on its oxygen to interact with the positively charged cations.

All in all, imidazolidinones are only marginally adept at binding  $Zn^{2+}$  and  $Ca^{2+}$ . The presence of the carbonyl next to N3 diminishes the basicity of the imidazole ring and prevents the cations from binding to it.

### 3.2.12– Imidazolidinethione

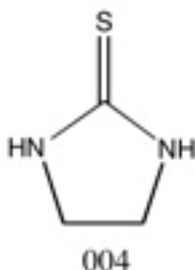


**Figure 3.16: Structure of imidazolidinethione.**

Imidazolidinethione (004) is an analogue of imidazolidinone in which the carbonyl oxygen is replaced with a sulfur atom. This molecule is worse at binding the cations than its oxygen-containing counterparts. As mentioned, the binding in imidazolidinones occurred via the carbonyl nitrogen due to oxygen's partial negative charge. Sulfur's electronegativity is lower than that of both oxygen and nitrogen. This means that the nitrogens will pull some electron density away from the sulfur, decreasing the partial negative charge compared to oxygen. This is corroborated by the fact that simulations in MOE with 004 show a  $\pi$ -type interaction. When the system was set up to be minimized, the cations were placed in the plane of the molecule three angstroms away from the imidazole nitrogen. After minimization, the cations moved to a position directly above the plane of the molecule about 2.6 angstroms from the middle of the ring. This is indicative of a weak  $\pi$ -type interaction. The binding energy for 004 was -6.315 kcal/mol

with  $\text{Zn}^{2+}$  and  $-4.277$  kcal/mol with  $\text{Ca}^{2+}$ , making imidazolidinethione a poor chelating agent for both cations.

### 3.2.13 – Benzimidazoles with Only Alkyl Substituents

Benzimidazoles (Figure 3.5) are a fusion of a benzene ring to C4 and C5 of imidazole. Data for benzimidazoles with only alkyl substituents interacting with zinc and calcium ions are listed in Tables 3.29 and 3.30.

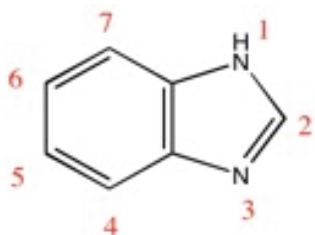


Figure 3.17: Benzimidazole.

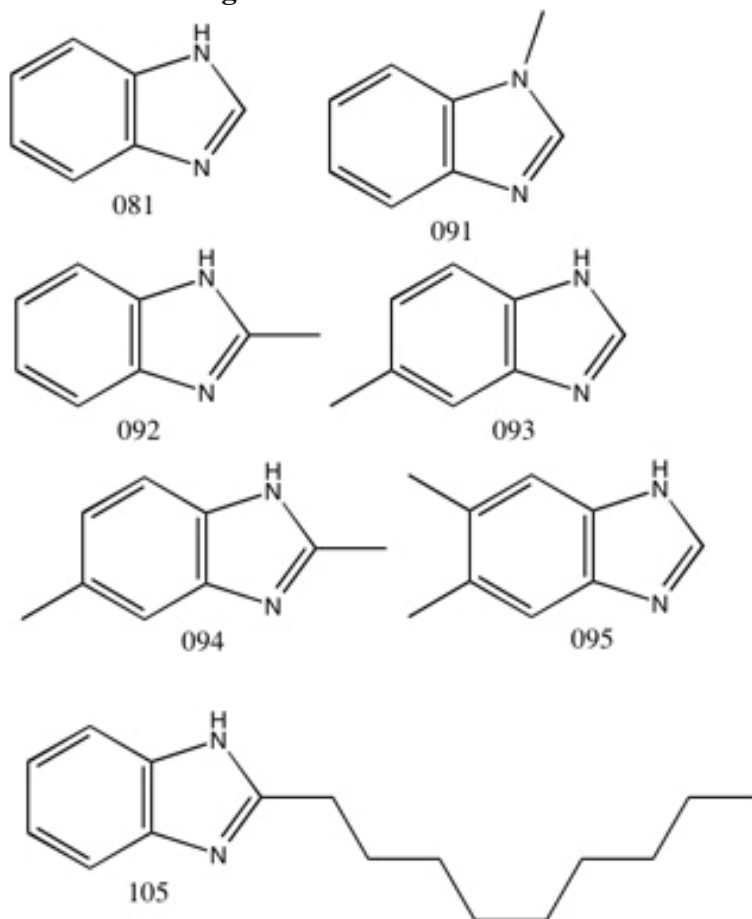


Figure 3.18: Structures for benzimidazoles with only alkyl substituents.

**Table 3.29: Gas-phase data for benzimidazoles with only alkyl substituents binding with Zn<sup>2+</sup>.**

| Molecule | Energy of Drug<br>kcal/mol | Energy of Complex<br>kcal/mol | $\Delta$ Energy<br>kcal/mol | Interactions |
|----------|----------------------------|-------------------------------|-----------------------------|--------------|
| 081      | 17.953                     | -6.507                        | -24.460                     | 1            |
| 091      | 50.312                     | 30.097                        | -20.215                     | N            |
| 092      | 16.042                     | -16.772                       | -32.814                     | 1            |
| 093      | 17.958                     | -8.790                        | -26.748                     | 1            |
| 094      | 15.967                     | -19.089                       | -35.056                     | 1            |
| 095      | 22.452                     | -5.227                        | -27.679                     | 1            |
| 105      | 28.595                     | -6.442                        | -35.037                     | 1            |

**Table 3.30: Gas-phase data for benzimidazoles with only alkyl substituents binding with Ca<sup>2+</sup>.**

| Molecule | Energy of Drug<br>kcal/mol | Energy of Complex<br>kcal/mol | $\Delta$ Energy<br>kcal/mol | Interactions |
|----------|----------------------------|-------------------------------|-----------------------------|--------------|
| 081      | 17.953                     | -1.946                        | -19.899                     | 1            |
| 091      | 50.312                     | 31.447                        | -18.865                     | N            |
| 092      | 16.042                     | -12.187                       | -28.229                     | 1            |
| 093      | 17.958                     | -4.260                        | -22.218                     | 1            |
| 094      | 15.967                     | -14.533                       | -30.500                     | 1            |
| 095      | 22.452                     | -1.376                        | -23.828                     | 1            |
| 105      | 28.595                     | -1.944                        | -30.539                     | 1            |

Molecule 081 is benzimidazole. It will be used as a reference point for the next several sections. The binding between benzimidazole and the cations occurs via electrostatic interactions at N3, similar to imidazoles. In fact, the binding energy of benzimidazole is quite a bit better than that of imidazole for both cations.

Molecules 091 (1-methylbenzimidazole), 092 (2-methylbenzimidazole) and 093 (5-methylbenzimidazole) all feature methyl substituents at different positions around the

ring system. Recall that, for imidazole, an alkyl substituent at N1 was very detrimental to the binding capability of the molecule. Similarly, 091 (which has a methyl group at N1), shows no binding with either cation. Correspondingly, 092 and 093 have methyl substituents at C2 and C5, respectively. As was the case with the imidazoles, these alkyl groups donate electron density to the ring system and increase the magnitude of the binding energy. Also note that 092, which has the methyl group adjacent to N3, has a better binding energy than 093, which has the methyl group several bonds away.

Molecule 094 (2,5-dimethylbenzimidazole) features a methyl group at C2 (like 092) and C5 (like 093). Not surprisingly, the binding energy for 094 is better than both 092 and 093 due to the extra electron-donating group. Similarly, 095 (5,6-dimethylbenzimidazole) has methyl groups at C5 and C6. The binding energy of 095 is larger in magnitude than that of 093 (which has a single methyl group at C5). Also, 095 has a smaller binding energy than 094 due to the location of the alkyl substituents. With the exception of N1, the closer the alkyl substituent is to N3, the better the resulting binding energy will be.

Molecule 105 (2-nonylbenzimidazole) has an extended alkyl group at C2. It has a less favourable binding energy than 092 (which has a methyl group at the same position), which may indicate some steric hindrance to cation binding. This effect is quite small.

### **3.2.14 – Benzimidazoles with Halide Substituents**

Next, selected benzimidazoles with halide substituents were analyzed. The results are summarized below in Tables 3.31 and 3.32.

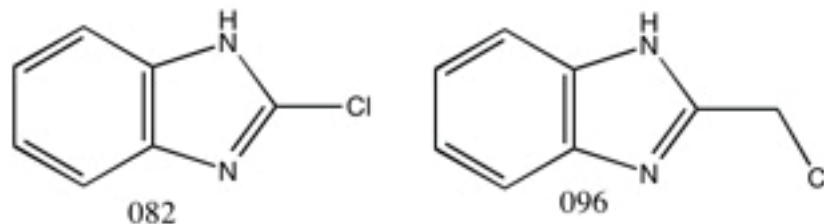


**Figure 3.19: Structures for benzimidazoles with halide substituents.**

**Table 3.31: Gas-phase data for benzimidazoles with halide substituents binding with Zn<sup>2+</sup>.**

| Molecule | Energy of Drug<br>kcal/mol | Energy of Complex<br>kcal/mol | ΔEnergy<br>kcal/mol | Interactions |
|----------|----------------------------|-------------------------------|---------------------|--------------|
| 082      | 17.994                     | -10.856                       | -28.850             | 1            |
| 096      | 18.619                     | -10.747                       | -29.366             | 1            |

**Table 3.32: Gas-phase data for benzimidazoles with halide substituents binding with Ca<sup>2+</sup>.**

| Molecule | Energy of Drug<br>kcal/mol | Energy of Complex<br>kcal/mol | ΔEnergy<br>kcal/mol | Interactions |
|----------|----------------------------|-------------------------------|---------------------|--------------|
| 082      | 17.994                     | -6.935                        | -24.929             | 1            |
| 096      | 18.619                     | -6.101                        | -24.720             | 1            |

Molecules 082 (2-chlorobenzimidazole) and 096 (2-(chloromethyl)-benzimidazole) both feature substituents containing chloride at C2. Halides are unique in that they can act as an electron-withdrawing group via induction, or as an electron-donating group via resonance. Because the binding energy of 082 is larger in magnitude than that of benzimidazole, it must be the resonance effect that dominates in this case. Figure 3.6 shows how a chloride substituent can donate one of its lone pairs to create a partial negative charge in the aromatic ring system.

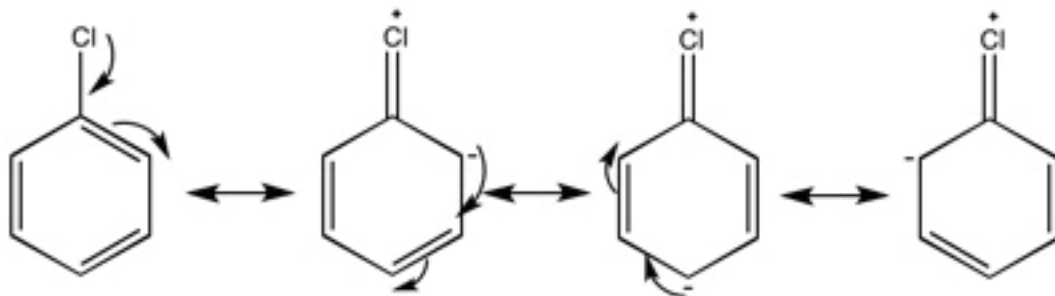


**Figure 3.20: Resonance of chloride in an aromatic ring.**

As the Figure indicates, the atom adjacent to the chloride experiences a partial negative charge. In the case of 082, this is enough to attract the cations and form an electrostatic interaction.

The resonance effect cannot take place in 096 because the chloride is one carbon removed from the aromatic ring system. This means that only the electron-withdrawing inductive effect will be active. In theory, the binding energy for 096 should be smaller for both zinc and calcium ions, compared to 082. This is true for  $\text{Ca}^{2+}$ , but not for  $\text{Zn}^{2+}$ . This particular simulation may be an anomaly.

### 3.2.15 – Benzimidazoles with Nitrogen-Containing Substituents

Simulations with benzimidazoles with nitrogen-containing substituents were also performed: these included nitro groups, piperidine, amino groups, cyano groups and pyrimidine. The data are summarized in Tables 3.33 and 3.34.

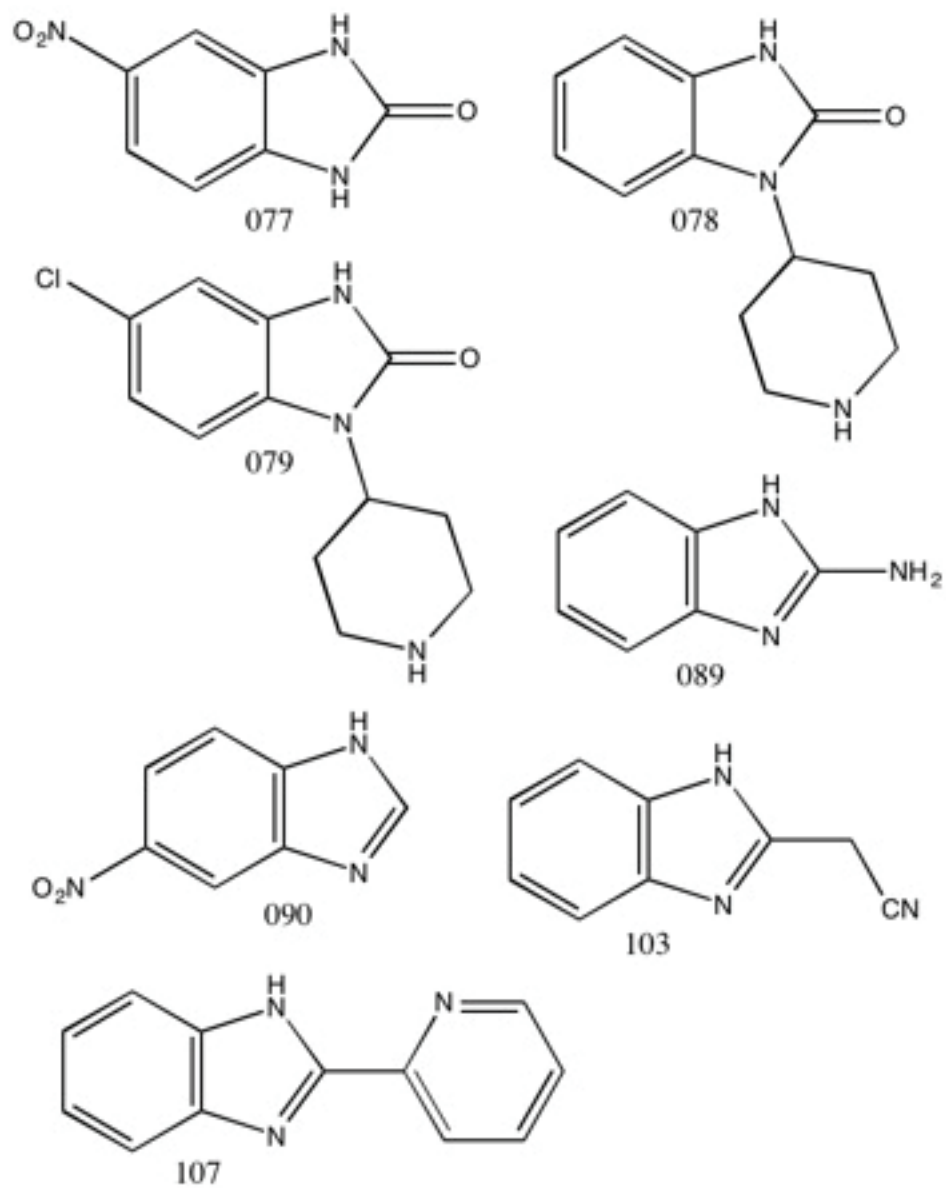


Figure 3.21: Structures for benzimidazoles with nitrogen-containing substituents.

**Table 3.33: Gas-phase data for benzimidazoles with nitrogen-containing substituents binding with Zn<sup>2+</sup>.**

| Molecule | Energy of Drug<br>kcal/mol | Energy of Complex<br>kcal/mol | ΔEnergy<br>kcal/mol | Interactions |
|----------|----------------------------|-------------------------------|---------------------|--------------|
| 077      | 52.148                     | 14.808                        | -37.340             | 1            |
| 078      | 65.123                     | 37.728                        | -27.395             | 1            |
| 079      | 65.241                     | 41.271                        | -23.970             | 1            |
| 089      | 19.921                     | 14.904                        | -5.017              | N            |
| 090      | 32.393                     | -2.164                        | -34.557             | 1            |
| 103      | 28.073                     | -16.089                       | -44.162             | 1            |
| 107      | 38.954                     | 14.334                        | -24.620             | 1            |

**Table 3.34: Gas-phase data for benzimidazoles with nitrogen-containing substituents binding with Ca<sup>2+</sup>.**

| Molecule | Energy of Drug<br>kcal/mol | Energy of Complex<br>kcal/mol | ΔEnergy<br>kcal/mol | Interactions |
|----------|----------------------------|-------------------------------|---------------------|--------------|
| 077      | 52.148                     | 17.504                        | -34.644             | 1            |
| 078      | 65.123                     | 40.371                        | -24.752             | 1            |
| 079      | 65.241                     | 44.096                        | -21.145             | 1            |
| 089      | 19.921                     | -13.874                       | -33.795             | N            |
| 090      | 32.393                     | 2.125                         | -30.268             | 1            |
| 103      | 28.073                     | -11.747                       | -39.820             | 1            |
| 107      | 38.954                     | 18.498                        | -20.456             | N            |

Molecules 077 (6-nitro-2-benzimidazolinone) and 090 (5-nitrobenzimidazole) have a nitro groups on C6 and C5, respectively. Benzimidazolinone is analogous to imidazolidinone, in that the C2 carbon is a carbonyl. Both of these molecules showed significant binding with both calcium and zinc ions. The resonance electron-withdrawal effect of the nitro group does not affect binding in either molecule because it is so far away from the binding site (the carbonyl oxygen for 077 and N3 for 090). Also note that

the benzimidazolinone (077) showed more efficient binding than the benzimidazole (090).

Molecules 078 (3-(4-piperidyl)-2-benzimidazolinone) and 079 (5-chloro-3-(4-piperidyl)-2-benzimidazolinone) each have a piperidine substituent on N3, blocking the normal binding site of the cations. Both 078 and 079 are benzimidazolinones, which have an alternate binding site at the carbonyl oxygen (as demonstrated by 077). Compared to the other benzimidazolinone (077), both 078 and 079 have a significantly less favourable binding energy. This indicates that the piperidine is detrimental to binding. Also the presence of the chloro substituent in 079 makes the binding energy even less favourable than 078 (which does not have a chloro group).

Molecule 089 (2-aminobenzimidazole) has an amino group adjacent to N3. As usual, the amino group is protonated at physiological pH. The positive charge on the amino nitrogen repels that cations and does not allow binding to take place. This is similar to the amino substituents on the imidazoles in section 3.2.4.

Molecule 103 (2-benzimidazolylacetonitrile) contains a cyano group one carbon removed from the aromatic ring system. Cyano groups that are directly attached to an aromatic ring system can exhibit an electron-withdrawing resonance effect. Since the cyano group is two bonds away from the benzimidazole ring, the resonance effect is muted. Instead, the cyano group further stabilizes the interaction between the cations and N3, as evidenced by the outstanding binding energy of 103.

Molecule 107 (2-(2-pyridyl)benzimidazole) features a pyridine substituent adjacent to N3. The pyridyl group has very little effect on the binding energy. This is indicated by the fact that the binding energy for 107 is nearly the same as that of bare

benzimidazole. As the tables above show,  $Zn^{2+}$  was able to bind with 107 at N3, but  $Ca^{2+}$  was not. Recall that  $Zn^{2+}$  has an ionic radius of 88 pm, while  $Ca^{2+}$  has an ionic radius of 114 pm. The pyridyl group is a fairly large group and may sterically hinder the binding of  $Ca^{2+}$ .

### 3.2.16 – Benzimidazoles with Oxygen-Containing Substituents

Next, benzimidazoles containing hydroxyl groups, ketone, aldehyde and carboxylic acid groups were tested. The results are summarized below in Tables 3.35 and 3.36.

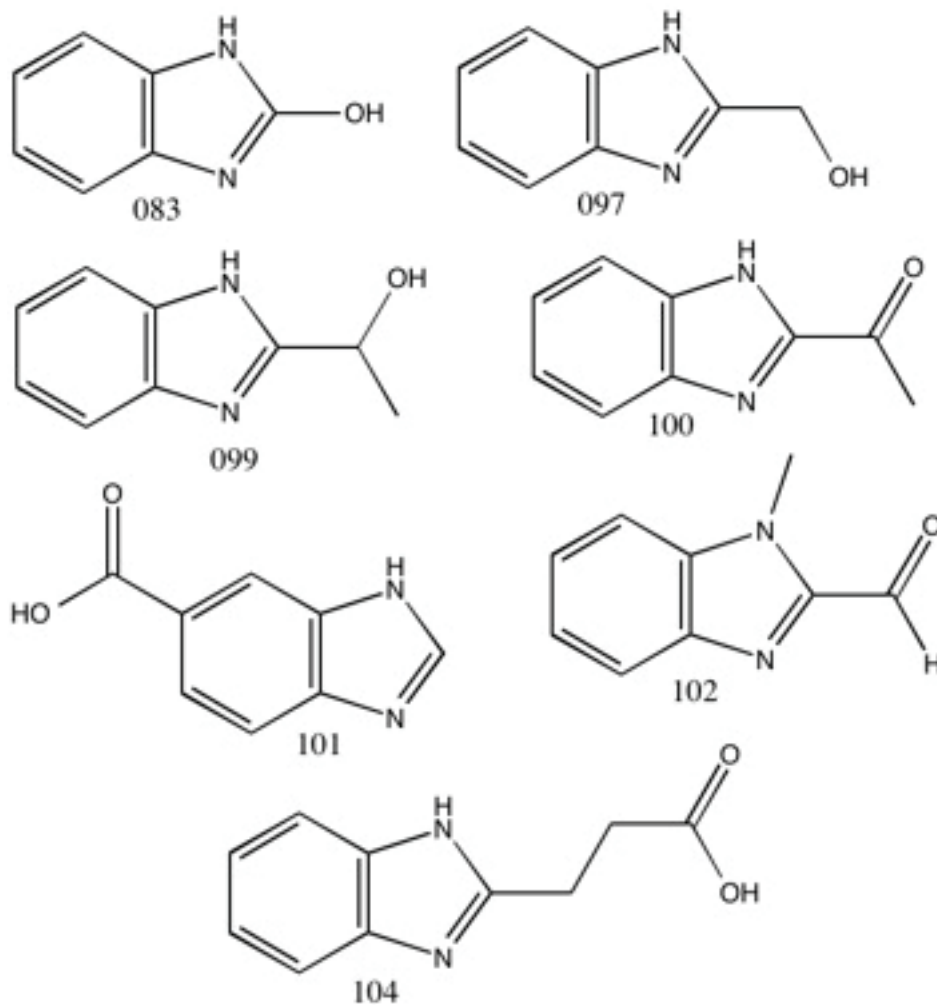


Figure 3.22: Structures for benzimidazoles with oxygen-containing substituents.

**Table 3.35: Gas-phase data for benzimidazoles with oxygen-containing substituents binding with Zn<sup>2+</sup>.**

| File Name | Energy of Drug<br>kcal/mol | Energy of Complex<br>kcal/mol | ΔEnergy<br>kcal/mol | Interactions |
|-----------|----------------------------|-------------------------------|---------------------|--------------|
| 083       | 19.527                     | -21.497                       | -41.024             | 1            |
| 097       | 20.605                     | -7.880                        | -28.485             | 2            |
| 099       | 19.881                     | 5.150                         | -14.731             | 1            |
| 100       | 20.802                     | 12.836                        | -7.966              | 1            |
| 101       | 33.054                     | -61.967                       | -95.021             | 1            |
| 102       | 46.445                     | 29.210                        | -17.235             | 1            |
| 104       | 27.488                     | -72.022                       | -99.510             | 1            |

**Table 3.36: Gas-phase data for benzimidazoles with oxygen-containing substituents binding with Ca<sup>2+</sup>.**

| Molecule | Energy of Drug<br>kcal/mol | Energy of Complex<br>kcal/mol | ΔEnergy<br>kcal/mol | Interactions |
|----------|----------------------------|-------------------------------|---------------------|--------------|
| 083      | 19.527                     | -17.096                       | -36.623             | 1            |
| 097      | 20.605                     | -0.201                        | -20.806             | 2            |
| 099      | 19.881                     | 9.187                         | -10.694             | 1            |
| 100      | 20.802                     | 16.547                        | -4.255              | 1            |
| 101      | 33.054                     | -48.293                       | -81.347             | 1            |
| 102      | 46.445                     | 32.359                        | -14.086             | 1            |
| 104      | 27.488                     | -57.752                       | -85.240             | 1            |

Molecules 083 (2-hydroxylbenzimidazole), 097 ((1H-benzimidazol-2-yl)methanol) and 099 (2-(1H-hydroxyethyl)benzimidazole) all have a hydroxyl substituent at C2, adjacent to N3. Recall that hydroxyl groups are proficient electron donating groups. This is evidenced by the binding energy of 083, which is significantly better than benzimidazole. In 097, the hydroxyl group is one carbon removed from the ring system. Instead of donating electrons as it did in 083, it withdraws electron density from the ring via induction. This explains the binding energy being slightly smaller in

magnitude than that of benzimidazole. Furthermore, 097 acts as a bidentate ligand for both cations. The free rotation about the  $sp^3$ -hybridized carbon on the hydroxyl substituent allows for the oxygen to orient itself in space in such a way that it can interact with the cations in the N3 binding site.

Contrary to 097, when the lowest energy conformation of 099 was identified, the hydroxyl group was facing away from the binding site of zinc and calcium ions. Instead of stabilizing the interaction between N3 and the cation, the hydroxyl group only acts as an inductive electron-withdrawing group. This explains the binding energy of 097 being much more favourable than that of 099.

Molecules 100 (2-acetylbenzimidazole) and 102 (1-methyl-1H-benzimidazol-2-carbaldehyde) contain a ketone and an aldehyde functionality at C2, adjacent to the N3 binding site. In both cases, the carbonyl acts as a moderate electron-withdrawing group. Both molecules have a binding energy that is less favourable than that of benzimidazole. Furthermore, 102 has a more favourable binding energy than 100, indicating that the keto group is a more effective electron-withdrawing group. This is because the extra carbon on the ketone helps to stabilize the partial positive charge on the carbonyl carbon.

As was the case with the imidazoles, the carboxylic acid-containing benzimidazoles were the most proficient at binding both calcium and zinc ions. As before, the carboxylic acids were manually deprotonated before running the simulations to produce a negatively charged carboxylate group, an ideal binding site for the cations. 101 (6-benzimidazolecarboxylic acid) and 104 (2-benzimidazolepropionic acid) each contain a carboxylate at C5 and C2, respectively. In both cases, the binding took place at the negatively charged carboxylate group. Note that the carboxylate group in 101 is quite

far away in space from N3. Despite the system being arranged such that the cation was placed in the plane of the ring system three angstroms away from N3, when minimized, the cations migrated to the other side of the molecule to form a strong electrostatic interaction with the carboxylate group. In 104, the carboxylate was two carbons removed from the ring system. Despite being fairly close in space to N3, there was no bidentate-type ligand interaction in this molecule. Instead, the cation migrated to the carboxylate, as it did in 101.

### 3.2.17 – Benzimidazoles with Sulfur-Containing Substituents

Benzimidazoles containing sulfur-base functional groups were also tested. The results are listed in Tables 3.37 and 3.38.

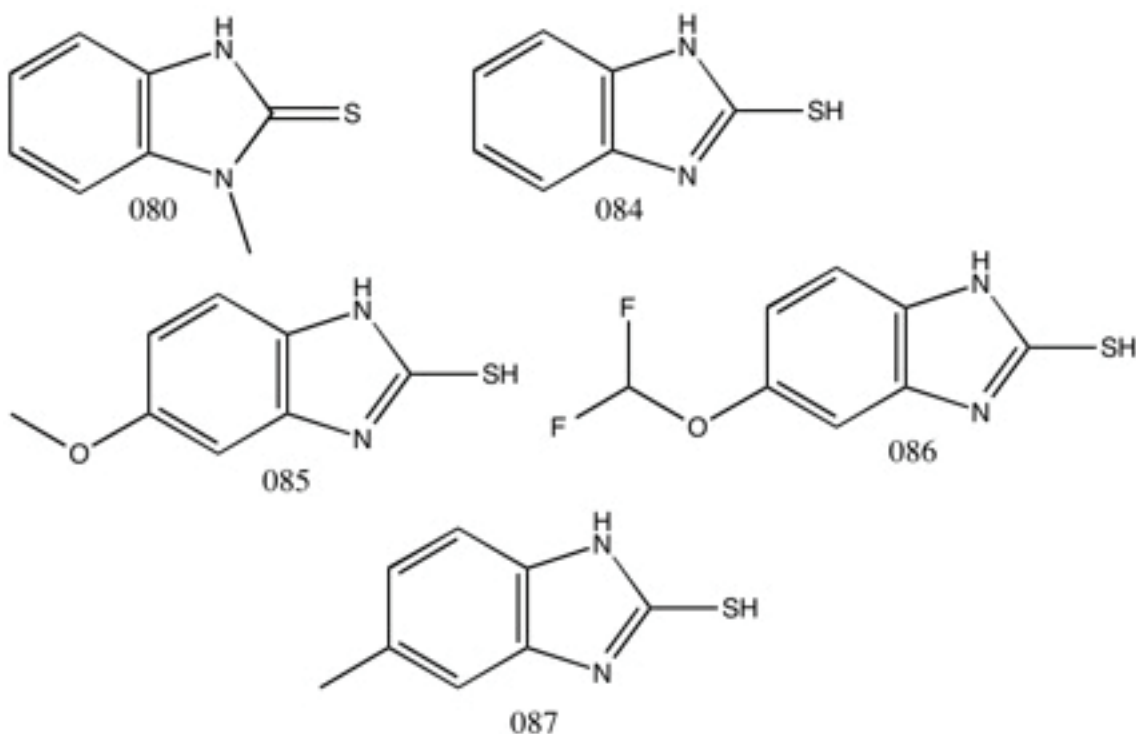


**Figure 3.23: Structures for benzimidazoles with sulfur-containing substituents.**

**Table 3.37: Gas-phase data for benzimidazoles with sulfur-containing substituents binding with Zn<sup>2+</sup>.**

| Molecule | Energy of Drug<br>kcal/mol | Energy of Complex<br>kcal/mol | ΔEnergy<br>kcal/mol | Interactions |
|----------|----------------------------|-------------------------------|---------------------|--------------|
| 080      | 62.936                     | 37.265                        | -25.671             | N            |
| 084      | 24.335                     | -12.799                       | -37.134             | 1            |
| 085      | 36.258                     | -13.122                       | -49.380             | 1            |
| 086      | 32.647                     | -17.428                       | -50.075             | 1            |
| 087      | 24.224                     | -15.159                       | -39.383             | 1            |

**Table 3.38: Gas-phase data for benzimidazoles with sulfur-containing substituents binding with Ca<sup>2+</sup>.**

| Molecule | Energy of Drug<br>kcal/mol | Energy of Complex<br>kcal/mol | ΔEnergy<br>kcal/mol | Interactions |
|----------|----------------------------|-------------------------------|---------------------|--------------|
| 080      | 62.936                     | 39.567                        | -23.369             | N            |
| 084      | 24.335                     | -8.349                        | -32.684             | 1            |
| 085      | 36.258                     | -8.926                        | -45.184             | 1            |
| 086      | 32.647                     | -13.352                       | -45.999             | 1            |
| 087      | 24.224                     | -10.741                       | -34.965             | 1            |

Molecule 080 (1-methyl-1H-benzimidazole-2-thione) is the sulfur analogue of benzimidazolinone (i.e. there is a sulfur in place of the carbonyl oxygen). In 080, a methyl group is attached to N3. Though it is a small substituent, it is directly on the binding site and may sterically hinder binding of the cations. This is corroborated by the lack of binding with 080.

Molecule 084 (2-mercaptobenzimidazole) features a mercapto group on the carbon adjacent to N3. The mercapto group acts as a moderate electron-donating group and increases electron density in the imidazole ring. This results in stronger binding with

the cations, as evidenced by their binding energies, which are more favourable than benzimidazole itself.

Molecules 085 (5-methoxy-2-benzimidazolethiol), 086 (5-(difluoromethoxy)-2-mercapto-1H-benzimidazole) and 087 (2-mercapto-5-methylbenzimidazole) all also feature a mercapto group at C2. They also each feature a different substituent at C5. 087 has a methyl group at C5, which slightly improves the binding energy as compared to 084. This is expected because of the methyl group's weak electron-donating ability. 085 and 086 both have ether groups at C5. Ethers are stronger electron donors than alkyl groups. This is confirmed by the fact that the binding energy for 086 is more favourable than that of 085.

### 3.2.18 – Benzimidazoles with Phenyl Substituents

Two benzimidazoles with phenyl substituents were studied next. The results are summarized in Tables 3.39 and 3.40.

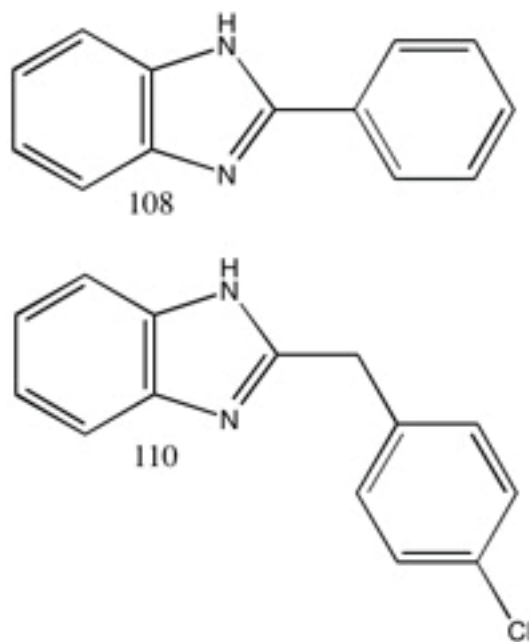


Figure 3.24: Structures for benzimidazoles with only alkyl substituents.

**Table 3.39: Gas-phase data for benzimidazoles with phenyl substituents binding with Zn<sup>2+</sup>.**

| Molecule | Energy of Drug<br>kcal/mol | Energy of Complex<br>kcal/mol | $\Delta$ Energy<br>kcal/mol | Interactions |
|----------|----------------------------|-------------------------------|-----------------------------|--------------|
| 108      | 34.514                     | 8.795                         | -25.719                     | 1            |
| 110      | 31.003                     | -4.640                        | -35.643                     | 1+P          |

**Table 3.40: Gas-phase data for benzimidazoles with phenyl substituents binding with Ca<sup>2+</sup>.**

| Molecule | Energy of Drug<br>kcal/mol | Energy of Complex<br>kcal/mol | $\Delta$ Energy<br>kcal/mol | Interactions |
|----------|----------------------------|-------------------------------|-----------------------------|--------------|
| 108      | 34.514                     | 13.451                        | -21.063                     | 1            |
| 110      | 31.003                     | 0.669                         | -30.334                     | 1+P          |

Molecule 108 (2-phenylbenzimidazole) features a phenyl substituent adjacent to N3. The weak electron-donating effect of the phenyl ring helps to improve the binding energy slightly as compared to benzimidazole.

In molecules 110 (2-(4-chlorobenzyl)benzimidazole), the phenyl group is one carbon removed from the ring. The free rotation about the extra sp<sup>3</sup> hybridized carbon allows the phenyl ring to orientate itself in space to bind with the cations via a  $\pi$ -type interaction. Also, the free rotation prevents the phenyl group from sterically hindering the binding of zinc and calcium ions; they are both able to bind at N3. The extra stabilizing effect of the  $\pi$ -type interaction improves the binding energy as compared to 108.

### 3.2.19 – Exceptions and Atypical Imidazoles

In this section, the results of imidazoles that did not fit into one of the previous categories will be summarized. The results are tabulated in Tables 3.41 and 3.42.

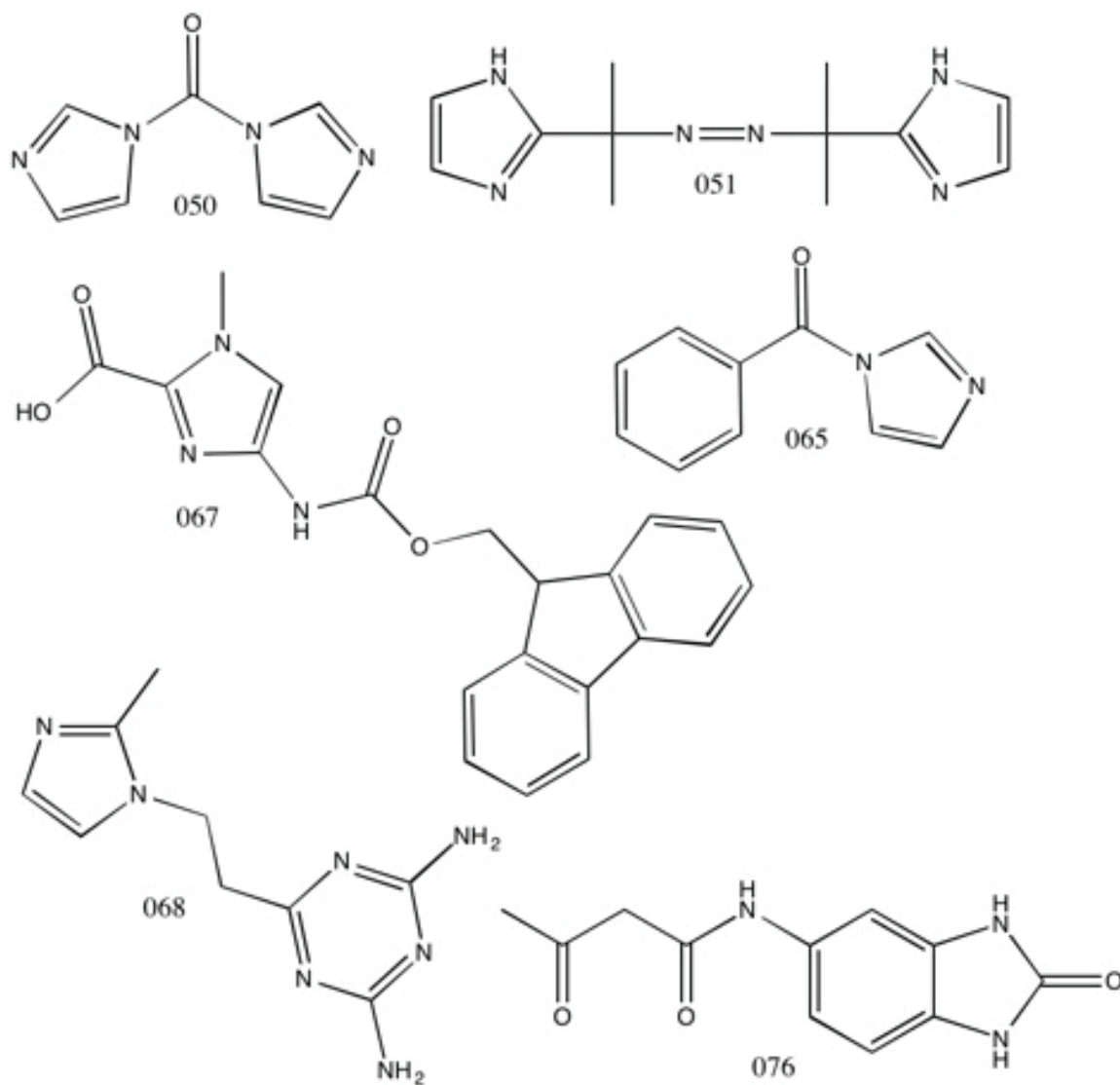


Figure 3.25: Structures for atypical imidazoles.

**Table 3.41: Gas-phase data for atypical imidazoles binding with Zn<sup>2+</sup>.**

| Molecule | Energy of Drug<br>kcal/mol | Energy of Complex<br>kcal/mol | $\Delta$ Energy<br>kcal/mol | Interactions |
|----------|----------------------------|-------------------------------|-----------------------------|--------------|
| 050      | 87.451                     | 32.279                        | -55.172                     | N            |
| 051      | 33.787                     | -12.059                       | -45.846                     | 2            |
| 065      | 61.391                     | 27.399                        | -33.992                     | 1            |
| 067      | 112.024                    | 19.563                        | -92.461                     | 1            |
| 068      | 82.383                     | 27.805                        | -54.578                     | N            |
| 076      | 27.974                     | -12.659                       | -40.633                     | 1            |

**Table 3.42: Gas-phase data for atypical imidazoles binding with Ca<sup>2+</sup>.**

| Molecule | Energy of Drug<br>kcal/mol | Energy of Complex<br>kcal/mol | $\Delta$ Energy<br>kcal/mol | Interactions |
|----------|----------------------------|-------------------------------|-----------------------------|--------------|
| 050      | 87.451                     | 32.202                        | -55.249                     | N            |
| 051      | 33.787                     | -0.927                        | -34.714                     | 2            |
| 065      | 61.391                     | 30.806                        | -30.585                     | 1            |
| 067      | 112.024                    | 30.992                        | -81.032                     | 1            |
| 068      | 82.383                     | 27.324                        | -55.059                     | N            |
| 076      | 27.974                     | -9.148                        | -37.122                     | 1            |

050 (N,N'-carbonylimidazole) is essentially two imidazoles connect by a carbonyl bridge at N1. No binding occurred for either cation during the molecular mechanics simulations. This may be due to the electron withdrawing effect of the carbonyl group. Also, recall that substituents on N1 tend to inhibit binding at N3.

Molecule 065 (N-benzoylimidazole) is similar to 050, except that one of the imidazole rings is replaced with a phenyl ring. Unlike 050, both cations were able to bind to 065 via the carbonyl oxygen. This interaction is stronger than that of imidazole.

Molecule 051 (2,2'-azobis[2-(2-imidazolin-2-yl)propane]) features two imidazoles bridged via C5 by an azobis group. The imidazole rings are arranged in such

a way that they are able to act as a bidentate ligand for both cations. The molecule essentially pinches the cations between N3 on both imidazole rings. 051 shows better binding than imidazole itself.

Molecule 067 (4-(Fmoc-amino)-1-methyl-1H-imidazole-2-carboxylic acid) showed a very favourable binding energy with calcium and zinc ions. As with all other molecules featuring a carboxylate group, the cations bound to 067 via the negatively charged oxygen. This is an ionic interaction.

Molecule 068 (2,4-diamino-6-[2-(2-methyl-1-imidazol-1-yl)ethyl]-1,3,5-triazine) features two protonate amino groups. The positive charge of these substituents repel the cations and no binding takes place, as expected.

Molecule 076 (5-acetoacetamido-2-benzimidazolinone) is a benzimidazolinone derivative that features a consecutive amido and carbonyl substituent on C6. The binding for 076 occurs via the carbonyl oxygen in the imidazole ring. This interaction is stronger than that of bare benzimidazole.

### ***3.3 – Solvation Simulations of Imidazoles with $Zn^{2+}$ and $Ca^{2+}$***

Once the gas-phase simulations were complete, solvation simulations were pursued with some of the more promising molecules. The cut-offs to move on to this stage are the following: for imidazoles, any molecule that bound both  $Zn^{2+}$  and  $Ca^{2+}$ , and exhibited a stronger binding energy than imidazole itself moved on to the solvation studies. For benzimidazoles, any molecule that bound both  $Zn^{2+}$  and  $Ca^{2+}$ , and exhibited a more favourable binding energy than benzimidazole itself moved on to solvation studies. The method described in section 2.2 was used to evaluate each molecule in a

water solvent box to mimic the aqueous environment of the blood. In some cases, the presence of water molecules altered or prevented binding of zinc and calcium ions. In this section, the interactions between the molecules and cations in solvent will be summarized and rationalized.

### 3.3.1 – Imidazoles with Only Alkyl Substituents in Water

As before, imidazoles with only alkyl substituents were tested first. The results are summarized in Tables 3.43 and 3.44. Refer to Figure 3.1 for structures.

**Table 3.43: Solvation data for imidazoles with alkyl substituents binding with Zn<sup>2+</sup>.**

| Molecule | Energy of Drug<br>kcal/mol | Energy of Complex<br>kcal/mol | ΔEnergy<br>kcal/mol | Interactions |
|----------|----------------------------|-------------------------------|---------------------|--------------|
| 000      | -0.329                     | -12.123                       | -11.794             | 1            |
| 017      | -8.785                     | -19.544                       | -10.759             | 1            |
| 018      | -6.754                     | -16.585                       | -9.831              | N            |
| 020      | 27.419                     | 24.998                        | -2.421              | N            |
| 021      | 11.155                     | -3.303                        | -14.458             | N            |
| 047      | -5.308                     | -23.729                       | -18.421             | 1            |

**Table 3.44: Solvation data for imidazoles with alkyl substituents binding with Ca<sup>2+</sup>.**

| Molecule | Energy of Drug<br>kcal/mol | Energy of Complex<br>kcal/mol | ΔEnergy<br>kcal/mol | Interactions |
|----------|----------------------------|-------------------------------|---------------------|--------------|
| 000      | -0.329                     | -12.128                       | -11.799             | 1            |
| 017      | -8.785                     | -15.578                       | -6.793              | N            |
| 018      | -6.754                     | -17.297                       | -10.543             | 1            |
| 020      | 27.419                     | 23.722                        | -3.697              | N            |
| 021      | 11.155                     | 5.363                         | -5.792              | 1            |
| 047      | -5.308                     | -14.461                       | -9.153              | N            |

Molecule 000 (imidazole) showed binding with both zinc and calcium ions. Not surprisingly, the addition of a solvent reduced the magnitude of the binding energy as

compared to the gas-phase simulations. The water molecules surrounding the system being studied have several effects. First, the water has a small inductive effect that removes electron density from the imidazole ring. Secondly, the water molecules can form hydrogen bonds with many of the functional groups present in the molecules being tested. Depending on the location and number of hydrogen bonds, the effects on binding energy vary.

Molecule 017 (2-methylimidazole) maintained its ability to chelate  $\text{Zn}^{2+}$ , but not  $\text{Ca}^{2+}$ , in the presence of solvent. In the case of  $\text{Zn}^{2+}$ , at the beginning of the simulation, the cation migrated directly toward the N3 binding site. Two water molecules stabilized the ligand-cation interaction. Also, hydrogen bonding occurred between the oxygen of a water molecule and the hydrogen on N1. In the case of  $\text{Ca}^{2+}$ , when the simulation began, several water molecules immediately solvated the cation. The cation was then unable to migrate to the N3 binding site. This was a common problem in the solution-phase simulations. Each time the periodic solvent box is created, the water molecules are placed at slightly different coordinates in 3-dimensional space. The arrangement of water molecules near the binding site can determine whether the cation binds to the molecule being tested or is solvated by a number of water molecules.

Molecule 018 (4-methylimidazole) maintained its ability to chelate  $\text{Ca}^{2+}$ , but not  $\text{Zn}^{2+}$ , in the presence of solvent. In the case of  $\text{Zn}^{2+}$ , at the beginning of the simulation, it was snatched up and solvated by neighbouring water molecules. In the case of  $\text{Ca}^{2+}$ , the cation immediately migrated to the binding site and two water molecules stabilized the interaction. Once again, hydrogen bonding occurred at N1.

Molecule 020 (1-butylimidazole) was unable to chelate either cation in the presence of solvent. Recall that alkyl substituents on N1 are very detrimental to the binding capability of imidazoles. In the gas-phase simulations for 020, the electron donating effect of the butyl group was enough to facilitate an interaction between the molecule and the cations. However, under the more strict conditions of the solvation study, no binding occurred for either cation.

Molecule 021 (2-undecylimidazole) maintained its ability to chelate  $\text{Ca}^{2+}$ , but not  $\text{Zn}^{2+}$ , in the presence of solvent. It was hypothesized that the large, non-polar alkyl chain on C2 would repel the polar water molecules and essentially clear the region of the binding site so that both cations could interact with N3. Unfortunately, in the lowest-energy conformation given by MOE, the undecyl group points away from the binding site and water molecules were able to pull  $\text{Zn}^{2+}$  away before an electrostatic interaction could form with the molecule.  $\text{Ca}^{2+}$ , on the other hand, immediately migrated to N3 and was stabilized by three water molecules.

Molecule 047 (2-ethyl-4-methylimidazole) maintained its ability to chelate  $\text{Zn}^{2+}$ , but not  $\text{Ca}^{2+}$ , in the presence of solvent. Similar to 021, it was hypothesized that the presence of two alkyl groups on the carbons adjacent to N3 might deter water molecule from entering the binding region. Unfortunately, the methyl and ethyl groups are too small to have any deterrent effect. In the end,  $\text{Ca}^{2+}$  was pulled away from the binding site and solvated, while  $\text{Zn}^{2+}$  formed an electrostatic interaction that was stabilized by two water molecules.

### 3.3.2 – Imidazoles with Nitrogen-Containing Substituents in Water

Next, solvation studies were carried out using imidazoles with nitrogen-containing substituents. The results are tabulated in Tables 3.45 and 3.46. Refer to Figure 3.3, 3.6 and 3.8 for structures.

**Table 3.45: Solvation data for imidazoles with nitrogen-containing substituents binding with Zn<sup>2+</sup>.**

| Molecule | Energy of Drug<br>kcal/mol | Energy of Complex<br>kcal/mol | $\Delta$ Energy<br>kcal/mol | Interactions |
|----------|----------------------------|-------------------------------|-----------------------------|--------------|
| 012      | 4.960                      | -6.502                        | -11.462                     | 1            |
| 013      | 7.237                      | -7.908                        | -15.145                     | 2            |
| 014      | -4.635                     | -20.757                       | -16.122                     | 1            |
| 015      | 31.504                     | 31.083                        | -0.421                      | N            |
| 038      | 11.531                     | 1.109                         | -10.422                     | 1            |

**Table 3.46: Solvation data for imidazoles with nitrogen-containing substituents binding with Ca<sup>2+</sup>.**

| Molecule | Energy of Drug<br>kcal/mol | Energy of Complex<br>kcal/mol | $\Delta$ Energy<br>kcal/mol | Interactions |
|----------|----------------------------|-------------------------------|-----------------------------|--------------|
| 012      | 4.960                      | -2.113                        | -7.073                      | 1            |
| 013      | 7.237                      | -4.081                        | -11.318                     | 2            |
| 014      | -4.635                     | -11.681                       | -7.046                      | 1            |
| 015      | 31.504                     | 29.188                        | -2.316                      | 1            |
| 038      | 11.531                     | 3.046                         | -8.485                      | N            |

Molecules 012 (2-nitroimidazole), 013 (4-nitroimidazole) and 014 (2-methyl-5-nitroimidazole) all maintained their ability to chelate both zinc and calcium ions in the solution phase. In 012 the electrostatic interaction took place at the negatively charged nitrogen of the nitro group. Even though the cation was placed next to N3, the proximity

of the nitro group allowed for the cation to be drawn away. The interactions were stabilized by two water molecules.

Unlike molecule 012, the binding with 014 took place at N3. In 014, the nitro group is three bonds away from N3. The attraction of the negative charge is not enough for the cation to migrate to the other side of the molecule. Instead, the nitro group's electron-withdrawing effect is lessened by hydrogen bonding with water molecules (i.e. the hydrogens in water donate some electron density to the nitro group).

Molecule 013 acted as a bidentate ligand for both cations. Like in 012, the nitro group in 013 is on the carbon adjacent to N3. The proximity of the negative charge to the binding site allowed for an electrostatic interaction to occur. Unlike in 012, 013 also chelated both cations via N3.

Molecule 015 (1,2-dimethyl-5-nitroimidazole) maintained its ability to bind  $\text{Ca}^{2+}$ , but not  $\text{Zn}^{2+}$ , in solvent. The nitro group in 015 sits on C5, three bonds away from N3. Like in 014, the cations did not migrate to the negative charge on the nitro oxygen. As usual, the alkyl substituent on N1 significantly affects the binding energy (as compared to 014, which only differs from 015 by a methyl group on N1). The interaction with  $\text{Ca}^{2+}$  was stabilized by two water molecules and multiple hydrogen bonds occurred at the nitro group.

Molecule 038 (4,5-imidazolecarboxamide) is the only amide in this group. As indicated in the tables above, 038 maintained its ability to chelate  $\text{Zn}^{2+}$ , but not  $\text{Ca}^{2+}$ . The interaction with  $\text{Zn}^{2+}$  occurred via N3 and was stabilized by one water molecule. Also, multiple hydrogen bonds formed with the two amido groups.

### 3.3.3 – Imidazoles with Oxygen-Containing Substituents in Water

Imidazoles with oxygen-containing function groups were also tested. The results are summarized in Tables 3.47 and 3.48. Refer to Figure 3.9, 3.10 and 3.11 for structures.

**Table 3.47: Solvation data for imidazoles with oxygen-containing substituents binding with Zn<sup>2+</sup>.**

| Molecule | Energy of Drug<br>kcal/mol | Energy of Complex<br>kcal/mol | ΔEnergy<br>kcal/mol | Interactions |
|----------|----------------------------|-------------------------------|---------------------|--------------|
| 026      | 2.376                      | -5.412                        | -7.788              | 1            |
| 027*     | -6.370                     | -62.156                       | -55.786             | 1            |
| 030      | 35.916                     | 36.285                        | 0.369               | N            |
| 031      | 0.492                      | -6.226                        | -6.718              | N            |
| 032      | -0.718                     | -13.694                       | -12.976             | 1            |
| 033      | -0.148                     | -12.127                       | -11.979             | 1            |
| 034      | 10.749                     | -10.161                       | -20.910             | 1            |
| 036*     | 25.391                     | -47.170                       | -72.561             | 1            |
| 037      | 15.119                     | 2.950                         | -12.169             | 1            |
| 045      | 6.365                      | -4.872                        | -11.237             | N            |

**Table 3.48: Solvation data for imidazoles with oxygen-containing substituents binding with Ca<sup>2+</sup>.**

| Molecule | Energy of Drug<br>kcal/mol | Energy of Complex<br>kcal/mol | ΔEnergy<br>kcal/mol | Interactions |
|----------|----------------------------|-------------------------------|---------------------|--------------|
| 026      | 2.376                      | -4.620                        | -6.996              | N            |
| 027*     | -6.370                     | -64.366                       | -57.996             | 1            |
| 030      | 35.916                     | 28.276                        | -7.640              | 1            |
| 031      | 0.492                      | -4.232                        | -4.724              | 1            |
| 032      | -0.718                     | -10.790                       | -10.072             | 1            |
| 033      | -0.148                     | -10.284                       | -10.136             | 1            |
| 034      | 10.749                     | -5.790                        | -16.539             | 1            |
| 036*     | 25.391                     | -31.657                       | -61.738             | 1            |
| 037      | 15.119                     | 11.210                        | -3.909              | N            |
| 045      | 6.365                      | -10.062                       | -16.427             | 1            |

\*indicates when the simulation was set up with the dithiocarboxylate as the binding site

026 (4-hydroxymethylimidazole) and 045 (5-methyl-4-hydroxymethylimidazole) both feature hydroxyl groups. In the solution phase, 026 was able to chelate  $\text{Zn}^{2+}$ , but not  $\text{Ca}^{2+}$ . This appears to be another case of the solvent being inconveniently arranged in space for the  $\text{Ca}^{2+}$  simulation because it was immediately taken away from the binding site and solvated by water molecules.  $\text{Zn}^{2+}$ , on the other hand, ended up bound to N3 and stabilized by two water molecules. In both case, hydrogen bonding occurred at the hydroxyl group.

Recall that in the gas-phase simulations, 045 acted as a bidentate ligand, via the N3 and the hydroxyl oxygen, for both cations. In the solution phase, the hydroxyl group was the site of hydrogen bonding and did not participate in the binding of  $\text{Ca}^{2+}$ . Instead,  $\text{Ca}^{2+}$  interacted solely with N3 and was stabilized by three water molecules. In the  $\text{Zn}^{2+}$  simulation, the cation was immediately solvated.

Molecules 030 (1-methyl-2-imidazolecarbaldehyde), 031 (2-methyl-4-formylimidazole), 032 (4-methyl-5-imidazolecarbaldehyde), 033 (2-ethyl-4-methyl-5-imidazolecarbaldehyde) and 034 (2-butyl-5-chloro-1H-imidazole-4-carbaldehyde) all contain an aldehyde group. All molecules in this group were able to chelate  $\text{Ca}^{2+}$ . All except 030 interacted with the cations via N3. The electrostatic interaction with 030 occurred at the carbonyl oxygen. All molecules in this group except 030 and 031 were able to bind  $\text{Zn}^{2+}$ .

Molecules 030 and 031 both had the aldehyde group on a carbon adjacent to N3. In 030, the lowest-energy conformation had the carbonyl oxygen orientated near enough to the binding site that the partial negative charge on the oxygen of the carbonyl was able to steal the calcium cation away from N3. Two water molecules stabilized this

interaction and hydrogen bonding occurred at N1. Conversely, in 031 the carbonyl oxygen was pointed away from the binding site in the lowest energy conformation, so  $\text{Ca}^{2+}$  was not able to bind to it. Instead, the carbonyl oxygen was the site of hydrogen bonding and the interaction between N3 and the cation was stabilized by one water molecule.

In molecules 032, 033 and 034, the carbonyl sits on C5, far away from the binding site. Unlike for 030 and 031,  $\text{Zn}^{2+}$  was able to bind with all of the aforementioned molecules. It may be true that aldehydes on carbons adjacent to the N3 binding site are detrimental to zinc binding specifically.

Molecule 037 (methyl-5-imidazolecarboxylate) is the only ester in this group. As indicated above, this molecule retained its ability to chelate  $\text{Zn}^{2+}$ , but not  $\text{Ca}^{2+}$ . This was another case of one of the cations being taken away by water molecules, while the other immediately migrated to N3.

Molecules 027 (imidazole-5-acetic acid) and 036 (4-imidazolecarboxylic acid) each contain a deprotonated carboxylate group. For both molecules in the gas phase, the primary interaction with the cations took place at the carboxylate group. For completeness, the simulations were performed in the usual way (with the cation three angstroms from N3), and separate simulations were performed with the cation three angstroms away from the carboxylate oxygens. In both cases, the cation being placed near the carboxylate led to the more favourable binding energy, so those values are reported in the tables above.

In molecule 027, the carboxylate sits on C5, away from the N3 binding site. As mentioned, binding took place at the carboxylate oxygen and was very favourable (as

evidenced by the binding energy). At the end of these simulations, the ligand-cation interaction was stabilized by four water molecules.

In molecule 036, the carboxylate sits on C4, adjacent to the N3 binding site. At the outset, it was hypothesized that 036 would act as a bidentate ligand, but it did not. Instead, binding occurred solely through the carboxylate group. In the case of  $Zn^{2+}$ , the interaction was stabilized by four water molecules, while five water molecules stabilized  $Ca^{2+}$ . Thus far, 036 is the only molecule to improve its binding energy on going from gas-phase to solution-phase simulations. This is likely due to the negative charge on the carboxylate group being stabilized by hydrogen bonds from water.

### 3.3.4 – Imidazoles with Sulfur-Containing Substituents in Water

Next, imidazoles with sulfur-containing substituents were evaluated. The results are listed below in Tables 3.49 and 3.50. Refer to Figure 3.12 for structures.

**Table 3.49: Solvation data for imidazoles with sulfur-containing substituents binding with  $Zn^{2+}$ .**

| Molecule | Energy of Drug<br>kcal/mol | Energy of Complex<br>kcal/mol | $\Delta$ Energy<br>kcal/mol | Interactions |
|----------|----------------------------|-------------------------------|-----------------------------|--------------|
| 009      | -13.090                    | -19.422                       | -6.332                      | N            |
| 039      | 5.650                      | -10.916                       | -16.566                     | 2            |
| 040*     | -6.380                     | -9.125                        | -2.745                      | 1            |
| 041      | 1.437                      | -12.219                       | -13.656                     | 1            |
| 042      | 0.953                      | -4.927                        | -5.880                      | N            |
| 044      | -11.835                    | -25.030                       | -13.195                     | 1            |
| 064      | 23.859                     | 7.626                         | -16.233                     | 2            |
| 112      | 14.787                     | 12.343                        | -2.444                      | N            |

**Table 3.50: Solvation data for imidazoles with sulfur-containing substituents binding with Ca<sup>2+</sup>.**

| Molecule | Energy of Drug<br>kcal/mol | Energy of Complex<br>kcal/mol | ΔEnergy<br>kcal/mol | Interactions |
|----------|----------------------------|-------------------------------|---------------------|--------------|
| 009      | -13.090                    | -23.564                       | -10.474             | 1            |
| 039      | 5.650                      | -8.616                        | -14.266             | 2            |
| 040*     | -6.380                     | -9.462                        | -3.082              | 1            |
| 041*     | 1.437                      | -2.984                        | -4.421              | 1            |
| 042      | 0.953                      | -5.648                        | -6.601              | N            |
| 044      | -11.835                    | -18.233                       | -6.398              | N            |
| 064      | 23.859                     | 10.729                        | -13.130             | 2            |
| 112      | 14.787                     | 12.951                        | -1.836              | N            |

*\*indicates when the simulation was set up with the dithiocarboxylate as the binding site*

Molecules 009 (2-mercapto-4,5-dimethylimidazole) and 044 (2-mercapto-4-methylimidazole) only differ by a methyl group at C5. Note that the binding energies for the simulations in which binding occurred differ by about 3 kcal/mol (i.e. 009 with Ca<sup>2+</sup> and 044 with Zn<sup>2+</sup>). This indicates that the presence of the second methyl group is detrimental to binding. In 009, two water molecules stabilized binding with Ca<sup>2+</sup>. The same can be said about 044 with Zn<sup>2+</sup>.

Molecules 039 (4-imidazoledithiocarboxylic acid), 040 (2-methylimidazole-4-dithiocarboxylic acid), 041(4-methylimidazole-5-dithiocarboxylic acid), 042 (2-ethyl-4-methylimidazole-5-dithiocarboxylic acid) and 064 (2-phenylimidazole-4-dithiocarboxylic acid) each contain the sulfur analogue of a carboxylate group. Recall that, in the gas-phase simulations, binding with these molecules took place at the negatively charged dithiocarboxylate. For completeness, separate solution-phase simulations were performed with the cations in proximity to both potential binding sites.

In molecules 039, 040 and 064, the dithiocarboxylate group is on the carbon adjacent to N3. 039 maintained its ability to act as a bidentate ligand for both cations. These interactions were heavily stabilized by hydrogen bonds and solvation. In fact, up to five hydrogen bonds formed with the dithiocarboxylate group and the cations were stabilized by four water molecules each.

Recall that in the gas-phase simulations, 064 only formed one electrostatic interaction with the zinc and calcium ions. In the solution face, 064 acted as a bidentate ligand. It was hypothesized that the large, non-polar phenyl group helped to repel the water from the binding site enough for the two interactions to take place. This is corroborated by the lack of water molecules present in the binding site. In the case of  $Zn^{2+}$ , only one water molecule was present, while none were present in the  $Ca^{2+}$  simulation. As in the simulations with 039, the interaction at the dithiocarboxylate was heavily stabilized by hydrogen bonds.

Molecule 040 did not act as a bidentate ligand, despite the fact that the dithiocarboxylate group was adjacent to N3. Therefore, separate simulations were performed with the cations placed near both potential binding sites. When placed in proximity to N3, no binding occurred. Contrarily, an interaction was formed with the dithiocarboxylate group. Each ligand-cation interaction was stabilized by three water molecules and the dithiocarboxylate group was stabilized by several hydrogen bonds.

In both 041 and 042, the dithiocarboxylate group sits three bonds away from N3. In these cases, it was definitely necessary to assess interactions at both possible binding site. 042 showed no binding with either cation at either binding site.

Molecule 041 yielded unusual results. When simulations using the N3 binding site were performed,  $\text{Zn}^{2+}$  showed a fairly strong electrostatic interaction (more so than imidazole itself). Three water molecules stabilized this interaction. In the case of  $\text{Ca}^{2+}$ , no binding occurred at N3 because it was taken and solvated by several water molecules at the outset. Multiple simulations were run with  $\text{Ca}^{2+}$  at the N3 binding site, but to no avail. Conversely, both cations were able to form an electrostatic interaction with the dithiocarboxylate group. Interestingly, the binding energy for  $\text{Zn}^{2+}$  was stronger at N3. This means that there are selective binding site for both ions of interest in this molecule. Another solution-phase simulation was performed in which molecule 041 and both cations were loaded into MOE.  $\text{Zn}^{2+}$  was placed near the N3 binding site and  $\text{Ca}^{2+}$  was placed near the dithiocarboxylate group. The system was then solvated and minimized in the usual way. The promising result is shown in Figure 3.7.

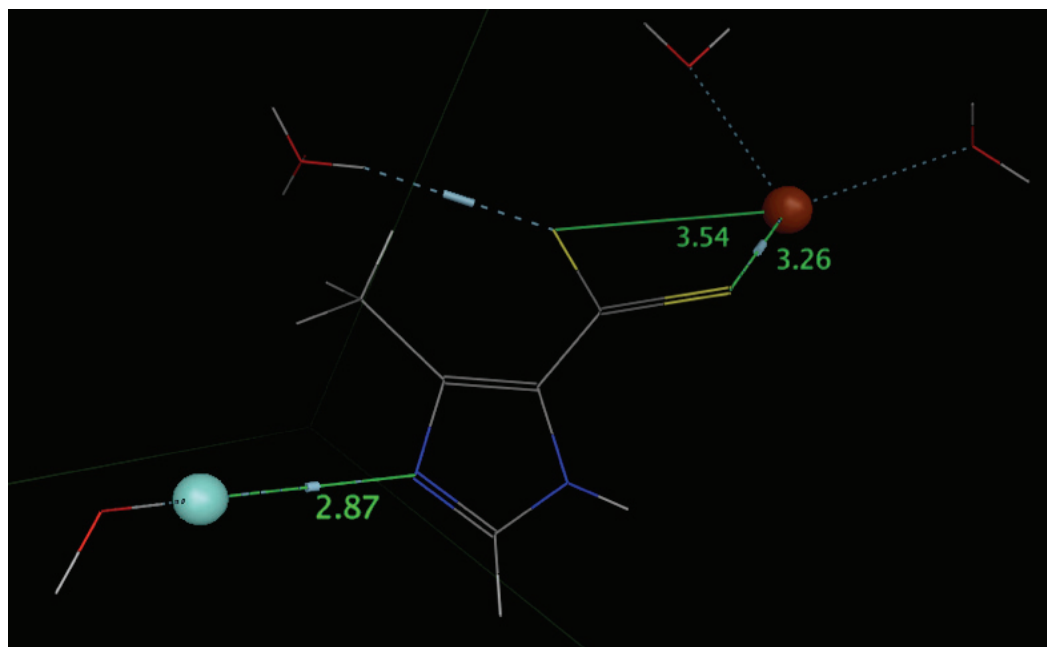


**Figure 3.26:** The resulting system after a solution-phase simulation with molecule 041,  $\text{Zn}^{2+}$  and  $\text{Ca}^{2+}$ .

For simplicity, any water molecules that were not directly involved in stabilizing the system were removed. Note that both cations formed electrostatic interactions with 041. This molecule is an excellent candidate for experimental testing.

Molecule 112 (2-ethylthio-2-imidazoline) showed no binding with either cation after several attempts.

### 3.3.5 – Imidazoles with Phenyl Substituents in Water

Imidazoles with phenyl substituents were solvated next. The results are listed in Tables 3.51 and 3.52. Refer to Figure 3.14 for structures.

**Table 3.51: Solvation data for imidazoles with phenyl substituents binding with  $Zn^{2+}$ .**

| Molecule | Energy of Drug<br>kcal/mol | Energy of Complex<br>kcal/mol | $\Delta$ Energy<br>kcal/mol | Interactions |
|----------|----------------------------|-------------------------------|-----------------------------|--------------|
| 052      | 17.551                     | 4.420                         | -13.131                     | 1            |
| 053      | 35.643                     | 32.179                        | -3.464                      | N            |
| 055      | 17.060                     | 8.531                         | -8.529                      | N            |
| 056      | 32.844                     | 30.060                        | -2.784                      | 1            |
| 059      | 43.991                     | 39.797                        | -4.194                      | 1            |
| 060      | 37.313                     | 35.389                        | -1.924                      | N            |
| 061      | 44.661                     | 42.160                        | -2.501                      | N            |
| 062      | 41.588                     | 40.331                        | -1.257                      | N            |
| 063      | 12.763                     | -4.183                        | -16.946                     | 1            |
| 069      | 39.796                     | 23.882                        | -15.914                     | 1            |
| 070      | 44.659                     | 34.639                        | -10.020                     | N            |
| 071      | 56.738                     | 52.956                        | -3.782                      | N            |
| 072      | 55.508                     | 39.650                        | -15.858                     | 1            |
| 074      | 40.718                     | 36.283                        | -4.435                      | N            |

**Table 3.52: Solvation data for imidazoles with phenyl substituents binding with  $\text{Ca}^{2+}$ .**

| Molecule | Energy of Drug<br>kcal/mol | Energy of Complex<br>kcal/mol | $\Delta$ Energy<br>kcal/mol | Interactions |
|----------|----------------------------|-------------------------------|-----------------------------|--------------|
| 052      | 17.551                     | 7.269                         | -10.282                     | 1            |
| 053      | 35.643                     | 30.926                        | -4.717                      | N            |
| 055      | 17.060                     | 9.264                         | -7.796                      | 1            |
| 056      | 32.844                     | 30.826                        | -2.018                      | N            |
| 059      | 43.991                     | 41.049                        | -2.942                      | N            |
| 060      | 37.313                     | 32.839                        | -4.474                      | 1            |
| 061      | 44.661                     | 38.860                        | -5.801                      | N            |
| 062      | 41.588                     | 40.407                        | -1.181                      | N            |
| 063      | 12.763                     | -0.636                        | -13.399                     | 1            |
| 069      | 39.796                     | 25.870                        | -13.926                     | 1            |
| 070      | 44.659                     | 33.803                        | -10.856                     | 1            |
| 071      | 56.738                     | 47.970                        | -8.768                      | N            |
| 072      | 55.508                     | 50.083                        | -5.425                      | 1            |
| 074      | 40.718                     | 33.607                        | -7.111                      | N            |

Molecules 052 (2-phenylimidazole), 053 (1-phenylimidazole) and 055 (4-phenylimidazole) each feature an unsubstituted phenyl substituent. 052 maintained its ability to chelate both calcium and zinc ions. The non-polar phenyl ring adjacent to N3 may act to repel water molecules from the binding site. This is evidenced by the lack of water molecules in the binding site at the end of the simulation (one for  $\text{Zn}^{2+}$  and zero for  $\text{Ca}^{2+}$ ). 053 has the phenyl ring on N1, which has proven to be detrimental to binding in previous simulations. Molecule 053 was unable to chelate either cation in the solution phase; 055 maintained its ability to chelate  $\text{Ca}^{2+}$ , but not  $\text{Zn}^{2+}$ . Two water molecules stabilized the interaction with  $\text{Ca}^{2+}$ . After multiple attempts,  $\text{Zn}^{2+}$  was unable to form an interaction with 053.

Molecules 056 (*p*-(1-imidazolyl)-phenol), 059 (1-(4-nitrophenyl)-1H-imidazole), 060 (4-(1H-imidazol-1-yl)benzotrile), 061 (4-(1H-imidazol-1-yl)benzaldehyde), and 062 (4-imidazol-1-yl)acetophenone) all feature substituted phenyl substituents on N1. At most, these molecules were able to bind with one of the cations. Any interactions that were formed were very weak (compared to imidazole). Molecules 056 and 059 were able to bind  $Zn^{2+}$ . Molecule 060 was able to bind  $Ca^{2+}$ . Molecules 061 and 061 were unable to bind either cation.

Molecules 063 and 052 only differ by a methyl group present at C4 in 063. Recall that molecule 052 was able to chelate both cations effectively. The extra electron donation from the methyl group on 063 allows for a stronger interaction to occur with both cations. As in 052, the phenyl group managed to keep water out of the binding site (zero for  $Zn^{2+}$  and two for  $Ca^{2+}$ ).

Molecules 069 (4,5-diphenylimidazole) and 070 (4,5-diphenylimidazolin-2-one) each feature two phenyl substituents. Molecule 069 chelated both zinc and calcium ions quite efficiently (better than imidazole in both cases). Three water molecules stabilized  $Zn^{2+}$ , while two water molecules stabilized  $Ca^{2+}$ . Molecule 070, an imidazolidinone, was able to chelate  $Ca^{2+}$ , but not  $Zn^{2+}$ . This trend will continue in the next section. The interaction took place at the carbonyl oxygen and was stabilized by four water molecules and two hydrogen bonds.

Molecules 071 (2,4,5-triphenylimidazole) and 072 (2-(*o*-chlorophenyl)-4,5-diphenyl-1H-imidazole) each feature three phenyl substituents. Molecule 071 was unable to chelate either cation in solvent, while 072, which only differs by a chloro substituent on one of the phenyl rings, chelated both cations effectively. At the outset, it was

expected that both molecules would be able to chelate zinc and calcium ions. It was hypothesized that the phenyl groups flanking the N3 binding site would deter water from solvating the cations. This was the case in 072, as there was only water molecule present at the periphery of the binding site at the end of the simulations. However, after several attempts, the cations never formed an electrostatic interaction with 071. Unlike in other simulations that resulted in no binding, the cation was not taken away by water molecules. Instead, the cations stayed in place approximately three angstroms from N3, where they were solvated by water molecules.

Molecule 074 (2-(1-naphthylmethyl)-2-imidazoline) showed no binding with either cation in solvent. It was hypothesized that, unlike in the gas-phase, the free rotation about the  $sp^3$ -hybridized carbon that separates the naphthyl group from the imidazole ring was hindered in the presence of solvent. As a result, the large naphthyl group would sterically hinder cation binding. As it turned out, the naphthyl group did not inhibit binding because of its size. After several attempts, the water molecules repeatedly solvated the cations on the periphery of the binding site.

### 3.3.6 – Imidazolidinones in Water

Next, a group of imidazolidinones were evaluated. The results are listed below in Tables 3.53 and 3.54. Refer to Figure 3.15 for structures.

**Table 3.53: Solvation data for imidazolidinones binding with  $Zn^{2+}$ .**

| Molecule | Energy of Drug<br>kcal/mol | Energy of Complex<br>kcal/mol | $\Delta$ Energy<br>kcal/mol | Interactions |
|----------|----------------------------|-------------------------------|-----------------------------|--------------|
| 001      | 10.599                     | -3.416                        | -14.015                     | 1            |
| 002      | 34.505                     | 27.084                        | -7.421                      | N            |
| 003      | 18.867                     | 14.717                        | -4.150                      | N            |

**Table 3.54: Solvation data for imidazolidinones binding with Ca<sup>2+</sup>.**

| Molecule | Energy of Drug<br>kcal/mol | Energy of Complex<br>kcal/mol | ΔEnergy<br>kcal/mol | Interactions |
|----------|----------------------------|-------------------------------|---------------------|--------------|
| 001      | 10.599                     | 0.951                         | -9.648              | 1            |
| 002      | 34.505                     | 26.543                        | -7.962              | 1            |
| 003      | 18.867                     | 11.596                        | -7.271              | 1            |

As mentioned in the previous section, imidazolidinones appear to have an affinity for binding Ca<sup>2+</sup>, but not Zn<sup>2+</sup>. Of the four imidazolidinones tested, only one of them was able to chelate Zn<sup>2+</sup>. Recall that, based on the EF hand motif, Ca<sup>2+</sup> tends to interact with oxygen-containing functional groups. With imidazolidinones, binding takes place at the carbonyl oxygen. This property makes imidazolidinones poor candidates for further testing.

### 3.3.7 – Benzimidazoles with Only Alkyl Substituents in Water

Next, benzimidazoles with only alkyl substituents were examined. The results are summarized below in Tables 3.55 and 3.56. Refer to Figure 3.18 for structures.

**Table 3.55: Solvation data for benzimidazoles with alkyl substituents binding with Zn<sup>2+</sup>.**

| Molecule | Energy of Drug<br>kcal/mol | Energy of Complex<br>kcal/mol | ΔEnergy<br>kcal/mol | Interactions |
|----------|----------------------------|-------------------------------|---------------------|--------------|
| 081      | 11.009                     | -4.101                        | -15.110             | 1            |
| 092      | 2.888                      | -12.507                       | -15.395             | 1            |
| 093      | 10.146                     | -6.793                        | -16.939             | 1            |
| 094      | -1.710                     | -13.778                       | -12.068             | 1            |
| 095      | 12.460                     | -2.082                        | -14.542             | 1            |
| 105      | 15.063                     | 8.323                         | -6.740              | N            |

**Table 3.56: Solvation data for benzimidazoles with alkyl substituents binding with  $\text{Ca}^{2+}$ .**

| Molecule | Energy of Drug<br>kcal/mol | Energy of Complex<br>kcal/mol | $\Delta$ Energy<br>kcal/mol | Interactions |
|----------|----------------------------|-------------------------------|-----------------------------|--------------|
| 081      | 11.009                     | 1.638                         | -11.936                     | 1            |
| 092      | 2.888                      | -8.799                        | -11.687                     | 1            |
| 093      | 10.146                     | 5.162                         | -4.984                      | N            |
| 094      | -1.710                     | -10.064                       | -8.354                      | 1            |
| 095      | 12.460                     | 2.559                         | -9.901                      | 1            |
| 105      | 15.063                     | 5.422                         | -9.641                      | N            |

Molecule 081 (benzimidazole) was able to chelate both cations quite effectively. It actually had a better binding energy than imidazole for both zinc and calcium ions. The interactions were each stabilized by two water molecules.

Molecules 092 (2-methylbenzimidazole), 093 (5-methylbenzimidazole) and 105 (2-nonylbenzimidazole) each have one alkyl substituent. Molecule 092 chelated both cations in solvent. In both cases, the binding energies were comparable to benzimidazole. The interaction with  $\text{Ca}^{2+}$  was stabilized by four water molecules, while the  $\text{Zn}^{2+}$  interaction was stabilized by just two. Molecule 093 was able to chelate  $\text{Zn}^{2+}$ , but not  $\text{Ca}^{2+}$ . After multiple simulations,  $\text{Ca}^{2+}$  showed no signs of binding, contrary to my hypothesis. It was predicted that both cations would interact with 093 and that the methyl group would donate electron density and improve the binding energy compared to benzimidazole. This was the case for  $\text{Zn}^{2+}$ , but not  $\text{Ca}^{2+}$ . The interaction with  $\text{Zn}^{2+}$  was stabilized by one water molecule. Molecule 105 was unable to chelate either cation in solvent. It was hypothesized that the large, non-polar nonyl group would protect the binding site from solvation of the cation by water molecules. This was not the case. After several attempts, both cations were consistently taken away and solvated by water.

Molecules 094 (2,5-dimethylbenzimidazole) and 095 (5,6-dimethylbenzimidazole) each have two alkyl substituents. The extra electron donation from the second alkyl group helps both of the molecules in this group to bind both cations effectively. For molecule 093, both cation interactions were stabilized by one water molecule. In the case of molecule 094,  $Zn^{2+}$  was stabilized by one water molecule, and  $Ca^{2+}$  by two.

### 3.3.8 – Benzimidazoles with Halide Substituents in Water

Benzimidazoles with halide substituents were also solvated and evaluated. The results are tabulated in Tables 3.57 and 3.58. Refer to Figure 3.19 for structures.

**Table 3.57: Solvation data for benzimidazoles with halide substituents binding with  $Zn^{2+}$ .**

| Molecule | Energy of Drug<br>kcal/mol | Energy of Complex<br>kcal/mol | $\Delta$ Energy<br>kcal/mol | Interactions |
|----------|----------------------------|-------------------------------|-----------------------------|--------------|
| 082      | 6.960                      | -5.380                        | -12.340                     | N            |
| 096      | 7.728                      | -6.113                        | -13.841                     | N            |

**Table 3.58: Solvation data for benzimidazoles with halide substituents binding with  $Ca^{2+}$ .**

| Molecule | Energy of Drug<br>kcal/mol | Energy of Complex<br>kcal/mol | $\Delta$ Energy<br>kcal/mol | Interactions |
|----------|----------------------------|-------------------------------|-----------------------------|--------------|
| 082      | 6.960                      | -1.132                        | -8.092                      | N            |
| 096      | 7.728                      | -3.565                        | -11.293                     | N            |

Molecules 082 (2-chlorobenzimidazole) and 096 (2-(chloromethyl)benzimidazole) both contain halides. Neither molecule showed any sign

of binding with zinc or calcium ions. Benzimidazoles with halide substituents are not ideal candidates for further testing and experimentation.

### 3.3.9 – Benzimidazoles with Nitrogen-Containing Substituents in Water

Next, solution-phase simulations were performed with benzimidazoles featuring nitrogen-containing substituents. The results are in Tables 3.59 and 3.60. Refer to Figure 3.21 for structures.

**Table 3.59: Solvation data for benzimidazoles with nitrogen-containing substituents binding with Zn<sup>2+</sup>.**

| Molecule | Energy of Drug<br>kcal/mol | Energy of Complex<br>kcal/mol | ΔEnergy<br>kcal/mol | Interactions |
|----------|----------------------------|-------------------------------|---------------------|--------------|
| 077      | 27.995                     | 20.286                        | -7.709              | N            |
| 078      | 55.888                     | 43.762                        | -12.126             | N            |
| 079      | 55.745                     | 54.111                        | -1.634              | N            |
| 090      | 14.454                     | 1.544                         | -12.910             | 1            |
| 103      | 2.046                      | -5.109                        | -7.155              | N            |

**Table 3.60: Solvation data for benzimidazoles with nitrogen-containing substituents binding with Ca<sup>2+</sup>.**

| Molecule | Energy of Drug<br>kcal/mol | Energy of Complex<br>kcal/mol | ΔEnergy<br>kcal/mol | Interactions |
|----------|----------------------------|-------------------------------|---------------------|--------------|
| 077      | 27.995                     | 23.880                        | -4.115              | N            |
| 078      | 55.888                     | 44.227                        | -11.661             | 1            |
| 079      | 55.745                     | 47.750                        | -7.995              | 1            |
| 090      | 14.454                     | 10.237                        | -4.217              | 1            |
| 103      | 2.046                      | -8.195                        | -10.241             | 1            |

Consistent with imidazolidinones, the benzimidazolinones showed preferential binding with Ca<sup>2+</sup> via their carbonyl carbon. Molecules 077 (5-nitro-2-

benzimidazolinone), 078 (1-(4-piperidyl)-2-benzimidazolinone) and 079 (5-chloro-1-(4-piperidyl)-2-benzimidazolinone) all contain the benzimidazolinone functionality. In the cases of 078 and 079, the ligand- $\text{Ca}^{2+}$  interaction was stabilized by two water molecules. Benzimidazolinones are not good candidates for further testing.

Molecule 090 (5-nitrobenzimidazole) was able to chelate both cations. The binding energy of  $\text{Zn}^{2+}$  and molecule 090 is significantly better than that of  $\text{Ca}^{2+}$  and molecule 090. Both interactions were stabilized by two water molecules. Also, hydrogen bonding occurred at the nitro group, perhaps further stabilizing the system.

Molecule 103 (2-benzimidazolylacetonitrile) showed binding with  $\text{Ca}^{2+}$ , but not  $\text{Zn}^{2+}$ . The interaction with  $\text{Ca}^{2+}$  was stabilized by two water molecules. The binding energy for this interaction was similar to that of benzimidazole.

### 3.3.10 – Benzimidazoles with Oxygen-Containing Substituents in Water

Benzimidazoles with oxygen-containing groups were investigated next. The results are summarized in Tables 3.61 and 3.62. Refer to Figure 3.22 for structures.

**Table 3.61: Solvation data for benzimidazoles with oxygen-containing substituents binding with  $\text{Zn}^{2+}$ .**

| Molecule | Energy of Drug<br>kcal/mol | Energy of Complex<br>kcal/mol | $\Delta$ Energy<br>kcal/mol | Interactions |
|----------|----------------------------|-------------------------------|-----------------------------|--------------|
| 083      | -5.221                     | -15.214                       | -9.993                      | 1            |
| 101      | 18.831                     | -54.324                       | -73.155                     | 1            |
| 104      | 8.626                      | -47.981                       | -56.607                     | 1            |

**Table 3.62: Solvation data for benzimidazoles with oxygen-containing substituents binding with Ca<sup>2+</sup>.**

| Molecule | Energy of Drug<br>kcal/mol | Energy of Complex<br>kcal/mol | ΔEnergy<br>kcal/mol | Interactions |
|----------|----------------------------|-------------------------------|---------------------|--------------|
| 083      | -5.221                     | -14.133                       | -8.912              | 1            |
| 101      | 18.831                     | -39.771                       | -58.602             | 1            |
| 104      | 8.626                      | -48.616                       | -57.242             | 1            |

Molecule 083 (2-hydroxybenzimidazole) has a hydroxyl group at C2. It maintained its ability to chelate both calcium and zinc ions. The interaction with Zn<sup>2+</sup> was stabilized by one water molecule, while the interaction with Ca<sup>2+</sup> was stabilized by three. Considering the strong electron donating nature of the hydroxyl group, its no surprise that binding was maintained on going from gas-phase to solution-phase simulations.

Two of the best molecules for chelating zinc and calcium ions are molecules 101 (5-benzimidazolecarboxylic acid) and 104 (2-benzimidazolecarboxylic acid). They both exhibited outstanding binding energies. As was done with the imidazoles that contained carboxylate groups, separate simulations were performed with the cations in proximity to both possible binding sites. The negatively charged carboxylate was the preferred binding site for both cations. The binding energies associated with both 101 and 104 are all far better than those of benzimidazole itself. Several hydrogen bonds helped to stabilize the carboxylate groups in these simulations. For molecule 101, the Zn<sup>2+</sup> interaction was stabilized by two water molecules compared to just one for Ca<sup>2+</sup>. For molecule 104, both ligand-ion interactions were stabilized by three water molecules. Either of these two would be an excellent candidate for further testing.

### 3.3.11 – Benzimidazoles with Sulfur-Containing Substituents in Water

Next, benzimidazoles with sulfur-containing functional groups were tested. The results are given in Tables 3.63 and 3.64. Refer to Figure 3.23 for structures.

**Table 3.63: Solvation data for benzimidazoles with sulfur-containing substituents binding with Zn<sup>2+</sup>.**

| Molecule | Energy of Drug<br>kcal/mol | Energy of Complex<br>kcal/mol | ΔEnergy<br>kcal/mol | Interactions |
|----------|----------------------------|-------------------------------|---------------------|--------------|
| 084      | 4.035                      | -7.714                        | -11.749             | 1            |
| 085      | 3.866                      | -8.372                        | -12.238             | 1            |
| 086      | -0.120                     | -13.761                       | -13.641             | N            |
| 087      | 2.643                      | -10.951                       | -13.594             | 1            |

**Table 3.64: Solvation data for benzimidazoles with sulfur-containing substituents binding with Ca<sup>2+</sup>.**

| Molecule | Energy of Drug<br>kcal/mol | Energy of Complex<br>kcal/mol | ΔEnergy<br>kcal/mol | Interactions |
|----------|----------------------------|-------------------------------|---------------------|--------------|
| 084      | 4.035                      | -7.263                        | -11.298             | 1            |
| 085      | 3.866                      | -5.061                        | -8.927              | 1            |
| 086      | -0.120                     | -3.858                        | -3.738              | 1            |
| 087      | 2.643                      | -4.953                        | -7.596              | 1            |

In general, benzimidazoles that feature mercapto groups are quite efficient at chelating both zinc and calcium ions. Molecules 084 (2-mercaptobenzimidazole), 085 (5-methoxy-2-mercaptobenzimidazole), 086 (5-difluoromethoxy-2-mercaptobenzimidazole) and 087 (2-mercapto-5-methylbenzimidazole) each contain this functional group on C2. All but 086 were able to chelate Zn<sup>2+</sup> with binding energies comparable to benzimidazole itself. Also, all of the molecules in this group successfully chelated Ca<sup>2+</sup>, although these interactions were less energetically favourable as compared to Zn<sup>2+</sup>.

For all molecules, the interaction with  $\text{Ca}^{2+}$  was stabilized with three water molecules. The interactions of  $\text{Zn}^{2+}$  with molecules 084 , 085 and 087 were stabilized by one, two and two water molecules, respectively. Also, in all simulations, there was hydrogen bonding at N1 and the mercapto hydrogen.

### 3.3.12 – Benzimidazoles with Phenyl Substituents in Water

Benzimidazoles with phenyl substituents were also tested in the solution-phase. The results are in Tables 3.65 and 3.66. Refer to Figure 3.24 for structures.

**Table 3.65: Solvation data for benzimidazoles with phenyl substituents binding with  $\text{Zn}^{2+}$ .**

| Molecule | Energy of Drug<br>kcal/mol | Energy of Complex<br>kcal/mol | $\Delta$ Energy<br>kcal/mol | Interactions |
|----------|----------------------------|-------------------------------|-----------------------------|--------------|
| 108      | 28.044                     | 12.976                        | -15.068                     | 1            |
| 110      | 18.297                     | 10.279                        | -8.018                      | 1            |

**Table 3.66: Solvation data for benzimidazoles with phenyl substituents binding with  $\text{Ca}^{2+}$ .**

| Molecule | Energy of Drug<br>kcal/mol | Energy of Complex<br>kcal/mol | $\Delta$ Energy<br>kcal/mol | Interactions |
|----------|----------------------------|-------------------------------|-----------------------------|--------------|
| 108      | 28.044                     | 17.086                        | -10.958                     | 1            |
| 110      | 18.297                     | 3.686                         | -14.611                     | 1            |

Molecules 108 (2-phenylbenzimidazole) and 110 (2-(4-chlorobenzyl)benzimidazole) were both quite effective at chelating both cations of interest. The phenyl rings adjacent to the N3 binding site repelled water and allowed electrostatic interactions to form. This is evidenced by the fact that only two water

molecules stabilized each ligand-cation interaction and they were on the periphery of the binding site.

### 3.3.13 – Exceptions and Atypical Imidazoles in Water

Finally, simulations with the imidazoles that did not fit into any one category above were investigated. The results of these simulations are tabulated below in Tables 3.67 and 3.68. Refer to Figure 3.25 for structures.

**Table 3.67: Solvation data for atypical imidazoles binding with Zn<sup>2+</sup>.**

| Molecule | Energy of Drug<br>kcal/mol | Energy of Complex<br>kcal/mol | ΔEnergy<br>kcal/mol | Interactions |
|----------|----------------------------|-------------------------------|---------------------|--------------|
| 051      | 29.214                     | 14.051                        | -15.163             | 1            |
| 065      | 40.525                     | 31.365                        | -9.160              | 1            |
| 076      | 8.135                      | -1.024                        | -9.159              | N            |

**Table 3.68: Solvation data for atypical imidazoles binding with Ca<sup>2+</sup>.**

| Molecule | Energy of Drug<br>kcal/mol | Energy of Complex<br>kcal/mol | ΔEnergy<br>kcal/mol | Interactions |
|----------|----------------------------|-------------------------------|---------------------|--------------|
| 051      | 29.214                     | 16.266                        | -12.948             | N            |
| 065      | 40.525                     | 32.441                        | -8.084              | 1            |
| 076      | 8.135                      | 0.336                         | -7.799              | N            |

Molecule 051 (2,2'-azobis[2-(2-imidazolin-2-yl)propane]) was able to chelate Zn<sup>2+</sup> quite efficiently. It has a more favourable binding energy with zinc than imidazole. This interaction was stabilized by three water molecules. No Ca<sup>2+</sup> binding was evident.

Molecule 065 (N-benzoylimidazole) managed to bind both metal cations in solvent with marginally effectiveness. The binding energies for 065 are quite a bit

smaller in magnitude than those of imidazole. The interaction with  $\text{Zn}^{2+}$  was stabilized by one water molecule and the interaction with  $\text{Ca}^{2+}$  was stabilized with four.

Molecule 076 (5-acetoacetamido-2-benzimidazolinone) did not show any binding with either cation. As stated previously, benzimidazolinones tend to bind  $\text{Ca}^{2+}$  preferably and not  $\text{Zn}^{2+}$ . This is a unique case in which no  $\text{Ca}^{2+}$  binding occurred. After multiple attempts with both zinc and calcium ions, the water molecules consistently pulled the cations from the binding site and solvated them.

### ***3.4 – Comments and Conclusions***

After systematically evaluating nearly 120 imidazole-based molecules, the database has been narrowed down to a list of several potential lead molecules. As far as binding energy is concerned, no other functional group came close to the carboxylates. Molecules 027, 036, 101 and 104 all had extremely favourable binding energies with both zinc and calcium ions. This is, of course, largely due to the presence of the negative charge on the deprotonated carboxylate, which served as an ideal binding site for the positively charged metal ions. These molecules were the only ones that compared to carnosine and the reference amino acids from chapter two.

The second group that showed promise was, predictably, the dithiocarboxylic acids. Molecules 039 and 064 both showed binding energies that were quite a bit lower than those of their oxygen analogues, but both of them acted as bidentate ligands in solvent. Going forward, it may be useful to run a simulation with either cation and two copies of 039 or 064 to see if the cations will accommodate two bidentate ligands. Perhaps the most interesting molecule was 041, another dithiocarboxylic acid. Recall

that this molecule was able to chelate both zinc and calcium ions at the same time, at different binding sites.

Finally, there was one other molecule that acted as a bidentate ligand for both zinc and calcium ions. Molecule 013, which contains a nitro group, was able to chelate both cations via N3, as usual, and one of the nitro group's oxygen atoms (which have a partial negative charge).

Thus, based on a comprehensive series of gas-phase and solution-phase simulations, the initial 120 molecule working set was significantly reduced to a select group of seven candidate molecules for subsequent *in vitro* testing.

## CHAPTER 4 – BIOLOGICALLY RELEVANT CATIONS

### *4.1 – General Trends*

For completeness,  $\text{Zn}^{2+}$  and  $\text{Ca}^{2+}$  were not the only two cations that were evaluated in this research. In total, 24 other biologically relevant cations were analyzed with all of the imidazoles from the previous chapter. For the purpose of this chapter, the term biologically relevant means that the cation is present in the human body.

This chapter will offer a brief overview of the biological function of each cation, its HSAB classification and reasoning for why it was able/unable to be bound by certain molecules. In each section, the four molecules that showed the most favourable binding energy with the cation in question will be presented. Table 4.1 gives a summary of the cations that were evaluated, along with some of their physical and chemical properties. In column 4, *L* denotes low-spin and *H* denotes high-spin. In column 5, H stands for hard, S for soft and I for intermediate. Column 6 (% Bound) gives the percentage of imidazoles that formed an electrostatic interaction with the cation being tested.

**Table 4.1: Overview of the cations evaluated in this chapter (Shannon 1976).**

| Ion              | Effective Ionic Radius (pm) | Electronic Configuration                              | Spin     | HSAB Class | % Bound |
|------------------|-----------------------------|---|----------|------------|---------|
| Li <sup>+</sup>  | 90                          | [He]  |          | H          | 86.1%   |
| Be <sup>2+</sup> | 59                          | [He]  |          | H          | 76.9%   |
| Na <sup>+</sup>  | 116                         | [Ne]  |          | H          | 83.3%   |
| Mg <sup>2+</sup> | 86                          | [Ne]  |          | H          | 86.1%   |
| Al <sup>3+</sup> | 68                          | [Ne]  |          | H          | 2.8%    |
| K <sup>+</sup>   | 152                         | [Ar]  |          | H          | 71.3%   |
| Ca <sup>2+</sup> | 114                         | [Ar]  |          | H          | 82.4%   |
| Cr <sup>2+</sup> | 87                          | [Ar]3d <sup>4</sup>                                   | <i>L</i> | I          | 87.0%   |
| Cr <sup>2+</sup> | 94                          | [Ar]3d <sup>4</sup>                                   | <i>H</i> | I          | 87.0%   |
| Cr <sup>3+</sup> | 76                          | [Ar]3d <sup>3</sup>                                   | <i>L</i> | H          | 88.9%   |
| Mn <sup>2+</sup> | 81                          | [Ar]3d <sup>5</sup>                                   | <i>L</i> | H          | 87.0%   |
| Mn <sup>2+</sup> | 97                          | [Ar]3d <sup>5</sup>                                   | <i>H</i> | H          | 87.0%   |
| Mn <sup>3+</sup> | 72                          | [Ar]3d <sup>4</sup>                                   | <i>L</i> | H          | 88.9%   |
| Mn <sup>3+</sup> | 79                          | [Ar]3d <sup>4</sup>                                   | <i>H</i> | H          | 88.9%   |
| Co <sup>2+</sup> | 79                          | [Ar]3d <sup>7</sup>                                   | <i>L</i> | I          | 88.0%   |
| Co <sup>2+</sup> | 89                          | [Ar]3d <sup>7</sup>                                   | <i>H</i> | I          | 88.0%   |
| Co <sup>3+</sup> | 69                          | [Ar]3d <sup>6</sup>                                   | <i>L</i> | H          | 88.9%   |
| Co <sup>3+</sup> | 75                          | [Ar]3d <sup>6</sup>                                   | <i>H</i> | H          | 88.9%   |
| Ni <sup>2+</sup> | 83                          | [Ar]3d <sup>8</sup>                                   | <i>L</i> | I          | 88.0%   |
| Cu <sup>+</sup>  | 91                          | [Ar]3d <sup>10</sup>                                  |          | S          | 81.5%   |
| Cu <sup>2+</sup> | 87                          | [Ar]3d <sup>9</sup>                                   |          | I          | 86.1%   |
| Zn <sup>2+</sup> | 88                          | [Ar]3d <sup>10</sup>                                  |          | I          | 85.2%   |
| Sr <sup>2+</sup> | 132                         | [Kr]  |          | H          | 80.6%   |
| Pd <sup>2+</sup> | 100                         | [Kr]4d <sup>8</sup>                                   |          | S          | 87.0%   |
| Ag <sup>+</sup>  | 129                         | [Kr]4d <sup>10</sup>                                  |          | S          | 86.1%   |
| Cd <sup>2+</sup> | 109                         | [Kr]4d <sup>10</sup>                                  |          | S          | 88.9%   |
| Sn <sup>2+</sup> | 118                         | [Kr]5s <sup>2</sup> 4d <sup>10</sup>                  |          | I          | 3.7%    |
| Sn <sup>4+</sup> | 83                          | [Kr]4d <sup>10</sup>                                  |          | H          | 1.9%    |
| Ba <sup>2+</sup> | 149                         | [Xe]  |          | H          | 82.4%   |
| Hg <sup>2+</sup> | 116                         | [Xe]4f <sup>14</sup> 5d <sup>10</sup>                 |          | S          | 87.0%   |
| Pb <sup>2+</sup> | 133                         | [Xe]4f <sup>14</sup> 5d <sup>10</sup> 6s <sup>2</sup> |          | I          | 2.8%    |

In general, for the d-block cations, oxidation state and binding energy are directly related. For example, the average binding energy exhibited by Co<sup>2+</sup> was -29.824

kcal/mol, while the average binding energy for  $\text{Co}^{3+}$  was -37.604 kcal/mol. This trend is also true on going from  $\text{Cu}^+$  to  $\text{Cu}^{2+}$ . When comparing isoelectronic cations, this trend is conserved. For instance,  $\text{Cr}^{2+}$  and  $\text{Mn}^{3+}$  are both  $3d^4$  metal cations. Their average binding energies are -29.239 kcal/mol and -37.994 kcal/mol, respectively. The same trend is demonstrated by the s-block cations.

The above trend is not true for p-block ions. Only four ions in the p-block were tested:  $\text{Al}^{3+}$ ,  $\text{Sn}^{2+}$ ,  $\text{Sn}^{4+}$  and  $\text{Pb}^{2+}$ . As indicated in Table 4.1, these cations exhibited minimal binding with the imidazole-based molecules in the working set.

Another trend that emerged is the relationship between ionic radius and binding energy. Small ions showed stronger binding energies with imidazoles than larger ions of the same oxidation state.

Recall that imidazole is an intermediate/borderline base according to HSAB. This property gives imidazoles the ability to form acid-base adducts with both hard and soft acids and bases. In most cases, soft cations exhibited binding energies that were comparable to hard cations.

## ***4.2 – Gas-Phase Simulations with Biologically Relevant Cations***

In this section, data for each of the 24 cations that were evaluated will be presented and analyzed. All simulations were done *in vacuo*, as described in Chapter 2. All cations were placed three angstroms from the appropriate binding site on each imidazole-based molecule.

### 4.2.1 – Gas-Phase Simulations with Li<sup>+</sup>

The Li<sup>+</sup> cation is ubiquitous in the human body. Trace amounts have been found in almost every type of vertebrate tissue. Though the mechanisms by which Li<sup>+</sup> acts in the human body are, for the most part, unknown, deficiencies have been linked to mood disorders and criminal behaviour. Evidence suggests that Li<sup>+</sup> is very important for psychological wellbeing (Schrauzer 2002). Because of their affinity for binding Li<sup>+</sup>, a lithium supplement may need to be coadministered with an imidazole-based therapeutic when treating stroke. Data from the gas-phase simulations of this ion with the four imidazoles that showed the most favourable binding energy are summarized in the table below.

**Table 4.2: Gas-phase data for imidazoles binding with Li<sup>+</sup>.**

| Molecule | Binding Energy<br>kcal/mol | Interactions |
|----------|----------------------------|--------------|
| 104      | -60.649                    | 1            |
| 050      | -56.561                    | 1            |
| 067      | -55.513                    | 1            |
| 042      | -54.013                    | 1            |

The lithium ion is a very hard, acidic cation with an ionic radius of 90 pm. Li<sup>+</sup> is smaller than Ca<sup>2+</sup> and larger than Zn<sup>2+</sup>, so no steric issues were expected. In fact, the lithium ion was chelated by more of the imidazoles than either Zn<sup>2+</sup> or Ca<sup>2+</sup>, though the binding energies were significantly small in magnitude for the monovalent cation.

Three of the four imidazoles that best chelated Li<sup>+</sup> feature a negatively charged functional group. Molecules 104 and 067 each contain a carboxylate group and molecule 042 contains a dithiocarboxylate group. The strong electrostatic interaction formed

between the positively charged metal ion and the negatively charged binding site in these molecules was matched by molecule 050, which chelated  $\text{Li}^+$  via a carbonyl oxygen.

#### 4.2.2 – Gas-Phase Simulations with $\text{Be}^{2+}$

$\text{Be}^{2+}$  is a proven carcinogen in laboratory animal studies. The beryllium ion is used in alloys to make surgical tools, non-sparking tools and springs, so human exposure is quite common. Most human exposure of  $\text{Be}^{2+}$  occurs via inhalation. Another application of imidazoles could be to chelate beryllium ions if they are detected in the blood above an acceptable concentration (1 ng/g) (Benbrahim, Tokar and Waalkes 2011). Data from the gas-phase simulations of this ion with the four imidazoles that showed the most favourable binding energy are summarized in the table below.

**Table 4.3: Gas-phase data for imidazoles binding with  $\text{Be}^{2+}$ .**

| Molecule | Binding Energy<br>kcal/mol | Interactions |
|----------|----------------------------|--------------|
| 104      | -103.972                   | 1            |
| 067      | -92.289                    | 1            |
| 027      | -82.508                    | 1            |
| 036      | -65.336                    | 2            |

The beryllium ion is a very hard, acidic cation with an ionic radius of 59 pm. Its small ionic radius was both beneficial and detrimental in binding with imidazoles. On the one hand, the small ionic radius allowed the positively charged nucleus of the ion to get closer to the binding site, forming a stronger interaction. This is evidenced by the average binding energy for  $\text{Be}^{2+}$  being -30.518 kcal/mol, as compared to -25.644 kcal/mol and -29.972 kcal/mol for  $\text{Ca}^{2+}$  and  $\text{Zn}^{2+}$ , respectively. On the other hand, due to its small size, the positive nucleus of the ion is also more exposed to solvation by water. This is indicated by the lower percentage of imidazoles that chelated  $\text{Be}^{2+}$  in Table 4.1.

Similar to the lithium ion, the imidazoles that best chelated  $\text{Be}^{2+}$  contained the negatively charged carboxylate functional group. Molecules 104, 067, 027 and 036 all contain this group and formed strong ligand-ion complexes with the beryllium ion.

### 4.2.3 – Gas-Phase Simulations with $\text{Na}^+$

The sodium ion is ubiquitous in the human body. Its roles include, but are not limited to, regulation of blood pressure, volume and pH, and maintenance of neuronal action potentials.  $\text{Na}^+$  is also thought to be involved in stroke pathophysiology. In the absence of ATP, the  $\text{Na}^+/\text{K}^+$ -ATPase ion pump cannot move  $\text{Na}^+$  out of the cell.  $\text{Na}^+$  contributes to the cell depolarization that leads to the release of glutamate and excitotoxicity (Li and Zhang 2012). Data from the gas-phase simulations of this ion with the four imidazoles that showed the most favourable binding energy are summarized in the table below.

**Table 4.4: Gas-phase data for imidazoles binding with  $\text{Na}^+$ .**

| Molecule | Binding Energy<br>kcal/mol | Interactions |
|----------|----------------------------|--------------|
| 050      | -55.413                    | 1            |
| 104      | -53.573                    | 1            |
| 042      | -51.651                    | 1            |
| 067      | -50.729                    | 1            |

The sodium ion is a very hard, acidic cation with an ionic radius of 116 pm. Because of its size similarity with  $\text{Ca}^{2+}$ , it experienced some of the steric problems. This is evidenced by the fact that  $\text{Na}^+$  formed an electrostatic interaction with 83.3% of the imidazoles, compared to 82.4% for  $\text{Ca}^{2+}$ . Comparing the binding energies of molecule 104 with  $\text{Na}^+$  (-53.573 kcal/mol) and  $\text{K}^+$  (-60.649 kcal/mol from Table 4.2) is evidence of

the trend that, for ions of like charge, the one with the smaller radius will have a stronger binding energy with the imidazoles.

The top four imidazoles for  $\text{Na}^+$  are the same as  $\text{K}^+$ . These include the negatively charged carboxylates (104 & 067), the dithiocarboxylate (042) and the carbonyl-bridged diimidazole (050).

#### 4.2.4 – Gas-Phase Simulations with $\text{Mg}^{2+}$

$\text{Mg}^{2+}$  is an extremely important mineral in human health. Deficiencies in the magnesium ion have been linked to diabetes, cardiovascular disease, anxiety disorders, osteoporosis and cerebral infarction (Larsson, Virtanen and Mars 2008).  $\text{Mg}^{2+}$  is also known to be involved in stroke pathophysiology. The magnesium ion is a cofactor in a number of enzymatic reactions, including ATP production. During an ischemic event, the magnesium ion acts as an antioxidant and destroys reactive oxygen species. It is often given as a therapeutic to stroke victims (Li and Zhang 2012). The ability of imidazoles to chelate  $\text{Mg}^{2+}$  effectively may require the co-administration of a magnesium supplement. Data from the gas-phase simulations of this ion with the four imidazoles that showed the most favourable binding energy are summarized in the table below.

**Table 4.5: Gas-phase data for imidazoles binding with  $\text{Mg}^{2+}$ .**

| Molecule | Binding Energy<br>kcal/mol | Interactions |
|----------|----------------------------|--------------|
| 104      | -104.469                   | 1            |
| 101      | -95.944                    | 1            |
| 067      | -93.918                    | 1            |
| 027      | -90.259                    | 1            |

The magnesium ion is a very hard, acidic cation with an ionic radius of 86 pm. Its ionic radius is very similar to that of  $\text{Zn}^{2+}$ . As a result,  $\text{Mg}^{2+}$  and  $\text{Zn}^{2+}$  showed very

comparable binding energies and affinities with imidazoles. As indicated in Table 4.1, the imidazoles chelated the magnesium ion 86.1% of the time, compared to 85.2% with the zinc ion. Also, the average binding energy of complexes with  $Mg^{2+}$  was -29.948 kcal/mol, very close to the average binding energy of -29.972 kcal/mol for  $Zn^{2+}$ .

The four imidazoles that most strongly interacted with  $Mg^{2+}$  are the same as those that chelated  $Be^{2+}$  the best. All four molecules (104, 101, 067 and 027) include a carboxylate group. The negatively charged functional group acted as the binding site for the positively charged metal ion, via electrostatic interactions.

#### 4.2.5 – Gas-Phase Simulations with $Al^{3+}$

$Al^{3+}$  is an exogenous metal cation that has no known biological function in humans. However, it is commonly ingested in food and high levels of the aluminum ion can be harmful. High levels of  $Al^{3+}$  have been linked to bone disease (osteomalacia, or bone softening) (Bernardo 2012). Also, if present in the brain in excess of 2  $\mu g/g$ ,  $Al^{3+}$  can cause cerebral oxidative stress (Li and Zhang 2012). Data from the gas-phase simulations of this ion with the four imidazoles that showed the most favourable binding energy are summarized in the table below.

**Table 4.6: Gas-phase data for imidazoles binding with  $Al^{3+}$ .**

| Molecule | Binding Energy<br>kcal/mol | Interactions |
|----------|----------------------------|--------------|
| 110      | -34.666                    | P            |
| 004      | -5.996                     | P            |

The aluminum ion is a moderately hard, acidic cation with an ionic radius of 68 pm. This is the first ion of a p-block element and showed very little binding affinity for

imidazoles, despite its high oxidation state. It is isoelectronic with  $\text{Na}^+$  and  $\text{Mg}^{2+}$ , but shows none of the binding affinity that these ions have.

No electrostatic interactions were formed between  $\text{Al}^{3+}$  and the imidazoles. In fact, only two of the imidazoles showed any type of interaction with the aluminum ion. Both were  $\pi$ -type interactions. In the case of molecule 110, which features a benzyl group adjacent to N3, the cation was sandwiched between the  $\pi$ -systems of the imidazole ring and the phenyl ring. With molecule 004, a thione, the aluminum ion migrated to the space directly above the imidazole ring.

#### 4.2.6 – Gas-Phase Simulations with $\text{K}^+$

Like  $\text{Na}^+$ , potassium ions are necessary for the normal propagation of neuronal action potentials.  $\text{K}^+$  serves countless biological functions in the human body (Campbell 1987). Potassium ions are also known to play a role in stroke pathophysiology. As mentioned, in the absence of ATP, the  $\text{Na}^+/\text{K}^+$ -ATPase ion pump fails to function. This pump is extremely important in maintaining a concentration gradient and the potential of the cell. Another approach to reducing the effects of a stroke is to design drug molecules that reactivate these ion pumps (Li and Zhang 2012). Data from the gas-phase simulations of this ion with the four imidazoles that showed the most favourable binding energy are summarized in the table below.

**Table 4.7: Gas-phase data for imidazoles binding with  $\text{K}^+$ .**

| Molecule | Binding Energy<br>kcal/mol | Interactions |
|----------|----------------------------|--------------|
| 050      | -54.784                    | 1            |
| 042      | -50.858                    | 1            |
| 104      | -50.812                    | 1            |
| 067      | -47.787                    | 1            |

The potassium ion is a very hard, acidic cation with an ionic radius of 152 pm. As the largest ion in the testing set, it was hypothesized that  $K^+$  would suffer from the most steric problems. This is confirmed by the fact that only 71.3% of the imidazoles were able to chelate the potassium ion, the lowest percentage excluding the p-block cations.  $K^+$  also has the lowest average binding energy of all of the cations, consistent with the binding energy-ionic radius relationship.

Like the other monovalent cations discussed so far, molecule 050 bound  $K^+$  very strongly via a carbonyl oxygen. The other three molecules in table 4.7 are a dithiocarboxylate (042) and two carboxylate-containing imidazoles (104 & 067).

#### 4.2.7 – Gas-Phase Simulations with Chromium Ions

Although present in trace amounts in the human body, the biological role of chromium ions remains unelucidated;  $Cr^{2+}$  and  $Cr^{3+}$  are thought to be benign when ingested. Problems arise when these cations are oxidized to  $Cr^{6+}$  in the body.  $Cr^{6+}$  is known to be very toxic and mutagenic and has been linked to cancer (ATSDR 2012). Data from the gas-phase simulations of this ion with the four imidazoles that showed the most favourable binding energy are summarized in the tables below.

**Table 4.8: Gas-phase data for imidazoles binding with  $Cr^{2+}$ .**

| Molecule | Binding Energy<br>kcal/mol | Interactions |
|----------|----------------------------|--------------|
| 104      | -101.567                   | 1            |
| 067      | -89.768                    | 1            |
| 027      | -86.556                    | 1            |
| 036      | -62.573                    | 1            |

**Table 4.9: Gas-phase data for imidazoles binding with Cr<sup>3+</sup>.**

| Molecule | Binding Energy<br>kcal/mol | Interactions |
|----------|----------------------------|--------------|
| 104      | -147.205                   | 2            |
| 101      | -133.753                   | 1            |
| 067      | -128.839                   | 1            |
| 027      | -125.444                   | 1            |

The chromium (II) ion is an intermediate, acidic cation with a low-spin ionic radius of 87 pm. As was the case with the magnesium ion, Cr<sup>2+</sup> has an ionic radius very similar to that of Zn<sup>2+</sup>. This similarity translated to similar results for Cr<sup>2+</sup> and Zn<sup>2+</sup>. The chromium (II) cation formed a complex with 87% of the imidazoles that were tested, compared to 85.2% for the zinc ion. The average binding energies were also very similar: -29.239 kcal/mol for chromium (II) and -29.972 kcal/mol for the zinc ion. All of the molecules in Table 4.8 contain a carboxylate group.

The chromium (III) ion is a moderately hard, acidic cation with an ionic radius of 76 pm. Cr<sup>3+</sup> had an average binding energy of -38.268 kcal/mol, which is significantly more favourable than its divalent counterpart. The combination of the small ionic radius and high oxidation number allowed chromium (III) to form complexes with 88.9% of imidazoles, tied for the highest percentage of all the ions. All of the molecules in Table 4.9 contain a carboxylate group.

#### **4.2.8 – Gas-Phase Simulations with Manganese Ions**

Manganese ions are common and important cofactors for a several classes of enzymes (Law, Caudle and Pecoraro 1998). Manganese ions also have a known role in the ischemic cascade. Overexposure to manganese ions may facilitate the release of excess glutamate from vesicles, leading to excitotoxicity (Li and Zhang 2012). Data from

the gas-phase simulations of this ion with the four imidazoles that showed the most favourable binding energy are summarized in the tables below.

**Table 4.10: Gas-phase data for imidazoles binding with Mn<sup>2+</sup>.**

| Molecule | Binding Energy<br>kcal/mol | Interactions |
|----------|----------------------------|--------------|
| 104      | -102.715                   | 1            |
| 067      | -90.908                    | 1            |
| 027      | -87.651                    | 1            |
| 036      | -63.702                    | 2            |

**Table 4.11: Gas-phase data for imidazoles binding with Mn<sup>3+</sup>.**

| Molecule | Binding Energy<br>kcal/mol | Interactions |
|----------|----------------------------|--------------|
| 104      | -149.095                   | 2            |
| 067      | -130.731                   | 1            |
| 027      | -127.176                   | 1            |
| 036      | -103.632                   | 2            |

The manganese (II) ion is a moderately hard, acidic cation with an ionic radius of 81 pm. Once again, a cation with an ionic radius similar to that of Zn<sup>2+</sup> shows comparable results. Manganese (II) was chelated by 87% of the imidazoles tested and showed an average binding energy of -29.502 kcal/mol. Both of these results are similar to those for the zinc ion. All of the molecules in Table 4.10 contain a carboxylate group.

The manganese (III) ion is a hard, acidic cation with an ionic radius of 72 pm. It is isoelectronic with Cr<sup>2+</sup>, but gave significantly different results due to its higher oxidation state. The average binding energy for Mn<sup>3+</sup> was -37.994 kcal/mol, much higher than the average value for Cr<sup>2+</sup> of -29.239 kcal/mol. Mn<sup>3+</sup> formed a complex with 88.9%

of the imidazoles being tested. All of the molecules in table 4.11 contain a carboxylate group.

#### 4.2.9 – Gas-Phase Simulations with Cobalt Ions

Cobalt ions are essential to humans. They are an essential component of vitamin B-12, which is required for normal functioning of the brain and nervous system (Cracan and Banerjee 2013). Data from the gas-phase simulations of this ion with the four imidazoles that showed the most favourable binding energy are summarized in the tables below.

**Table 4.12: Gas-phase data for imidazoles binding with Co<sup>2+</sup>.**

| Molecule | Binding Energy<br>kcal/mol | Interactions |
|----------|----------------------------|--------------|
| 104      | -103.605                   | 1            |
| 067      | -91.802                    | 1            |
| 027      | -88.406                    | 1            |
| 036      | -64.567                    | 2            |

**Table 4.13: Gas-phase data for imidazoles binding with Co<sup>3+</sup>.**

| Molecule | Binding Energy<br>kcal/mol | Interactions |
|----------|----------------------------|--------------|
| 104      | -150.518                   | 2            |
| 101      | -136.790                   | 1            |
| 067      | -134.610                   | 1            |
| 027      | -128.518                   | 1            |

The cobalt (II) ion is an intermediate, acidic cation with an ionic radius of 79 pm. The ionic radius of Co<sup>2+</sup> is almost identical to that of Mn<sup>2+</sup>. It had a slightly better average binding energy of -29.824 kcal/mol and was chelated by 88% of the imidazoles. All of the molecules in Table 4.12 feature a carboxylate group.

The cobalt (III) ion is a moderately hard, acidic cation with an ionic radius of 69 pm. Compared with its trivalent manganese counterpart, which has a similar ionic radius, it had a very comparable average binding energy of -37.604 kcal/mol and bound 88.9% of the imidazoles. All of the molecules in Table 4.13 feature a carboxylate group.

#### 4.2.10 – Gas-Phase Simulations with Ni<sup>2+</sup>

Nickel ions have been linked to numerous medical conditions. Compounds containing nickel ions are believed to be carcinogenic. Allergies to nickel can also lead to dermatitis (Barceloux 1999). Ni<sup>2+</sup> has also been linked to oxidative stress and mitochondrial dysfunction during a stroke (Li and Zhang 2012). Data from the gas-phase simulations of this ion with the four imidazoles that showed the most favourable binding energy are summarized in the table below.

**Table 4.14: Gas-phase data for imidazoles binding with Ni<sup>2+</sup>.**

| Molecule | Binding Energy<br>kcal/mol | Interactions |
|----------|----------------------------|--------------|
| 104      | -98.845                    | 1            |
| 067      | -92.085                    | 1            |
| 027      | -88.668                    | 1            |
| 036      | -64.837                    | 2            |

The nickel (II) ion is an intermediate, acidic cation with an ionic radius of 83 pm. Like its divalent counterparts with a similar radius (Mn<sup>2+</sup> & Co<sup>2+</sup>), it had an average binding energy of nearly -30 kcal/mol. Its average binding energy was -29.624 kcal/mol and it formed complexes with 88% of the imidazoles. All of the molecules in Table 4.14 contain a carboxylate group.

#### 4.2.11 – Gas-Phase Simulations with Copper Ions

Copper ions are essential to human life. They are incorporated in the structure of many metalloenzymes that perform metabolic functions throughout the human body.  $\text{Cu}^{2+}$  is also thought to have a role in stroke pathophysiology similar to that of  $\text{Zn}^{2+}$ . In fact, it is believed that  $\text{Cu}^{2+}$  may also be contained in the same vesicles as glutamate and  $\text{Zn}^{2+}$ . Copper ions have been linked to ischemic oxidative stress (Li and Zhang 2012). Data from the gas-phase simulations of this ion with the four imidazoles that showed the most favourable binding energy are summarized in the tables below.

**Table 4.15: Gas-phase data for imidazoles binding with  $\text{Cu}^+$ .**

| Molecule | Binding Energy<br>kcal/mol | Interactions |
|----------|----------------------------|--------------|
| 104      | -57.099                    | 1            |
| 050      | -55.533                    | 1            |
| 042      | -52.297                    | 1            |
| 067      | -51.772                    | 1            |

**Table 4.16: Gas-phase data for imidazoles binding with  $\text{Cu}^{2+}$ .**

| Molecule | Binding Energy<br>kcal/mol | Interactions |
|----------|----------------------------|--------------|
| 104      | -94.463                    | 1            |
| 067      | -87.645                    | 1            |
| 027      | -84.334                    | 1            |
| 042      | -60.937                    | 1            |

The copper (I) ion is a soft, acidic cation with an ionic radius of 91 pm.  $\text{Cu}^+$  formed complexes with 81.5% of the imidazoles and had an average binding energy of -21.259 kcal/mol. This is similar to other monovalent ions  $\text{Li}^+$  and  $\text{Na}^+$ . Molecules 104 and 067 each bound  $\text{Cu}^+$  via a carboxylate group. Copper (I) interacted with 042 via a

dithiocarboxylate group. Finally,  $\text{Cu}^+$  formed an electrostatic interaction with molecule 050 via a carbonyl oxygen.

The copper (II) ion is an intermediate, acidic cation with an ionic radius of 87 pm. Its atomic radius is almost identical to that of  $\text{Zn}^{2+}$ . As a result, its average binding energy of -28.709 kcal/mol is very similar to that of the zinc ion. Copper (II) managed to form a complex with 86.1% of the imidazoles, comparable to other divalent cations in the working set. Molecules 104, 067 and 027 all interacted with  $\text{Cu}^{2+}$  via a negatively charged carboxylate group. Similarly, copper (II) formed an electrostatic interaction with molecule 042 via a negatively charged dithiocarboxylate group.

#### 4.2.12 – Gas-Phase Simulations with $\text{Sr}^{2+}$

Due to its chemical similarity with  $\text{Ca}^{2+}$ , the body readily absorbs  $\text{Sr}^{2+}$ . Exposure to strontium ions has been linked to bone disease and/or cancer (ATSDR 2004). Data from the gas-phase simulations of this ion with the four imidazoles that showed the most favourable binding energy are summarized in the table below.

**Table 4.17: Gas-phase data for imidazoles binding with  $\text{Sr}^{2+}$ .**

| Molecule | Binding Energy<br>kcal/mol | Interactions |
|----------|----------------------------|--------------|
| 104      | -80.657                    | 1            |
| 067      | -78.905                    | 1            |
| 101      | -78.063                    | 1            |
| 027      | -74.232                    | 1            |

The strontium ion is a moderately hard, acidic cation with an ionic radius of 132 pm. Though  $\text{Sr}^{2+}$  is quite a bit smaller than  $\text{K}^+$ , it still experienced many of the same steric problems. This is evidenced by the fact that the strontium ion only managed to form an electrostatic interaction with 80.6% of the imidazoles, the second lowest

percentage among divalent metal cations (only  $\text{Be}^{2+}$  was lower). This lack of affinity for interacting with imidazoles is corroborated by the fact that the average binding energy for the strontium ion was  $-26.750$  kcal/mol, quite a bit lower than most of the other divalent cations. All of the molecules in Table 4.17 contain a negatively charged carboxylate group that served as the binding site for  $\text{Sr}^{2+}$ .

#### 4.2.13 – Gas-Phase Simulations with $\text{Pd}^{2+}$

Although  $\text{Pd}^{2+}$  is not present in the human body under normal conditions, exposure to it can lead to an allergic response. People who suffer from a nickel allergy are especially susceptible. Like many metal ions,  $\text{Pd}^{2+}$  has been linked to cancer as well. Palladium is present in dental appliances, jewelry and electrical appliance, among other common objects (Keilhorn, Melber, Keller and Mangelsdorf 2002). Data from the gas-phase simulations of this ion with the four imidazoles that showed the most favourable binding energy are summarized in the table below.

**Table 4.18: Gas-phase data for imidazoles binding with  $\text{Pd}^{2+}$ .**

| Molecule | Binding Energy<br>kcal/mol | Interactions |
|----------|----------------------------|--------------|
| 104      | -100.037                   | 1            |
| 101      | -90.473                    | 1            |
| 067      | -88.812                    | 1            |
| 027      | -84.874                    | 1            |

The palladium (II) ion is a soft, acidic cation with an ionic radius of 100 pm. The average binding energy of  $-28.938$  kcal/mol is consistent with other divalent metal cations in the working set.  $\text{Pd}^{2+}$  managed to form complexes with 87% of the imidazoles being evaluated. All of the molecules in Table 4.18 interacted with palladium (II) via a negatively charged carboxylate group.

#### 4.2.14 – Gas-Phase Simulations with Ag<sup>+</sup>

Silver ions play no clearly defined role in human biology. When silver (I) salts enter the circulatory system, they can accumulate in different tissues, resulting in a condition called argyria. The silver deposits in the skin, causing it to turn grey (Hammond 2000). Also, exposure to silver ions has been linked to liver and kidney disease (Drake 2005). Data from the gas-phase simulations of this ion with the four imidazoles that showed the most favourable binding energy are summarized in the table below.

**Table 4.19: Gas-phase data of imidazoles with Ag<sup>+</sup>**

| Molecule | Binding Energy<br>kcal/mol | Interactions |
|----------|----------------------------|--------------|
| 050      | -55.522                    | 1            |
| 104      | -54.174                    | 1            |
| 042      | -52.343                    | 1            |
| 067      | -51.354                    | 1            |

The silver (I) ion is a soft, acidic cation with an ionic radius of 129 pm. Despite being larger than the strontium ion, silver (I) formed complexes with 86.1% of the imidazoles (compared to 80.6% for Sr<sup>2+</sup>). The average binding energy for Ag<sup>+</sup> was -21.537 kcal/mol, a value comparable to the other monovalent cations in the working set. The fact that the silver (I) ion was bound by such a high percentage of imidazoles (compared to other, hard monovalent cations) may indicate a preference of imidazoles for soft acids.

Like many other monovalent cations, Ag<sup>+</sup> formed a very strong interaction with the carbonyl oxygen of molecule 050. The silver (I) ion also formed strong electrostatic

interactions with the carboxylate groups of molecules 104 and 067, as well as the dithiocarboxylate group of molecule 042.

#### 4.2.15 – Gas-Phase Simulations with Cd<sup>2+</sup>

Exposure to cadmium and cadmium compounds is associated with an increased risk of stroke and heart failure. Cd<sup>2+</sup> acts as a neurotoxin by disturbing cellular redox balance (i.e. formation of reactive oxygen species) (Li and Zhang 2012). Prolonged exposure to cadmium and its compounds has also been linked to cancer (Tokar, Benbrahim and Waalkes 2011). Data from the gas-phase simulations of this ion with the four imidazoles that showed the most favourable binding energy are summarized in the table below.

**Table 4.20: Gas-phase data for imidazoles binding with Cd<sup>2+</sup>.**

| Molecule | Binding Energy<br>kcal/mol | Interactions |
|----------|----------------------------|--------------|
| 104      | -97.253                    | 1            |
| 101      | -87.241                    | 1            |
| 067      | -85.458                    | 1            |
| 027      | -82.039                    | 1            |

The cadmium (II) ion is a soft, acidic cation with an ionic radius of 109 pm. It formed a ligand-cation complex with 88.9% of the imidazoles that were tested and had a binding energy of -27.721 kcal/mol. Both of these values are comparable to those of Pd<sup>2+</sup>, another divalent cation with a similar ionic radius. Cd<sup>2+</sup> is isoelectronic with Ag<sup>+</sup>, but its higher oxidation state results in stronger interactions and binding energies of larger magnitude. All of the molecules in Table 4.20 have carboxylate groups.

#### 4.2.16 – Gas-Phase Simulations with Tin Ions

Salts of tin ions do not serve any biological purpose in the human body. However, chronic exposure to tin and its ions can have detrimental effects on human health. Tin (IV) oxide, in particular, has been linked to an increased risk of heart disease (Gunat, Aksoy, Davutoglu, Yildirim and Ege 2006). Data from the gas-phase simulations of this ion with the four imidazoles that showed the most favourable binding energy are summarized in the tables below.

**Table 4.21: Gas-phase data for imidazoles binding with Sn<sup>2+</sup>.**

| Molecule | Binding Energy<br>kcal/mol | Interactions |
|----------|----------------------------|--------------|
| 110      | -29.404                    | P            |
| 004      | -4.600                     | P            |

**Table 4.22: Gas-phase data for imidazoles binding with Sn<sup>4+</sup>.**

| Molecule | Binding Energy<br>kcal/mol | Interactions |
|----------|----------------------------|--------------|
| 004      | -8.097                     | P            |

The tin (II) ion is an intermediate, acidic cation with an ionic radius of 118 pm. Like aluminum, tin is a p-block element. Like the aluminum ion, tin (II) was not successful at binding with the imidazoles. In fact, only two of the gas-phase simulations resulted in any type of interaction with Sn<sup>2+</sup>. Similar to the case of Al<sup>3+</sup>, molecule 110 essentially pinched the tin (II) cation between two  $\pi$ -systems (a phenyl ring and the imidazole ring). This  $\pi$ -type interaction was much weaker than most of the electrostatic interactions between imidazoles and most of the other cations. Sn<sup>2+</sup> also formed a  $\pi$ -type

interaction with molecule 004 by migrating to the space directly above the imidazole ring.

The tin (IV) ion is a moderately hard, acidic cation with an ionic radius of 83 pm. Like its divalent counterpart, tin (IV) showed very little affinity for binding with imidazoles. This is counterintuitive because, with the high oxidation state, one would expect tin (IV) to readily form an electrostatic interaction with imidazoles. Contrarily,  $\text{Sn}^{4+}$  only formed a  $\pi$ -type interaction with molecule 004, in the same way as  $\text{Sn}^{2+}$ .

#### 4.2.17 – Gas-Phase Simulations with $\text{Ba}^{2+}$

Barium metal is highly reactive and its compounds are highly toxic.  $\text{Ba}^{2+}$  can interfere with the normal functioning of potassium ion channels and lead to unwanted neurological activity. Barium ions have been linked to heart disease, anxiety, tremors and several other disorders. Unlike most of the other metal ions in this study,  $\text{Ba}^{2+}$  is not carcinogenic (Patnaik 2003). Data from the gas-phase simulations of this ion with the four imidazoles that showed the most favourable binding energy are summarized in the table below.

**Table 4.23: Gas-phase data for imidazoles binding with  $\text{Ba}^{2+}$**

| Molecule | Binding Energy<br>kcal/mol | Interactions |
|----------|----------------------------|--------------|
| 104      | -79.706                    | 1            |
| 067      | -77.991                    | 1            |
| 101      | -76.554                    | 1            |
| 027      | -73.145                    | 1            |

The barium ion is a hard, acidic cation with an ionic radius of 149 pm.  $\text{Ba}^{2+}$  has the second largest ionic radius of the cations being studied. Much like the potassium and

strontium ions (ionic radii of 152 pm and 132 pm, respectively), many of the interactions with the imidazoles did not take place due to steric hindrance.  $\text{Ba}^{2+}$  was able to form complexes with 82.4% of the imidazoles with an average binding energy of -26.600 kcal/mol. This average binding energy is lower than most of its divalent counterparts. All of the molecules in Table 4.23 contain the carboxylate functionality.

#### 4.2.18 – Gas-Phase Simulations with $\text{Hg}^{2+}$

Mercury and the majority of its compound are extremely toxic. Some of its neurological effects include hallucinations, excitability, insomnia, tremors (which, if exposure is chronic, can become more violent) and suicidal tendencies. Mercury ions have also been linked to the generation of reactive oxygen species during the ischemic cascade (Li and Zhang 2012). Data from the gas-phase simulations of this ion with the four imidazoles that showed the most favourable binding energy are summarized in the table below.

**Table 4.24: Gas-phase data for imidazoles binding with  $\text{Hg}^{2+}$ .**

| Molecule | Binding Energy<br>kcal/mol | Interactions |
|----------|----------------------------|--------------|
| 104      | -98.070                    | 1            |
| 101      | -87.814                    | 1            |
| 067      | -85.975                    | 1            |
| 027      | -82.586                    | 1            |

The mercury (II) ion is a soft, acidic cation with an ionic radius of 116 pm. Although its ionic size and oxidation state are similar to  $\text{Ca}^{2+}$ ,  $\text{Hg}^{2+}$  showed more favourable and more frequent binding with the imidazoles. 87% of the molecules in the working set were able to chelate the mercury (II) ion with an average binding energy of -29.207 kcal/mol (compared to 82.4% and -25.644 kcal/mol for the calcium ion). Based

on this result, for cations of the same oxidation state, imidazole may prefer to interact with soft acids. All of the molecules in Table 4.24 have a carboxylate group.

#### 4.2.19 – Gas-Phase Simulations with $\text{Pb}^{2+}$

Long-term exposure to lead metal and its ionic salts can lead to severe kidney disease and gastrointestinal distress. It has also been linked to blood and brain disorders (ATSDR 2006). In children, lead is thought to be involved in the development of learning disabilities (Hu 1991). Data from the gas-phase simulations of this ion with the four imidazoles that showed the most favourable binding energy are summarized in the table below.

**Table 4.25: Gas-phase data for imidazoles binding with  $\text{Pb}^{2+}$ .**

| Molecule | Binding Energy<br>kcal/mol | Interactions |
|----------|----------------------------|--------------|
| 110      | -29.813                    | P            |
| 004      | -4.827                     | P            |

The lead (II) ion is an intermediate, acidic cation with an ionic radius of 133 pm. Like its p-block counterparts,  $\text{Pb}^{2+}$  showed very little affinity for binding with the imidazoles being evaluated. The two interactions that did take place were  $\pi$ -type interactions with aromatic rings. As was the case with  $\text{Al}^{3+}$  and  $\text{Sn}^{2+}$ , the two  $\pi$ -systems in molecule 110 (a phenyl ring and the imidazole ring) essentially sandwiched the cation. In comparison to the electrostatic interactions formed by most of the cations, these  $\pi$ -type interactions were quite weak. Also similar to the aluminum and tin ions, the lead ion migrated to the space directly above the imidazole ring in molecule 004, creating a  $\pi$ -type interaction.

### ***4.3 – Conclusion***

This chapter explored the interactions that took place between a database of imidazole-based molecules and 24 biologically relevant metal cations. After performing a comprehensive series of gas-phase simulations, it has become clear that imidazoles are very effective at chelating several cations. In fact, imidazoles showed significant binding with every s- and d-block cation that was evaluated. Also, p-block cations showed almost no binding with imidazole-based molecules.

In general, as oxidation state increases, so does the average binding energy exhibited by each cation. One exception to this rule is the case of tin (IV), which showed no electrostatic interaction with any of the imidazoles. Furthermore, for cations of the same oxidation state, the one with the smaller ionic radius showed the most favourable binding energy.

If imidazoles are to be used as a therapeutic for ischemic stroke, a few points need to be considered. The imidazoles in the testing set showed significant binding with several cations that are necessary for normal central nervous system functioning. These cations include  $\text{Na}^+$ ,  $\text{K}^+$  and  $\text{Li}^+$ , among others. To avoid these side effects, it may be useful to administer supplements of these cations shortly after administering the imidazole compound.

## CHAPTER 5 – FUTURE WORK AND CONCLUSIONS

This chapter will include a summary of future experimental work and some closing comments about the research presented in this thesis.

### *5.1 – Future Experimental Work*

There are two experiments that would be excellent complements to the computational work presented in this thesis. The first, another solution-phase study, would provide more information about the binding interactions between imidazoles and  $\text{Zn}^{2+}$  and  $\text{Ca}^{2+}$ . The other is an *in vitro* experiment that would provide information about the imidazole-based molecules' ability to cross lipid membranes.

One of the most significant problems in performing the solution-phase simulations was the ability of solvent molecules to displace the cations away from the binding site and solvate them. To counter this, a new *in silico* solution-phase study was devised. In the solution-phase simulations performed in Chapter 3, the imidazole-based molecule and cation were loaded into MOE separately. They were then manipulated such that the cation of interest was placed approximately three angstroms away from the potential metal-binding site. The separation of the molecule and cation was the cause of the removal of the cation from the binding site and subsequent solvation. In order to address this problem, in the new study, optimized systems from the gas-phase simulations were loaded into MOE. In these optimized systems, the ligand-ion complexes are already formed at the outset. Next, a solvent box will be created and filled with a periodic array of water molecules. Once solvated, the system will be minimized again. The purpose of

this study is to evaluate how the presence of a solvent affects the interaction between the imidazole and the cation. The previous experiment accomplished this goal, but only if the cation was able to escape the pull of the solvent molecules in the first place. In this new study, the binding step is taken out of the equation since the interaction is already formed.

The second experiment will be performed *in vitro*. Figure 4.1 shows the proposed apparatus for the experiment. It involves two beakers connected by a glass bridge. First, compartment A will be filled about three-quarters of the way to the bridge with a 10 mM solution of the imidazole being tested. Next, a 1mM solution of a zinc or calcium salt will be added to the same height in compartment B. *n*-Octanol will then be slowly and carefully added, making an effort to keep the layers as separate as possible. After twenty-four hours, a sample will be taken from compartment A and analyzed for cation content.

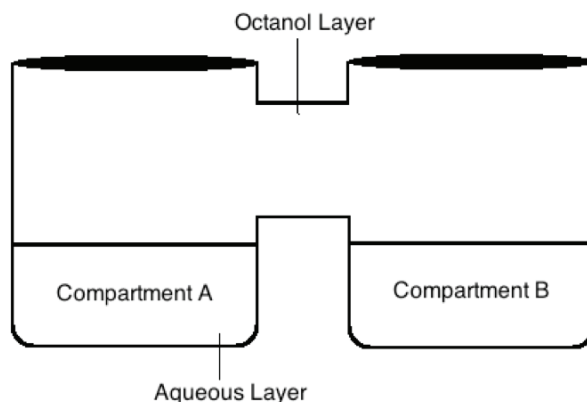


**Figure 5.1: Apparatus for an *in vitro* study.**

Ideally, the imidazole-based molecule will traverse the octanol-water interface, migrate to compartment B and then traverse the octanol-water interface again. Once in the aqueous layer of compartment B, the imidazole will chelate the metals cation of

interest and then return to compartment A in the same way. This is an economical and time-efficient experiment for evaluating a number of useful properties.

Once inside the human body, the imidazole-based drug molecule must cross a lipid membrane to enter the blood (unless it is injected). The octanol-water interface will simulate the lipid membrane. Once inside the blood, the drug must then cross another lipid membrane to reach its target. The second octanol-water interface will mimic this part of the drug's action. Once in the aqueous layer of compartment B, the imidazole must chelate the cation and return through the membranes again. This experiment evaluates the drug molecule's ability to get absorbed by the small intestine, transported through a lipophilic medium to a second aqueous compartment and then return to be metabolized or excreted.

Once this initial experiment is carried out, further experiments with biological concentrations of  $Zn^{2+}$  and  $Ca^{2+}$  can be done. It would also be useful to try lowering the concentration of the drug molecule with each successive trial as well. Finally, altering the amount of time allowed to elapse before testing the sample in compartment A could be altered as well.

## ***5.2 – Concluding Comments***

Stroke is the third leading cause of death in the developed countries. At present, there is not a sufficiently efficacious drug molecule that therapeutically interrupts the ischemic cascade in time to preserve normal motor and cognitive function. It would be beneficial to individual patients, their families, and society in general if a truly successful therapeutic were developed.

There are many chemical species involved in the ischemic cascade. Two such species are calcium ions and zinc ions. When present in the brain in excess, these cations become neurotoxic. They cause extreme depolarization in healthy neurons, causing the release of glutamate and setting the ischemic cascade into motion.

The purpose of the research presented in this thesis was to evaluate a class of molecules (imidazoles) for their therapeutic potential as chelating agents for both zinc and calcium ions in both gas- and solution-phase molecular mechanics simulations. After systematically testing approximately 120 imidazole-based molecules, a set of seven lead molecules was identified for *in vitro* experiments. These *in silico* studies suggest that imidazoles are a possible therapeutic platform around which an anti-stroke drug development program could be initiated.

In order to be thorough, 24 other biologically relevant cations were also put through the same series of *in silico* tests. Significant binding was shown for 22 of the 26 cations that were evaluated (including zinc and calcium ions). These results indicate that, when the imidazole platform is being optimized as an anti-ischemic therapeutic, the issue of selectivity and the issue of off-target binding site induced toxicity will have to be considered.

In conclusion, according to the *in silico* studies that were performed, imidazole-based molecules have worthwhile potential as a therapeutic platform for the prevention of the ischemic neuronal degradation associated with stroke. Pending the results of complementary *in vitro* studies, further experimentation with imidazoles should be done to fully characterize this class of molecules for their possible role in stroke therapy.

## REFERENCES

---

- “ToxFAQs: Chromium.” *Agency for Toxic Substances and Disease Registry* (2012).
- “ToxFAQs: Lead.” *Agency for Toxic Substances and Disease Registry* (2006).
- “ToxFAQs: Strontium.” *Agency for Toxic Substances and Disease Registry* (2004).
- Aggarwal, A; Aggarwal, P.; Khatak, M.; Khatak, S. “Cerebral Ischemic Stroke: Sequels of Cascades.” *International Journal of Pharma and Bio Science* 1.3 (2010) : 1-24.
- Barceloux, D. G. “Nickel.” *Clinical Toxicology* 37.2 (1999) : 239-258.
- Bernardo, J. “Aluminum Toxicity.” *Medscape Reference* (2012).
- Bhatnagar, A.; Sharma, P. K. and Kumar, N. “A Review on “Imidazoles”: Their Chemistry and Pharmacological Potentials.” *Int. J. of PharmaTech Research*. 3.1 (2011) : 268-282.
- Bogousslavsky, J. and Fisher, M. *Cerebrovascular Disease*. Philadelphia: Current Medicine, Inc., 2000.
- Boldyrev, A. et al. “Carnosine Protects Against Excitotoxic Cell Death Independently of Effects on Reactive Oxygen Species.” *Neuroscience* 94.2 (1999) : 571-577.
- Brown, C.E. and Antholine, W. E. “Chelation Chemistry of Carnosine.” *J. Phys. Chem.* 83.26 (1979) : 3314-3319.
- Campbell, N. *Biology*. 10<sup>th</sup> ed. Menlo Park: Benjamin Cummings (2010).
- Cracan, V.; Banerjee, R. “Cobalt and Corrinoid Transport and Biochemistry.” *Metal Ions in Life Science*. Springer. 2013.

- Drake, P.; Hazelwood, K. "Exposure-Related Health Effects of Silver and Silver Compounds: A Review." *The Annals of Occupational Hygiene* 9.7 (2005) : 575-585.
- Dyck, R.; Gasso, S. "The Role of Zinc in Cerebral Ischemia." *Mol. Med.* 13.7-8 (2007) : 380-387.
- Gunay, N. et al. "Cardiac Damage Secondary to Occupational Exposure to Tin Vapour." *Inhalation Toxicology* 18.1 (2006) : 53-56.
- Hu. H. "Knowledge of Diagnosis and Reproductive History Among Survivors of Childhood Plumbism." *Am. J. of Pub. Health* 81.8 (1991) : 1070-1072.
- Jolly, W. L. *Modern Inorganic Chemistry*. New York: McGraw-Hill. 1984.
- Kielhorn, J. et al. "Palladium: A review of exposure and effects to human health." *Int. J. Hyg. Env. Health* 205.6 (2002) : 417-432.
- Kohen, R. et al. "Antioxidant activity of carnosine, homocarnosine, and anserine present in muscle and brain." *Proc. Natl. Acad. Sci.* 85 (1988) : 3175-3179.
- Larsson, S. C.; Virtanen, M. J.; Mars, N. "Magnesium, Calcium, Potassium and Sodium Intakes and Risk of Stroke in Male Smokers." *Arch. Intern. Med.* 168.5 (2008) : 459-465.
- Law, N.; Caudle, M.; Pecoraro, V. "Manganese Redox Enzymes and Model Systems." *Advances in Inorganic Chemistry* 46 (1998) : 305.
- Leach, A. R. *Molecular Modeling: Principles and Applications*. 2<sup>nd</sup> ed. Toronto: Pearson Education Limited. 2001. Print
- Lewit-Bentley, A.; Rety, S. "EF Hand Calcium Binding Proteins." *Current Opinion in Structural Biology* 10 (2000) : 637-643.

- Li, Y. V.; Zhang, J. H. "Metal Ions in Stroke Pathophysiology." *Springer Series in Translational Stroke Research*. 2012. Print.
- Lipinski, C. A. et al. *J. Adv. Drug Deliv. Rev.* 46 (2001) : 3-26.
- MacKerell *et al.* "All-Atom Empirical Potential for Molecular Modeling and Dynamics Studies of Proteins." *J. Phys. Chem.* 102 (1998) : 3586-3616.
- Mandal, S.; Mandal, S.; Moudgil, M. "Rational Drug Design." *European Journal of Pharmacology* 635 (2009) : 90-100.
- McDowall, J. "Zinc Fingers." *Interpro Protein Data Bank* (2007).
- Nogarty, T. and Weaver, D. F. *Medicinal Chemistry: A Molecular and Biochemical Approach*. 3<sup>rd</sup> ed. Toronto: Oxford University Press, Inc. 2005.
- Orlowski, P. et al. "Modeling of pH dynamics in brain cells after stroke." *Interface Focus* (2011): 1-9.
- Patnaik, P. *Handbook of Inorganic Chemicals*. New York: McGraw-Hill. 2003. 77-78.
- Pearson, R. G. "Hard and Soft Acids and Bases, HSAB, Part 1." *J. Chem. Ed.* 45.9 (1968): 581-587
- Rajanikant, G.K. et al. "Carnosine Is Neuroprotective Against Permanent Focal Cerebral Ischemia in Mice." *Stroke* 38 (2007) : 3023-3031.
- Rang, H. P.; Dale, M. M.; Ritter, J. M. "Amino Acid Transmitters." *Pharmacology*, 3<sup>rd</sup> ed. Edinburgh: Harcourt Publishers Ltd. 2001. Print.
- Rogers, D. *Computational Chemistry Using The PC*. 3<sup>rd</sup> ed. Hoboken: John Wiley and Sons, Inc. 2003. Print.
- Sakurai, E. et al. "Uptake of L-histidine and histamine biosynthesis at the blood-brain barrier." *Inflammation Research* 58.1 (2009) : 34-35.

- Schrauzer, G. N. "Lithium: Occurrence, dietary intakes, nutritional essentiality." *J. Am. Coll. Nutr.* 1 (2002) : 14-21.
- Selnes, O. A. et al. "Cognitive and Neurologic Outcomes after Coronary-Artery Bypass Surgery." *The New England Journal of Medicine* 366 (2012) : 250-257.
- Shannon, R. D. "Revised effective ionic radii and systematic studies of interatomic distances in halides and chalcogenides." *Acta Cryst A* 22 (1976) : 751-767.
- Tokar, E.J.; Benbrahim-Tallaa, L.; Waalkes, M. P. "Metal ions in human cancer development." *Metal Ions: Life Science* 8 (2011) : 375-401.
- Truelove, S. "A Brief History of Taxol." *Virginia Tech Research Magazine* (1999).
- von Kummer, R. et al. "Acute Stroke." *Radiology* 205 (1997) : 327-333.